

Identification of novel proteins that regulate the amino acid-sensitive mTORC1 pathway

by

Lawrence D. Schweitzer

B.A. Molecular Biology
Colgate University

SUBMITTED TO THE DEPARTMENT OF BIOLOGY IN PARTIAL FULFILLMENT
OF THE REQUIREMENTS FOR THE DEGREE OF

DOCTOR OF PHILOSOPHY IN BIOLOGY
AT THE
MASSACHUSETTS INSTITUTE OF TECHNOLOGY

FEBRUARY 2016

© Lawrence D. Schweitzer. All rights reserved.

The author hereby grants to MIT permission to reproduce and to distribute publicly paper and electronic copies of this thesis in whole or in part in any medium now known or hereafter created.


Signature redacted

Signature of Author: _____

Department of Biology
December 2, 2015


Signature redacted

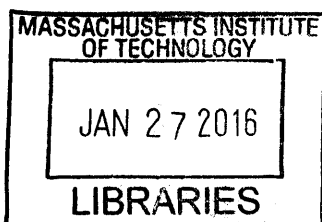
Certified by: _____

David M. Sabatini
Professor of Biology
Member, Whitehead Institute


Signature redacted

Accepted by: _____

Michael Hemann
Associate Professor of Biology
Co-Chair, Committee for Graduate Students



ARCHIVES

Identification of novel proteins that regulate the amino acid-sensitive mTORC1 pathway

by

Lawrence D. Schweitzer

Submitted to the Department of Biology on ____ in partial fulfillment of the requirements for the degree of Doctor of Philosophy in Biology

ABSTRACT

mTOR is a serine-threonine kinase that, as the catalytic subunit of mTORC1, promotes growth and anabolism. Due to its central role in metabolism, the local and systemic environment surrounding the cell tightly regulate mTORC1. Growth factors and nutrients are each required to activate mTORC1 and promote growth. Activation of mTORC1 by growth factors has been well-elucidated, but it is only recently becoming clear how nutrients, specifically amino acids, activate mTORC1. The presence of amino acids leads to the recruitment of mTORC1 from the cytosol to the surface of the lysosomal membrane, allowing it to be activated downstream of growth factors. This amino acid-induced translocation is mediated by the Rag GTPases and Ragulator (the scaffold for the Rag GTPases and mTORC1 on the lysosomal membrane). Here we describe the identification of two new components of Ragulator, HBXIP and c7orf59, that are required for the lysosomal localization of both the Rag GTPases and mTORC1 and that allowed us to identify new functions that Ragulator fulfills. We also characterized RagA-null mice and RagA-null mouse embryonic fibroblasts (MEFs). RagA is required for embryonic development, and, surprisingly, its deletion in adult mice leads to an expansion of monocytes. MEFs derived from RagA-null embryos display atypical, nutrient-insensitive mTORC1 activation. Finally, we identified c17orf59, a new Ragulator-interacting protein that inhibits the interaction between the Rag GTPases and Ragulator, inhibiting mTORC1 activation by amino acids. We report here our progress in characterizing the components of the amino acid-sensitive mTORC1 pathway and their physiological roles and we discuss the many open questions that remain to be studied regarding how amino acid sufficiency promotes the lysosomal localization of mTORC1.

Acknowledgements

I would like to thank David Sabatini for his guidance over the last six years. His insight and advice have shaped my scientific training ever since he led my section of Methods and Logic with Frank Solomon during my first year and through my recent decisions regarding my future professional steps. David's enthusiasm for science convinced me to rotate in and ultimately join his lab. I have learned more about how to think about science from David than I even imagined possible at the outset of graduate school and I hope that I am able to maintain the rigor, critical thinking and attention to detail that marks David's instruction as I move forward with my career.

Throughout my graduate years, my thesis committee has provided me with advice, both on my projects and presentations and, lately, on how to evaluate scientists and consider labs for my postdoctoral position. I am grateful to Hidde Ploegh and Matt Vander Heiden for the time they have taken to listen to me in my committee meetings and in less formal meetings. I would also like to thank Brendan Manning for serving on my committee for my thesis defense.

I would never have survived in the lab without constant help and support from dozens of people. Alejo has been a mentor and close friend and I cannot thank him enough for his advice over the years; he has made an enormous contribution to my growth as a scientist and as a person. For almost all of my time in the Sabatini lab, I have lived in room 357 and shared a bay with Heather. Our scientific conversations have always been constructive and she has been a part of my daily life. Kivanc and Roberto both continually gave me advice and always made sure I was on the right track in lab. Carson is a fountain of knowledge that I leaned on throughout the time we overlapped in lab, and someone that I am lucky to consider a friend. Brian has been a good friend whose enthusiasm for science, life and fishing is infectious. Bill was instrumental in completing my paper, sacrificing his time and energy to help with imaging experiments. Pekka and Amanda were often my partners in crime, and with Alejo made up the best times I had in lab.

There are nearly innumerable people I need to thank for allowing me to distract them with conversations, coffee, beer, and scientific discussions: Tim Peterson, Jan, Rich, Do, Dudley, Peggy, Tim Wang, Walter, Mike, Monther, Andrew, Greg, and just about anyone else that I overlapped with in the Sabatini lab. I learned most of the techniques that I use from Liron, with whom I collaborated in my early work.

I cannot express enough thanks to my family. They have kept me fed, loved, and happy. My mom has read and edited almost every important thing I have written, regardless of how boring or terribly written. My dad has endured

countless scientific conversations over dinner and is continually supportive and curious. And my brother Karl has always been there for me. I appreciate everything you have done for me.

Naama: you are awesome, and I am lucky to have you and Ron in my life.

TABLE OF CONTENTS

Abstract	3
Acknowledgements	4
Table of contents	6
Chapter 1: Introduction	7
Introduction.....	8
Conclusion.....	23
References.....	25
Chapter 2: Identification of HBXIP and c7orf59 as members of Ragulator	33
Introduction.....	34
Results.....	36
Discussion.....	54
Materials and Methods.....	56
Acknowledgements.....	62
References.....	63
Chapter 3: RagA deletion in the mouse	66
Introduction.....	67
Results.....	69
Discussion.....	84
Materials and Methods.....	86
Acknowledgements.....	89
References.....	90
Chapter 4: Disruption of the Rag-Ragulator complex by c17orf59 inhibits mTORC1	93
Introduction.....	94
Results.....	96
Discussion.....	119
Materials and Methods.....	122
Acknowledgements.....	130
References.....	131
Chapter 5: Discussion and Future Directions	134
Summary and Outstanding Questions.....	135
Conclusion.....	142
References.....	143

Chapter 1

Introduction

Lawrence D. Schweitzer¹

¹ Whitehead Institute for Biomedical Research and Massachusetts Institute of Technology, Department of Biology, Nine Cambridge Center, Cambridge, MA 02142

mechanistic Target of Rapamycin (mTOR)

The mechanistic Target of Rapamycin (mTOR) is a serine threonine kinase that phosphorylates a broad spectrum of protein substrates to affect anabolic and catabolic processes and regulate cellular growth. mTOR is evolutionarily conserved and found in nearly all eukaryotic organisms that have been examined and TOR activity is required for proliferation in organisms from yeast *Saccharomyces cerevisiae* to mammals.

mTOR activity is essential across nearly all eukaryotes due to its central role in controlling growth and anabolism. mTOR regulates processes that produce the building blocks, energy and proteins required for cell division and survival; active mTOR promotes mRNA translation, lipid and nucleotide biosynthesis, mitochondrial biogenesis, and specific metabolic pathways, while inactivated mTOR can signal a cell to choose between either autophagy, the process of salvaging pieces of the cell to survive under stress, or apoptosis, programmed cell death. As a regulator of processes that are required for survival and proliferation, mTOR responds to a number of important stimuli, including growth factors and growth factor signaling, nutrients, and cellular stresses.

Discovery of mTOR

TOR activity was known to be vital for cellular growth long before the identification of the kinase itself. Rapamycin, the bacterially-produced macrolide that can inhibit TOR, was discovered and shown to have anti-fungal activity in 1975 (Vézina et al., 1975). The drug is sufficient to inhibit growth of yeast, including *Candida albicans* as well as *S. cerevisiae*. Subsequently, it was found that rapamycin acts as an immunosuppressant in humans and other mammals and can inhibit proliferation of mammalian cells (Sehgal and Bansbach, 1993).

With the knowledge that rapamycin inhibited growth in fungal as well as mammalian cells, it became clear that the molecular target of the drug was

conserved and that the target of rapamycin would likely be an important mediator of proliferation from yeast to mammals. The identification of TOR was complicated by the mechanism of action of rapamycin, which requires the prolyl isomerase FKB12 as a co-factor for binding and inhibiting the kinase (Abraham and Wiederrecht, 1996). However, in the mid-1990's multiple groups found the protein that is inhibited by rapamycin in both *S. cerevisiae* and human cells, which was named the Target of Rapamycin (Kunz et al., 1993; Sabatini et al., 1994; Sabers et al., 1995; Brown et al., 1994). The identification of mTOR was followed by the discovery of the proteins that bind to and regulate the kinase, as well as further elucidation of its functions.

Two mTOR-containing complexes: mTORC1 and mTORC2

Work in both fungal and mammalian systems revealed that mTOR is found in two distinct multi-protein complexes: mTOR complex 1 and mTOR complex 2 (mTORC1 and mTORC2, respectively). Each of the complexes contains mTOR, but is composed of different sets of proteins that interact with and regulate mTOR. As such, each complex has distinct substrates and modes of regulation, despite the unifying presence of mTOR (Figure 1a and 1b).

mTORC1 is composed of the kinase mTOR, Raptor, mLST8 (also known as GβL), as well as two inhibitory or regulatory subunits: PRAS40 (Proline Rich Akt Substrate of 40kD) and DEPTOR (Kim et al., 2002; Hara et al., 2002; Kim et al., 2003; Sancak et al., 2007; Oshiro et al., 2007; Thedieck et al., 2007; Vander Haar et al., 2007; Wang et al., 2007; Fonseca et al., 2007; Peterson et al., 2009). mTORC2 includes mTOR, Rictor, mLST8, mSIN1, Protor1/2 and DEPTOR (Sarbossov et al., 2004; Frias et al., 2006; Thedieck et al., 2007; Pearce et al., 2007; Peterson et al., 2009). Raptor and Rictor are the defining components of mTORC1 and mTORC2, respectively. Both of these subunits are important structurally and for the recruitment of specific mTOR substrates, and can also be modified to alter the activity of their complexes.

mLST8, which is a component of both mTORC1 and mTORC2, binds directly to the kinase domain of mTOR and is important for mTOR kinase activity, particularly within mTORC2 (Kim et al., 2003; Guertin et al., 2006). mSin1 binds to Rictor and is required for mTORC2 assembly, stability and activity (Frias et al., 2006; Yang et al., 2006). mSin1 has three different isoforms that participate in mTORC2 and the different potential mTORC2 complexes (as defined by mSin1 isoforms) have different sensitivities to insulin, a major input into mTORC2 signaling, likely due to the presence or absence of Pleckstrin-homology domains in the mSin1 isoforms (Frias et al., 2006; Liu et al., 2015). The final constitutive component of mTORC2, Protor1/2, binds Rictor and is important for phosphorylation of a subset of mTORC2 substrates (Pearce et al., 2006; Pearce et al., 2011).

DEPTOR and PRAS40 are two mTOR-associated inhibitors, which are often considered to be part of the core complexes. Both proteins inhibit the kinase activity of mTOR. PRAS40 only interacts with and inhibits mTORC1 (Sancak et al., 2007), while DEPTOR binds and inhibits both mTORC1 and mTORC2 (Peterson et al., 2009). The binding of each to mTOR is regulated, providing a layer of control over mTOR activity.

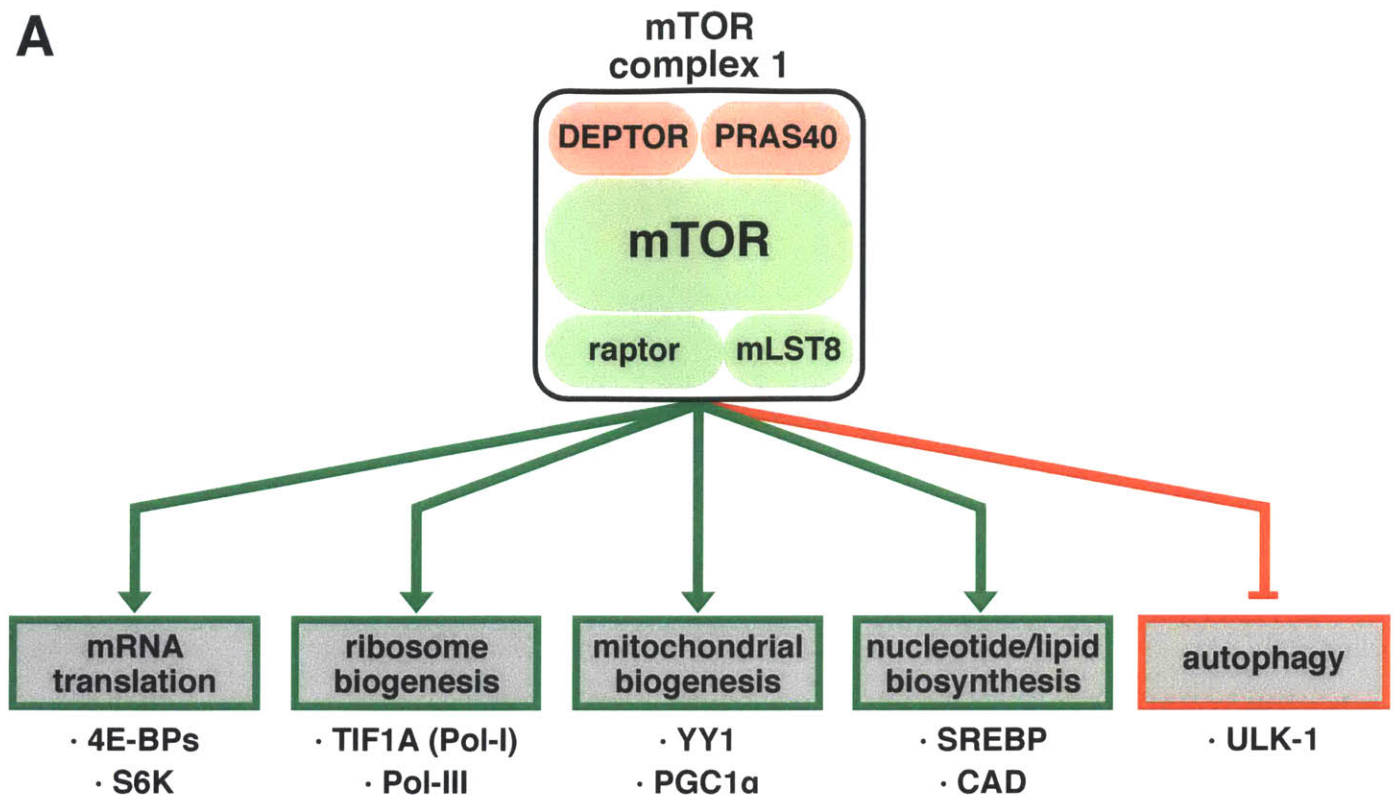
Functions and substrates of mTORC1

Despite sharing the same catalytic subunit, mTORC1 and mTORC2 participate in distinct signaling pathways; the complexes are activated and inhibited by different stimuli and in turn phosphorylate different substrates. Of the two complexes, the regulation and function of mTORC1 is much better understood, and will be discussed extensively.

mTORC1 balances the metabolic state of the cell with its environmental conditions. The complex positively regulates anabolic processes to promote growth, and also controls the availability of the building blocks required for these processes by controlling catabolic pathways. The anabolic processes regulated

Figure 1: mTOR complex 1 and 2 components and functions

A



B

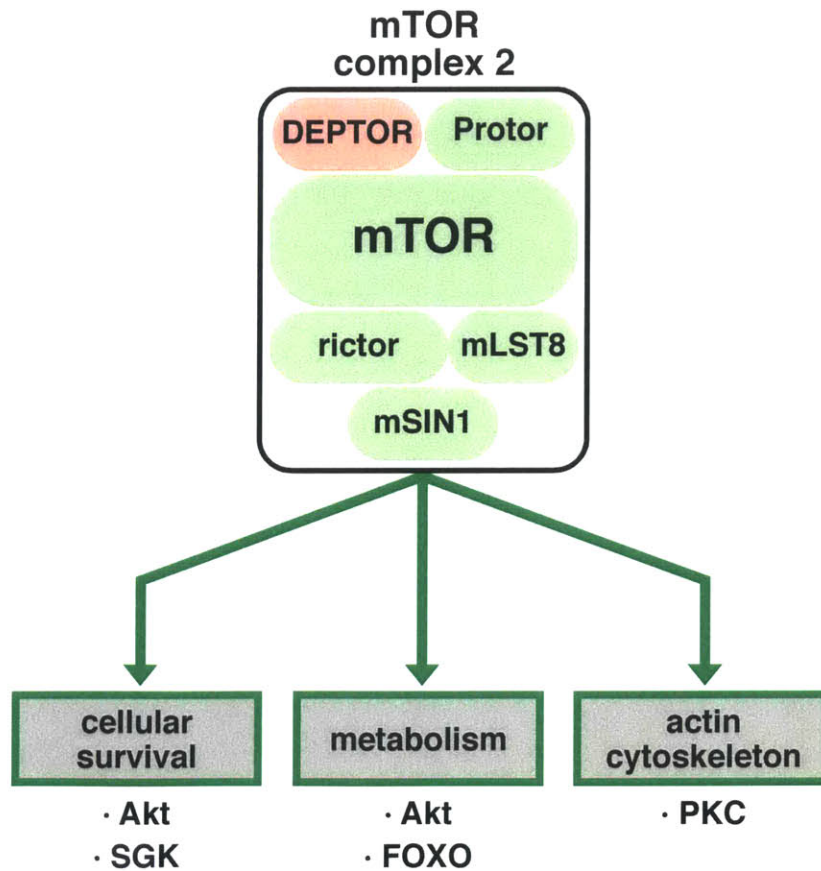


Figure 1: mTOR complex 1 and 2 components and functions

A) mTOR complex 1 and its functions. mTORC1 is composed of mTOR, raptor, mLST8 and two inhibitory proteins DEPTOR and PRAS40. When active mTORC1 promotes mRNA translation, ribosome and mitochondrial biogenesis, nucleotide and lipid biosynthesis and inhibits autophagy through phosphorylating a number of substrates. Proteins listed below each pathway are the factors regulated by mTORC1 that participate in the indicated process. These factors are either direct substrates of mTORC1 or are indirectly regulated by mTORC1 activity.

B) mTOR complex 2 and its functions. mTORC2 is composed of mTOR, rictor, mLST8, Protor and the inhibitor DEPTOR. When active, mTORC2 promotes cellular survival, metabolic changes and modifies the actin cytoskeleton through regulation of a number of substrates, listed below each indicated process. Proteins listed below each pathway are the factors regulated by mTORC2 that participate in the indicated process. These factors are either direct substrates of mTORC2 or are indirectly regulated by mTORC2 activity.

by mTORC1 include mRNA translation, ribosomal biogenesis, and lipid and nucleotide biosynthesis. Autophagy and proteasomal degradation are the major catabolic degradation pathways influenced by mTORC1 activity (Laplante and Sabatini, 2012; Zhang et al., 2014) (Figure 1a). Coordination of these anabolic and catabolic processes is vital for proliferation and growth, as a cell needs to increase its protein, ribosome, nucleotide and lipid pools in order to create a daughter cell.

mTORC1 regulates mRNA translation, particularly at the level of translation initiation. Under mTORC1 inhibition, total protein synthesis drops drastically. For example, there is a 65% suppression of protein synthesis in cells that have been treated with an ATP-competitive inhibitor of mTOR (Thoreen et al., 2012). The suppression of mRNA translation upon mTORC1 inhibition is due in large part to the loss of the mTORC1-mediated phosphorylation of the translation initiation repressors, 4E-BPs (Thoreen et al., 2012). When mTORC1 is inactive, the 4E-BP proteins are hypophosphorylated and bind to the translation initiation factor 4E (eIF4E), reducing its affinity for the mRNA m⁷GpppN cap. When 4E-BP is bound to eIF4E, it prevents eIF4E from binding to and recruiting eIF4G to the 5' end of the mRNA, which in turn strongly inhibits translation initiation. When mTORC1 is active, it phosphorylates 4E-BP, preventing it from binding to eIF4E and promoting mRNA translation initiation (Mamane et al., 2006).

The mTORC1 substrate S6 kinase 1 (S6K1) also regulates mRNA translation. When mTORC1 is active, it phosphorylates and activates S6K1. In addition to phosphorylating ribosomal protein S6, which is a part of the 40S ribosome subunit, S6K1 phosphorylates or binds to a number of components of the mRNA translation machinery to promote protein synthesis when active, including eIF4B, S6K1 Aly/REF-like substrate (SKAR), programmed cell death 4 (PDCD4), eukaryotic elongation factor 2 kinase (eEF2K), eukaryotic initiation factor 3 (eIF3) and 80 kD nuclear cap-binding protein (CBP80). (Magnuson et al., 2012)

mTORC1 also regulates mRNA translation at the level of ribosome biogenesis. mTORC1 promotes rRNA synthesis through the positive regulation of RNA polymerase I, by regulating Pol I-recruiting transcription factors especially transcription initiation factor 1A (TIF1A). mTORC1 positively regulates RNA Pol III, which transcribes genes important for rRNA processing. Finally, a class of transcripts with 5' terminal oligopyrimidine (5'-TOPs) are among the most strongly regulated by mTORC1 and include a number of ribosomal protein genes (Iadevaia et al., 2014; Thoreen et al., 2012).

Another important function of mTORC1 is in the negative regulation of autophagy. Autophagy is a cellular process in which cytoplasmic contents, including organelles, are degraded in lysosomes to recycle building blocks in cells that have been deprived of nutrients. mTORC1 inhibits autophagy through phosphorylation and inhibition of ULK1, a kinase that coordinates the early steps of autophagy (autophagosome formation). mTORC1 also phosphorylates AMBRA1, inhibiting a TRAF6-dependent K63-ubiquitination event on ULK1 (Nazio et al., 2013). By controlling ULK1 activity, mTORC1 can coordinate the initiation of autophagy. When mTORC1 is inhibited under nutrient deprivation (see below), autophagy is strongly upregulated by other pathways that respond to nutrient deprivation or stress (Dunlop and Tee, 2014).

mTORC1 has been implicated in a number of facets of metabolism both in cell culture and in whole body metabolism, through regulation of gluconeogenesis

and glucose transport in the liver, glycogen synthesis in the liver and muscle, and adipogenesis and lipogenesis in white adipose tissue. Many of the pathways that mTORC1 controls in tissues are maintained in cultured cells and are found to be dysregulated in tumors (Zoncu et al., 2011b; Laplante and Sabatini, 2012).

mTORC1 increases lipid biosynthesis, largely by promoting the processing of the transcription factor sterol-regulatory-element-binding protein (SREBP), which is responsible for upregulating expression of enzymes that are involved in lipid synthesis pathways (Horton et al., 2002). Lipin1 promotes the processing and nuclear localization of SREBP downstream of mTORC1 in a manner that involves restructuring of the nuclear lamina (Peterson et al., 2011). More directly, the mTORC1 substrate S6K1 is required for SREBP activation as well. Thus, mTORC1 controls at least two mechanisms of SREBP activation and lipid biosynthesis (Howell et al., 2013).

SREBP activation by mTORC1 also increases the expression of a number of genes whose products are important for the pentose phosphate pathway (PPP), which can lead to the biosynthesis of both purines and pyrimidines (Duvel et al., 2010). In addition to SREBP-mediated upregulation of the PPP, mTORC1 activates the enzyme carbamoyl-phosphate synthetase 2 (CAD2), which itself is involved in the production of pyrimidines (Ben-Sahra et al., 2013). By activating SREBP and CAD, mTORC1 also controls nucleotide biosynthesis.

Finally, mTORC1 has a role in mitochondrial biogenesis and metabolism. There is evidence that mTORC1 activation promotes mitochondrial DNA synthesis and expression of oxidative genes. Some aspects of the regulation of mitochondrial biogenesis may be mediated through mTORC1's regulation of yin-yang 1 (YY1) and PPAR γ coactivator-1 (PGC1 α). mTORC1 also regulates glycolysis and glucose uptake via the Hypoxia-inducible factor 1 α (HIF1 α) pathway. mTORC1 alters HIF1 α at the levels of transcription and translation, increasing energy production under stress conditions (Laplante and Sabatini, 2012).

Regulation of mTORC1

Because mTORC1 activity promotes growth processes, which are energy intensive and vital for cell division and the functions of terminally differentiated cells, it is not surprising that multiple cellular fitness parameters control mTORC1 activation. Intracellular conditions, including low energy levels, DNA damage, and other stress signals regulate mTORC1. Environmental cues that control mTORC1 activity represent the general nutritional status of the cell or organism so that mTORC1 is activated by growth factors and nutrients, including amino acids and glucose, and is inhibited under hypoxia (Zoncu et al., 2011b; Shimobayashi and Hall, 2014; Jewell et al., 2013; Gomes and Blenis, 2015; Zhang et al., 2014).

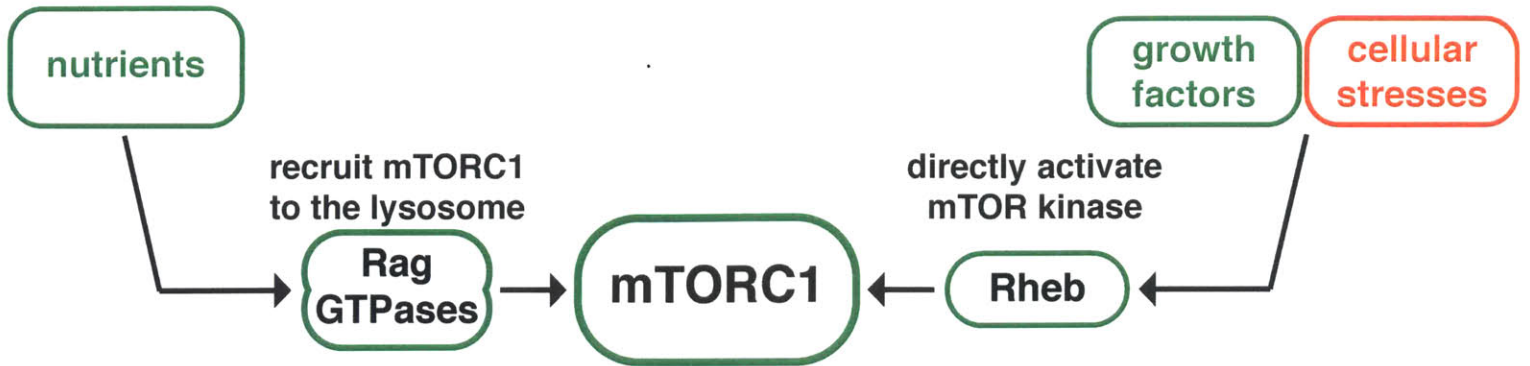
A. The Rag and Rheb GTPases

The mTORC1 pathway integrates different environmental signals by distinct mechanisms, well-exemplified by the contrast in pathway activation by growth factors as compared to nutrients (Figure 2a). Growth factors activate mTORC1 downstream of canonical phosphatidylinositol-3-kinase (PI3K)/Akt signaling. Growth factor-stimulated Akt activates the small GTPase Rheb by inhibiting its GTPase activating protein (GAP), tuberous sclerosis complex (TSC). GTP-bound Rheb activates the mTOR kinase activity (Tee et al., 2003; Inoki et al., 2003; Inoki et al., 2002; Garami et al., 2003; Long et al., 2005a; Manning et al., 2002; Zhang et al., 2003).

In order for Rheb to control the kinase activity of mTORC1, it must interact with the mTORC1 complex. This interaction is regulated independently of TSC/Rheb activity, and is controlled by intracellular amino acid and glucose availability (Sancak et al., 2008; Sancak et al., 2010; Efeyan et al., 2013; Long et al., 2005(b); Kim et al., 2008; Smith et al., 2005; Hara et al., 1998; Lynch et al., 2000; Nobukuni et al., 2005). Specifically, Rheb resides at the cytosolic face of

Figure 2: Regulation of mTORC1

A



B

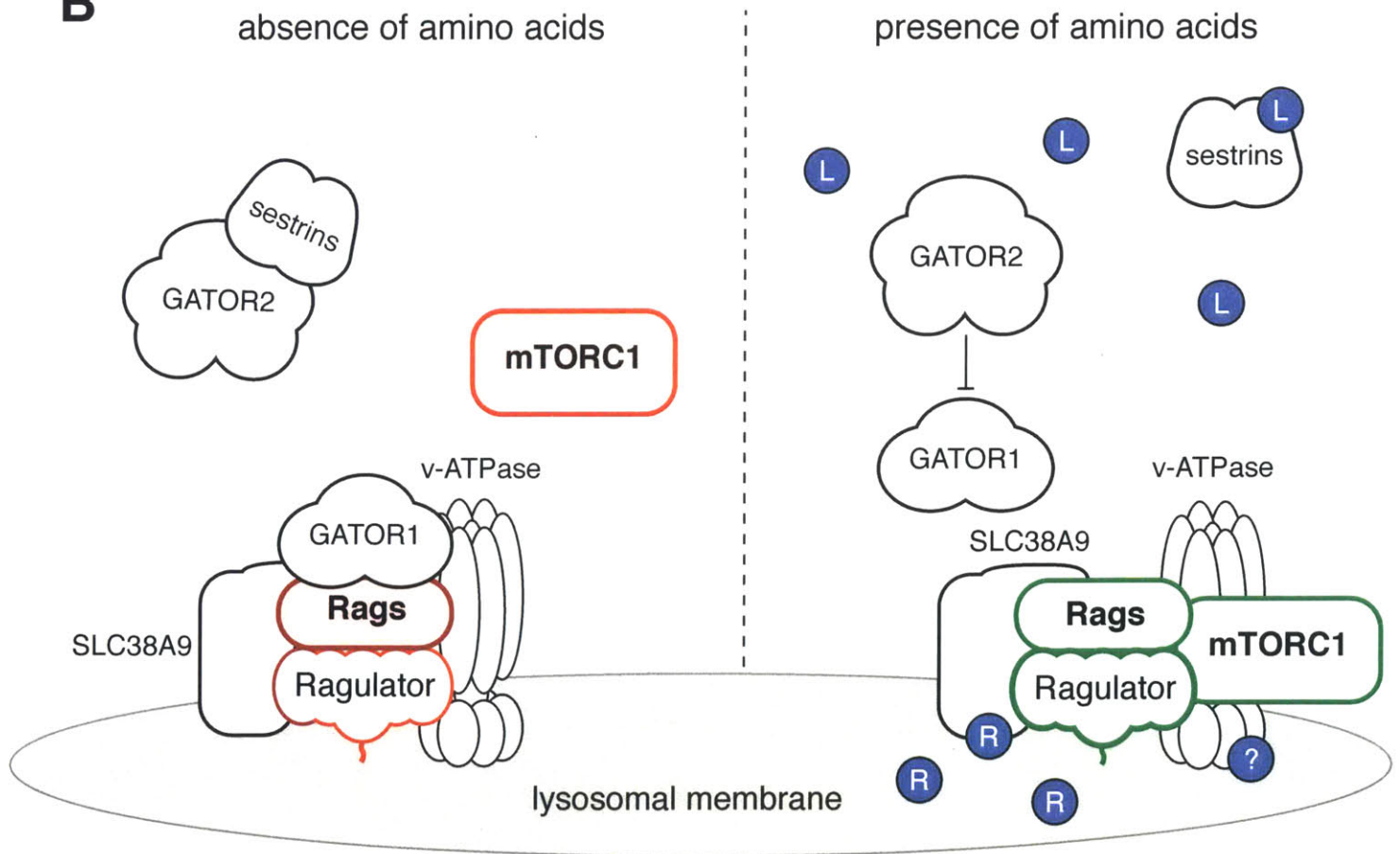


Figure 2: Regulation of mTORC1

A) Nutrients and growth factors are both required to activate mTORC1. Growth factors coupled with the absence of cellular stresses lead to the activation of mTORC1 through the small GTPase Rheb, which directly activates the kinase of mTOR within the complex. Nutrients act through the Heterodimeric Rag GTPases to promote mTORC1 localization to the lysosomal membrane, where it can interact with and be activated by Rheb.

B) Activation of mTORC1 by amino acids. In the absence of amino acids Sestrins are bound to GATOR2, relieving its inhibition upon GATOR1. Thus, GATOR1 can interact with and facilitate GTP hydrolysis in the RagA or RagB, preventing the Rag GTPases from recruiting mTORC1 to the lysosome. The absence of lysosomal amino acids simultaneously inhibits the GEF activity of Ragulator, likely because both SLC38A9 and the v-ATPase cannot induce activation of Ragulator. Upon stimulation with amino acids, Sestrins bind to cytosolic leucine (labeled as "L") and dissociate from GATOR2. Dissociation of Sestrins from GATOR2 leads to inhibition of the GAP activity of GATOR1; the inhibitory signal from GATOR1 to the Rag GTPases is relieved. Amino acids within the lysosomal lumen induce the activation of the GEF activity of Ragulator, through binding of arginine ("R") to SLC38A9 and some aspect of lysosomal amino acids (labeled "?") to the v-ATPase. Activated Ragulator facilitates nucleotide exchange in RagA and RagB, leading to an activated Rag conformation and recruitment of mTORC1 to the lysosomal membrane. The Ragulator-c17orf59 complex also exists on the lysosome.

late endosomal and lysosomal membranes (Menon et al., 2014), and mTORC1 localizes to these organelles in an amino acid- and glucose-dependent manner in order to be activated.

The Rag GTPases regulate mTORC1 localization and recruitment to lysosomes in response to intracellular nutrient availability (Sancak et al., 2008; Kim et al., 2008; Sancak et al., 2010). The Rags are small GTPases encoded by four separate genes (RRAGA, -B, -C, and -D; coding for RagA, -B, -C, and -D), which form heterodimers in which a single RagA or RagB protein is paired with a single RagC or RagD. The Rags localize to the cytosolic surface of the lysosomal membrane (Sancak et al., 2008; Sancak et al., 2010). Evidence suggests that the nucleotide-bound state of each Rag protein in the dimer tends to be opposite that of its partner (Sancak et al., 2008). In the absence of amino acids, the RagA/B component of the dimer binds GDP and the RagC/D component binds GTP, and the dimer does not bind mTORC1 and therefore cannot recruit it to the lysosome.

Within minutes of the addition of amino acids to the media of starved cells, the nucleotide-bound state is reversed such that RagA/B is GTP-bound and

RagC/D is GDP-bound, leading to the binding and lysosomal recruitment of mTORC1, where it can be activated by Rheb, downstream of growth factor signaling (Figure 2a). Expression of “active” Rag dimer mutants where RagA or B mimics the GTP-bound state (RagA/B^{GTP}) is sufficient to constitutively localize mTORC1 to the lysosomal membrane and activate mTORC1, even in the absence of amino acids. Conversely, mTORC1 activity is inhibited by “inactive” Rag mutant dimers consisting of RagA/B^{GDP} even when amino acids are present (Sancak et al., 2008; Kim et al., 2008).

B. The Ragulator complex and lysosomal regulation of mTORC1

The Ragulator complex maintains the Rags on the lysosome, and serves as a lysosomal docking site for the Rag dimers. Five proteins make up Ragulator: p18, p14, MP1, HBXIP, and c7orf59 (Wunderlich et al., 2001; Nada et al., 2009; Sancak et al., 2010; Bar-Peled et al., 2012; described in detail in Chapter 2). The complete Ragulator complex is required for mTORC1 activation by amino acids and for the appropriate lysosomal localization of the Rags and mTORC1. Loss of any component of Ragulator inhibits mTORC1 activation by amino acids and mis-localizes both the Rags and mTORC1 away from the lysosomes, even when amino acids are present (Sancak et al., 2010; Bar-Peled et al., 2012). Ragulator fulfills two major functions in mTORC1 activation: it acts as a scaffold and landing pad for the Rags and mTORC1 at the lysosome, and serves as the guanine nucleotide exchange factor (GEF) for RagA and RagB, activating the mTORC1 pathway in response to amino acids (Bar-Peled et al., 2012). Ragulator components and their identification will be the topic of Chapter 2, in which the characterization of HBXIP and c7orf59 are described.

Recently, the cellular mechanisms to regulate the nucleotide-bound state of the Rag GTPases and thus mTORC1 activation by amino acids through Ragulator have begun to be elucidated (Figure 2b). The GEF activity of Ragulator requires interaction with and signals from the vacuolar ATPase (v-

ATPase) at the lysosomal membrane (Zoncu et al., 2011a). While the molecular signal that the v-ATPase sends to Ragulator is unclear, it is apparent that lysosomal membrane integrity and the presence of amino acids within the lysosomal lumen are required for the activation of the v-ATPase-Ragulator-Rag pathway (Zoncu et al., 2011a).

Lysosomal amino acids also activate the Ragulator-Rag pathway through an interaction with another lysosomal transmembrane protein, SLC38A9. SLC38A9 interacts with the Rags and Ragulator and binds to arginine, likely from within the lumen of the lysosome, to promote the activation of the Rag GTPases and recruitment of mTORC1. The binding to arginine and regulation of mTORC1 localization by SLC38A9 indicates that the protein might be an amino acid sensor that signals through Ragulator and the Rag GTPases to activate mTORC1 (Wang et al. 2015).

C. Cytosolic regulation of mTORC1

While recent work indicates that the signal to recruit mTORC1 originates from the lysosome, there have also been advances in understanding the proteins that respond to cytosolic amino acids and inhibit mTORC1. In order to inactivate the RagA or RagB GTPase in the Rag heterodimer, the bound GTP must be hydrolyzed to GDP. A GTPase activating protein (GAP) facilitates this hydrolysis. The GAP for RagA/B is a complex of three proteins and named GATOR1 (“GAP Activity Towards the Rags”; composed of DEPDC5, Npr12 and Npr13) (Bar-Peled et al., 2013).

By promoting the hydrolysis of GTP to GDP in RagA or B, GATOR1 strongly inhibits mTORC1 signaling by preventing it from localizing to the lysosome. GATOR1 is inhibited by another complex of proteins, GATOR2 (composed of Mios, WDR24, WDR59, Seh1L, and Sec13). Both GATOR1 and GATOR2 are cytosolic, though they must interact with RagA/B at the lysosomal membrane (Bar-Peled et al., 2013). Cytosolic amino acid levels

control GATOR2 activity (i.e. inhibition of GATOR1 and activation of Rags and mTORC1).

Sestrins are cytosolic proteins that bind to GATOR2 and control its activity (Chantranupong et al., 2014). Sestrin1 and 2 bind to leucine directly, which regulates the Sestrin-GATOR2 interaction (Wolfson et al., 2015). Thus a decrease in cytosolic leucine (as in amino acid starvation) inhibits GATOR2, leading to the activation of GATOR1. Active GATOR1 inhibits the Rag GTPases and prevents mTORC1 from being recruited to the lysosome.

The combination of the GATOR and lysosomal mechanisms of controlling the nucleotide-bound state of the Rag GTPases indicates the emerging, complex regulation of mTORC1 by lysosomal and cytoplasmic amino acids (Figure 2b). It appears that positive signals, through the GEF activity of Ragulator, emanate from the lysosome and amino acids within the lysosomal lumen. Indeed, the presence of amino acids in the lumen of lysosomes is sufficient to recruit mTORC1 in a cell-free setting (Zoncu et al., 2011a). However, negative signals that inhibit the Rag GTPases and mTORC1 originate in the cytosol and utilize the GATOR1-GATOR2 complexes to induce RagA/B^{GDP} loading in cells.

D. Other mechanisms

In addition to the regulation of mTORC1 through its interaction with Rheb at the lysosome, mTORC1 can be inhibited by a handful of other mechanisms. The binding of the two mTORC1-contained inhibitors, PRAS40 and DEPTOR, is controlled independently of Rag or Rheb activity. As its name implies, PRAS40 is a substrate of Akt. Phosphorylation of PRAS40 by Akt, downstream of growth factor signaling and PI3K, leads to the release of inhibition. Upon phosphorylation, PRAS40 becomes a 14-3-3 substrate and is sequestered away from mTORC1 (Sancak et al., 2007; Vander Haar et al., 2007).

Similarly, the interaction of DEPTOR with mTORC1 (as well as mTORC2) is regulated at the protein level. There is an increase of DEPTOR mRNA levels

and protein stability following mTORC1 inactivation (Peterson et al., 2009). The mechanism of transcriptional control of DEPTOR by mTORC1 is not clear, but it was shown that DEPTOR is phosphorylated by mTORC1 or 2, which acts to prime the ubiquitination of DEPTOR by SCF/ β TrCP, which promotes its degradation (Duan et al., 2011; Gao et al., 2011; Zhao et al., 2011). This allows for a feed-forward loop in which mTORC1 can increase its own activity by degrading an mTORC1 inhibitor.

There are also phosphorylation events on mTORC1 itself that can alter pathway activation. One of these phosphorylation events is carried out by AMP-activated protein kinase (AMPK). AMPK responds to energy stress; when there is a decrease in the ATP:AMP ratio (indicating a decrease in cellular energy), AMPK is activated (Hardie, 2007). AMPK phosphorylates Raptor when activated, and this phosphorylation can inhibit mTORC1 via allosteric mechanisms. AMPK also phosphorylates TSC2, which impinges on Rheb activity. In all, AMPK and energy stress can inhibit mTORC1 in a variety of ways (Zoncu et al., 2011b).

mTORC1 as a sensor of nutritional status

Once active, mTORC1 controls a number of crucial cellular processes that contribute to growth, proliferation and metabolism. mTORC1 signaling increases the levels of building blocks that would be required for division, such as lipids and nucleotides, while also increasing ribosome activity and number. In contrast, under stress, such as nutrient or growth factor deprivation, mTORC1 is inactivated, leading to the inhibition of each of these processes. Not only does inactive mTORC1 cease to promote anabolism, but also loss of mTORC1 activity activates autophagy, restoring some level of nutrients to cells in a nutrient-deprived environment. Thus, mTORC1 inhibition by nutrient deprivation induces a catabolic state in which the cell attempts to rescue itself and re-activate mTORC1.

By acting as a coincidence detector that requires inputs from both nutrients and growth factors, mTORC1 is a sensor of the nutritional status of a cell. The nucleotide-bound state of the Rag GTPases reflects the intracellular and local nutrient environment; mTORC1 is recruited to lysosomes only when there is an abundance of amino acids and glucose available to a cell. This recruitment could be a cellular readout for the availability of building blocks required for cell division. mTORC1 activation also depends on the feeding status of an entire organism, which is reflected by growth factor levels. Growth factors are released following meals, which might serve as a signal for cells to proliferate and grow or become metabolically active. Thus, it is critical for a cell to integrate both local and global signals prior to activating mTORC1.

Functions and regulation of mTORC2

mTORC2 phosphorylates a number of proteins that control cellular survival, metabolism and proliferation, and regulates actin cytoskeletal organization and migration (Figure 1b). One major mTORC2 substrate is the protein kinase Akt/PKB. mTORC2 phosphorylates Akt at Ser-473 (Sarbossov et al., 2005), which is important for the complete activation of Akt, priming the protein for phosphorylation on its activation loop (Thr-308) by PDK1 downstream of phosphoinositide 3-kinase (PI3K) signaling (Scheid et al., 2002; Yang et al., 2002; Alessi et al., 1996). The phosphorylation of Akt on Ser-473 is important for the phosphorylation and modulation of FOXO1 and other factors such as glucokinase and SREBP1c by Akt, regulating apoptosis and cellular metabolism (Guertin et al., 2006; Hagiwara et al., 2012; Zhang et al., 2006). mTORC2 also phosphorylates other kinases of the same family as Akt, including the AGC kinases SGK and PKC. In addition, mTORC2 regulates the actin cytoskeleton, potentially through its phosphorylation of PKC, a function conserved to *S. cerevisiae* TORC2 (Sarbossov et al., 2004; Jacinto et al., 2004; Loewith et al., 2002).

While mTORC2 controls a number of important aspects of cellular survival and metabolism, the regulation of the kinase is not entirely clear. In metazoans, mTORC2 responds to insulin and other growth factors, downstream of PI3K, likely by virtue of the Pleckstrin-homology domains in mSin1 that can bind to PtdIns(3,4,5)P3 (PIP3), the output of PI3K (Liu et al., 2015). However, there are versions of mTORC2 (depending on the mSin1 isoform bound) that do not respond to insulin (Frias et al., 2006), indicating that there may be other mechanisms of activation of mTORC2. Additionally, TORC2 is conserved to *S. cerevisiae*, but yeast do not have any PI3K homologs, so other mechanisms to activate mTORC2 must be assumed to exist.

Conclusion

As a member of two complexes, mTOR is a central regulator growth and survival of the cell and organism. Nutrients, growth factors, and cellular stresses regulate mTORC1, which in turn promotes a number of anabolic processes and pathways while inhibiting autophagy, a major nutrient-responsive catabolic process. mTORC2 responds to growth factors and regulates other aspects of metabolism and survival, largely through its phosphorylation of Akt and other AGC kinases.

In this thesis, we will discuss the characterization of newly-identified proteins that interact with and regulate the amino acid-sensing pathway upstream of mTORC1. We identified two Ragulator-interacting proteins that we concluded to be new members of the Ragulator, allowing us to identify a novel role that the Ragulator plays in the activation of the Rag GTPases, namely by acting as a GEF for RagA. In addition, we characterized RagA-knockout mice and cells generated from these mice. RagA is required for embryonic development, but its loss leads aberrant, nutrient-insensitive activation of mTORC1 in cells derived from RagA-null embryos. In adult mice, loss of RagA can lead to a malignant expansion of monocytes. These advances help describe how mTORC1 is

activated in the presence of amino acids and what happens when this regulation is disrupted, but leave a number of questions open for the field to examine in the future.

REFERENCES

- Abraham RT, Wiederrecht GJ. Immunopharmacology of rapamycin. *Annu Rev Immunol.* 1996;14:483-510.
- Alessi DR, Andjelkovic M, Caudwell B, Cron P, Morrice N, Cohen P, Hemmings BA. Mechanism of activation of protein kinase B by insulin and IGF-1. *EMBO J.* 1996 Dec 2;15(23):6541-51.
- Bar-Peled L, Schweitzer LD, Zoncu R, Sabatini DM. Ragulator is a GEF for the rag GTPases that signal amino acid levels to mTORC1. *Cell.* 2012 Sep 14;150(6):1196-208.
- Bar-Peled L, Chantranupong L, Cherniack AD, Chen WW, Ottina KA, Grabiner BC, Spear ED, Carter SL, Meyerson M, Sabatini DM. A Tumor suppressor complex with GAP activity for the Rag GTPases that signal amino acid sufficiency to mTORC1. *Science.* 2013 May 31;340(6136):1100-6.
- Ben-Sahra I, Howell JJ, Asara JM, Manning BD. Stimulation of de novo pyrimidine synthesis by growth signaling through mTOR and S6K1. *Science.* 2013 Mar 15;339(6125):1323-8.
- Brown EJ, Albers MW, Shin TB, Ichikawa K, Keith CT, Lane WS, Schreiber SL. A mammalian protein targeted by G1-arresting rapamycin-receptor complex. *Nature.* 1994 Jun 30;369(6483):756-8.
- Chantranupong L, Wolfson RL, Orozco JM, Saxton RA, Scaria SM, Bar-Peled L, Spooner E, Isasa M, Gygi SP, Sabatini DM. The Sestrins interact with GATOR2 to negatively regulate the amino-acid-sensing pathway upstream of mTORC1. *Cell Rep.* 2014 Oct 9;9(1):1-8.
- Duan S, Skaar JR, Kuchay S, Toschi A, Kanarek N, Ben-Neriah Y, Pagano M. mTOR generates an auto-amplification loop by triggering the β TrCP- and CK1 α -dependent degradation of DEPTOR. *Mol Cell.* 2011 Oct 21;44(2):317-24.
- Dunlop EA, Tee AR. mTOR and autophagy: a dynamic relationship governed by nutrients and energy. *Semin Cell Dev Biol.* 2014 Dec;36:121-9.
- Düvel K, Yecies JL, Menon S, Raman P, Lipovsky AI, Souza AL, Triantafellow E, Ma Q, Gorski R, Cleaver S, Vander Heiden MG, MacKeigan JP, Finan PM, Clish CB, Murphy LO, Manning BD. Activation of a metabolic gene regulatory network downstream of mTOR complex 1. *Mol Cell.* 2010 Jul 30;39(2):171-83.

Efeyan A, Zoncu R, Chang S, Gumper I, Snitkin H, Wolfson RL, Kirak O, Sabatini DD, Sabatini DM. Regulation of mTORC1 by the Rag GTPases is necessary for neonatal autophagy and survival. *Nature*. 2013 Jan 31;493(7434):679-83.

Fonseca BD, Smith EM, Lee VH, MacKintosh C, Proud CG. PRAS40 is a target for mammalian target of rapamycin complex 1 and is required for signaling downstream of this complex. *J Biol Chem*. 2007 Aug 24;282(34):24514-24.

Frias MA, Thoreen CC, Jaffe JD, Schroder W, Sculley T, Carr SA, Sabatini DM. mSin1 is necessary for Akt/PKB phosphorylation, and its isoforms define three distinct mTORC2s. *Curr Biol*. 2006 Sep 19;16(18):1865-70.

Gao D, Inuzuka H, Tan MK, Fukushima H, Locasale JW, Liu P, Wan L, Zhai B, Chin YR, Shaik S, Lyssiotis CA, Gygi SP, Toker A, Cantley LC, Asara JM, Harper JW, Wei W. mTOR drives its own activation via SCF(β TrCP)-dependent degradation of the mTOR inhibitor DEPTOR. *Mol Cell*. 2011 Oct 21;44(2):290-303.

Garami A, Zwartkuis FJ, Nobukuni T, Joaquin M, Roccio M, Stocker H, Kozma SC, Hafen E, Bos JL, Thomas G. Insulin activation of Rheb, a mediator of mTOR/S6K/4E-BP signaling, is inhibited by TSC1 and 2. *Mol Cell*. 2003 Jun;11(6):1457-66.

Gomes AP, Blenis J. A nexus for cellular homeostasis: the interplay between metabolic and signal transduction pathways. *Curr Opin Biotechnol*. 2015 Aug;34:110-7.

Guertin DA, Stevens DM, Thoreen CC, Burds AA, Kalaany NY, Moffat J, Brown M, Fitzgerald KJ, Sabatini DM. Ablation in mice of the mTORC components raptor, rictor, or mLST8 reveals that mTORC2 is required for signaling to Akt-FOXO and PKC α , but not S6K1. *Dev Cell*. 2006 Dec;11(6):859-71.

Hagiwara A, Cornu M, Cybulski N, Polak P, Betz C, Trapani F, Terracciano L, Heim MH, Rüegg MA, Hall MN. Hepatic mTORC2 activates glycolysis and lipogenesis through Akt, glucokinase, and SREBP1c. *Cell Metab*. 2012 May 2;15(5):725-38.

Hara K, Maruki Y, Long X, Yoshino K, Oshiro N, Hidayat S, Tokunaga C, Avruch J, Yonezawa K. Raptor, a binding partner of target of rapamycin (TOR), mediates TOR action. *Cell*. 2002 Jul 26;110(2):177-89.

Hara K, Yonezawa K, Weng QP, Kozlowski MT, Belham C, Avruch J. Amino acid sufficiency and mTOR regulate p70 S6 kinase and eIF-4E BP1 through a common effector mechanism *J Biol Chem*. 1998 Jun 5;273(23):14484-94.

Hardie, D. G. AMP-activated/SNF1 protein kinases: conserved guardians of cellular energy. *Nature Rev. Mol. Cell Biol.* 8, 774–785 (2007).

Horton JD, Goldstein JL, Brown MS. SREBPs: activators of the complete program of cholesterol and fatty acid synthesis in the liver. *J Clin Invest.* 2002 May;109(9):1125-31.

Howell JJ, Ricoult SJ, Ben-Sahra I, Manning BD. A growing role for mTOR in promoting anabolic metabolism. *Biochem Soc Trans.* 2013 Aug;41(4):906-12.

Iadevaia V, Liu R, Proud CG. mTORC1 signaling controls multiple steps in ribosome biogenesis. *Semin Cell Dev Biol.* 2014 Dec;36:113-20.

Inoki K, Li Y, Zhu T, Wu J, Guan KL. TSC2 is phosphorylated and inhibited by Akt and suppresses mTOR signalling. *Nat Cell Biol.* 2002 Sep;4(9):648-57.

Inoki K, Li Y, Xu T, Guan KL. Rheb GTPase is a direct target of TSC2 GAP activity and regulates mTOR signaling. *Genes Dev.* 2003 Aug 1;17(15):1829-34.

Jacinto E, Loewith R, Schmidt A, Lin S, Ruegg MA, Hall A, Hall MN. Mammalian TOR complex 2 controls the actin cytoskeleton and is rapamycin insensitive. *Nat Cell Biol.* 2004 Nov;6(11):1122-8.

Jewell JL, Russell RC, Guan KL. Amino acid signalling upstream of mTOR. *Nat Rev Mol Cell Biol.* 2013 Mar;14(3):133-9.

Kim DH, Sarbassov DD, Ali SM, King JE, Latek RR, Erdjument-Bromage H, Tempst P, Sabatini DM. mTOR interacts with raptor to form a nutrient-sensitive complex that signals to the cell growth machinery. *Cell.* 2002 Jul 26;110(2):163-75.

Kim DH, Sarbassov DD, Ali SM, Latek RR, Guntur KV, Erdjument-Bromage H, Tempst P, Sabatini DM. GbetaL, a positive regulator of the rapamycin-sensitive pathway required for the nutrient-sensitive interaction between raptor and mTOR. *Mol Cell.* 2003 Apr;11(4):895-904.

Kim, E., Goraksha-Hicks, P., Li, L., Neufeld, T.P. and Guan, K.L. Regulation of TORC1 by Rag GTPases in nutrient response. *Nat Cell Biol.* 2008 Aug;10(8):935-45.

Kunz J, Henriquez R, Schneider U, Deuter-Reinhard M, Movva NR, Hall MN. Target of rapamycin in yeast, TOR2, is an essential phosphatidylinositol kinase homolog required for G1 progression. *Cell.* 1993 May 7;73(3):585-96.

Laplante M, Sabatini DM. mTOR signaling in growth control and disease. *Cell*. 2012 Apr 13;149(2):274-93.

Liu P, Gan W, Chin YR, Ogura K, Guo J, Zhang J, Wang B, Blenis J, Cantley LC, Toker A, Su B, Wei W. PtdIns(3,4,5)P₃-Dependent Activation of the mTORC2 Kinase Complex. *Cancer Discov*. 2015 Nov;5(11):1194-209.

Loewith R, Jacinto E, Wullschlegel S, Lorberg A, Crespo JL, Bonenfant D, Oppliger W, Jenoe P, Hall MN. Two TOR complexes, only one of which is rapamycin sensitive, have distinct roles in cell growth control. *Mol Cell*. 2002 Sep;10(3):457-68.

(a) Long X, Lin Y, Ortiz-Vega S, Yonezawa K, Avruch J. Rheb binds and regulates the mTOR kinase. *Curr Biol*. 2005 Apr 26;15(8):702-13.

(b) Long X, Ortiz-Vega S, Lin Y, Avruch J. Rheb binding to mammalian target of rapamycin (mTOR) is regulated by amino acid sufficiency. *J Biol Chem*. 2005 Jun 24;280(25):23433-6.

Lynch CJ, Fox HL, Vary TC, Jefferson LS, Kimball SR. Regulation of amino acid-sensitive TOR signaling by leucine analogues in adipocytes. *J Cell Biochem*. 2000 Mar;77(2):234-51.

Magnuson B, Ekim B, Fingar DC. Regulation and function of ribosomal protein S6 kinase (S6K) within mTOR signalling networks. *Biochem J*. 2012 Jan 1;441(1):1-21.

Manning BD, Tee AR, Logsdon MN, Blenis J, Cantley LC. Identification of the tuberous sclerosis complex-2 tumor suppressor gene product tuberlin as a target of the phosphoinositide 3-kinase/akt pathway. *Mol Cell*. 2002 Jul;10(1):151-62.

Mamane Y, Petroulakis E, LeBacquer O, Sonenberg N. mTOR, translation initiation and cancer. *Oncogene*. 2006 Oct 16;25(48):6416-22.

Menon S, Dibble CC, Talbott G, Hoxhaj G, Valvezan AJ, Takahashi H, Cantley LC, Manning BD. Spatial control of the TSC complex integrates insulin and nutrient regulation of mTORC1 at the lysosome. *Cell*. 2014 Feb 13;156(4):771-85.

Nada S, Hondo A, Kasai A, Koike M, Saito K, Uchiyama Y, Okada M. The novel lipid raft adaptor p18 controls endosome dynamics by anchoring the MEK-ERK pathway to late endosomes. *EMBO J*. 2009 Mar 4;28(5):477-89.

Nazio F, Strappazzon F, Antonioli M, Bielli P, Cianfanelli V, Bordi M, Gretzmeier C, Dengjel J, Piacentini M, Fimia GM, Cecconi F. mTOR inhibits autophagy by controlling ULK1 ubiquitylation, self-association and function through AMBRA1 and TRAF6. *Nat Cell Biol.* 2013 Apr;15(4):406-16.

Nobukuni T, Joaquin M, Roccio M, Dann SG, Kim SY, Gulati P, Byfield MP, Backer JM, Natt F, Bos JL, Zwartkruis FJ, Thomas G. Amino acids mediate mTOR/raptor signaling through activation of class 3 phosphatidylinositol 3OH-kinase. *Proc Natl Acad Sci U S A.* 2005 Oct 4;102(40):14238-43.

Oshiro N, Takahashi R, Yoshino K, Tanimura K, Nakashima A, Eguchi S, Miyamoto T, Hara K, Takehana K, Avruch J, Kikkawa U, Yonezawa K. The proline-rich Akt substrate of 40 kDa (PRAS40) is a physiological substrate of mammalian target of rapamycin complex 1. *J Biol Chem.* 2007 Jul 13;282(28):20329-39.

Pearce LR, Huang X, Boudeau J, Pawłowski R, Wullschleger S, Deak M, Ibrahim AF, Gourlay R, Magnuson MA, Alessi DR. Identification of Protor as a novel Rictor-binding component of mTOR complex-2. *Biochem J.* 2007 Aug 1;405(3):513-22.

Pearce LR, Sommer EM, Sakamoto K, Wullschleger S, Alessi DR. Protor-1 is required for efficient mTORC2-mediated activation of SGK1 in the kidney. *Biochem J.* 2011 May 15;436(1):169-79.

Peterson TR, Laplante M, Thoreen CC, Sancak Y, Kang SA, Kuehl WM, Gray NS, Sabatini DM. DEPTOR is an mTOR inhibitor frequently overexpressed in multiple myeloma cells and required for their survival. *Cell.* 2009 May 29;137(5):873-86.

Peterson TR, Sengupta SS, Harris TE, Carmack AE, Kang SA, Balderas E, Guertin DA, Madden KL, Carpenter AE, Finck BN, Sabatini DM. mTOR complex 1 regulates lipin 1 localization to control the SREBP pathway. *Cell.* 2011 Aug 5;146(3):408-20.

Sabatini DM, Erdjument-Bromage H, Lui M, Tempst P, Snyder SH. RAFT1: a mammalian protein that binds to FKBP12 in a rapamycin-dependent fashion and is homologous to yeast TORs. *Cell.* 1994 Jul 15;78(1):35-43.

Sabers CJ, Martin MM, Brunn GJ, Williams JM, Dumont FJ, Wiederrecht G, Abraham RT. Isolation of a protein target of the FKBP12-rapamycin complex in mammalian cells. *J Biol Chem.* 1995 Jan 13;270(2):815-22.

Sancak Y, Bar-Peled L, Zoncu R, Markhard AL, Nada S, Sabatini DM. Ragulator-Rag complex targets mTORC1 to the lysosomal surface and is necessary for its activation by amino acids. *Cell*. 2010 Apr 16;141(2):290-303.

Sancak Y, Peterson TR, Shaul YD, Lindquist RA, Thoreen CC, Bar-Peled L, Sabatini DM. The Rag GTPases bind raptor and mediate amino acid signaling to mTORC1. *Science*. 2008 Jun 13;320(5882):1496-501.

Sancak Y, Thoreen CC, Peterson TR, Lindquist RA, Kang SA, Spooner E, Carr SA, Sabatini DM. PRAS40 is an insulin-regulated inhibitor of the mTORC1 protein kinase. *Mol Cell*. 2007 Mar 23;25(6):903-15.

Sarbassov DD, Ali SM, Kim DH, Guertin DA, Latek RR, Erdjument-Bromage H, Tempst P, Sabatini DM. Rictor, a novel binding partner of mTOR, defines a rapamycin-insensitive and raptor-independent pathway that regulates the cytoskeleton. *Curr Biol*. 2004 Jul 27;14(14):1296-302.

Sarbassov DD, Guertin DA, Ali SM, Sabatini DM. Phosphorylation and regulation of Akt/PKB by the rictor-mTOR complex. *Science*. 2005 Feb 18;307(5712):1098-101.

Scheid MP, Marignani PA, Woodgett JR. Multiple phosphoinositide 3-kinase-dependent steps in activation of protein kinase B. *Mol Cell Biol*. 2002 Sep;22(17):6247-60.

Sehgal SN, Bansbach CC. Rapamycin: in vitro profile of a new immunosuppressive macrolide. *Ann N Y Acad Sci*. 1993 Jun 23;685:58-67.

Shimobayashi M, Hall MN. Making new contacts: the mTOR network in metabolism and signalling crosstalk. *Nat Rev Mol Cell Biol*. 2014 Mar;15(3):155-62.

Smith, EM, Finn, SG, Tee, AR, Browne, GJ and Proud, CG. The tuberous sclerosis protein TSC2 is not required for the regulation of the mammalian target of rapamycin by amino acids and certain cellular stresses. *J Biol Chem*. 2005 May 13;280(19):18717-27.

Thedieck K, Polak P, Kim ML, Molle KD, Cohen A, Jenö P, Arriemerlou C, Hall MN. PRAS40 and PRR5-like protein are new mTOR interactors that regulate apoptosis. *PLoS One*. 2007 Nov 21;2(11):e1217.

Thoreen CC, Chantranupong L, Keys HR, Wang T, Gray NS, Sabatini DM. A unifying model for mTORC1-mediated regulation of mRNA translation. *Nature*. 2012 May 2;485(7396):109-13.

Vander Haar E, Lee SI, Bandhakavi S, Griffin TJ, Kim DH. Insulin signalling to mTOR mediated by the Akt/PKB substrate PRAS40. *Nat Cell Biol.* 2007 Mar;9(3):316-23.

Vézina C, Kudelski A, Sehgal SN. Rapamycin (AY-22,989), a new antifungal antibiotic. I. Taxonomy of the producing streptomycete and isolation of the active principle. *J Antibiot (Tokyo).* 1975 Oct;28(10):721-6.

Wang L, Harris TE, Roth RA, Lawrence JC Jr. PRAS40 regulates mTORC1 kinase activity by functioning as a direct inhibitor of substrate binding. *J Biol Chem.* 2007 Jul 6;282(27):20036-44.

Wang S, Tsun ZY, Wolfson RL, Shen K, Wyant GA, Plovanich ME, Yuan ED, Jones TD, Chantranupong L, Comb W, Wang T, Bar-Peled L, Zoncu R, Straub C, Kim C, Park J, Sabatini BL, Sabatini DM. Lysosomal amino acid transporter SLC38A9 signals arginine sufficiency to mTORC1. *Science.* 2015 Jan 9;347(6218):188-94.

Wolfson RL, Chantranupong L, Saxton RA, Shen K, Scaria SM, Cantor JR, Sabatini DM. Sestrin2 is a leucine sensor for the mTORC1 pathway. *Science.* 2015 Oct 8. pii: aab2674.

Wunderlich W, Fialka I, Teis D, Alpi A, Pfeifer A, Parton RG, Lottspeich F, Huber LA. A novel 14-kilodalton protein interacts with the mitogen-activated protein kinase scaffold mp1 on a late endosomal/lysosomal compartment. *J Cell Biol.* 2001 Feb 19;152(4):765-76.

Yang J, Cron P, Thompson V, Good VM, Hess D, Hemmings BA, Barford D. Molecular mechanism for the regulation of protein kinase B/Akt by hydrophobic motif phosphorylation. *Mol Cell.* 2002 Jun;9(6):1227-40.

Yang Q, Inoki K, Ikenoue T, Guan KL. Identification of Sin1 as an essential TORC2 component required for complex formation and kinase activity. *Genes Dev.* 2006 Oct 15;20(20):2820-32.

Zhang W, Patil S, Chauhan B, Guo S, Powell DR, Le J, Klotsas A, Matika R, Xiao X, Franks R, Heidenreich KA, Sajan MP, Farese RV, Stolz DB, Tso P, Koo SH, Montminy M, Unterman TG. FoxO1 regulates multiple metabolic pathways in the liver: effects on gluconeogenic, glycolytic, and lipogenic gene expression. *J Biol Chem.* 2006 Apr 14;281(15):10105-17.

Zhang Y, Gao X, Saucedo LJ, Ru B, Edgar BA, Pan D. Rheb is a direct target of the tuberous sclerosis tumour suppressor proteins. *Nat Cell Biol.* 2003 Jun;5(6):578-81.

Zhang Y, Nicholatos J, Dreier JR, Ricoult SJ, Widenmaier SB, Hotamisligil GS, Kwiatkowski DJ, Manning BD. Coordinated regulation of protein synthesis and degradation by mTORC1. *Nature.* 2014 Sep 18;513(7518):440-3.

Zhao Y, Xiong X, Sun Y. DEPTOR, an mTOR inhibitor, is a physiological substrate of SCF(β TrCP) E3 ubiquitin ligase and regulates survival and autophagy. *Mol Cell.* 2011 Oct 21;44(2):304-16.

(a) Zoncu R, Bar-Peled L, Efeyan A, Wang S, Sancak Y, Sabatini DM. mTORC1 senses lysosomal amino acids through an inside-out mechanism that requires the vacuolar H(+)-ATPase. *Science.* 2011 Nov 4;334(6056):678-83.

(b) Zoncu R, Efeyan A, Sabatini DM. mTOR: from growth signal integration to cancer, diabetes and ageing. *Nat Rev Mol Cell Biol.* 2011 Jan;12(1):21-35.

CHAPTER 2

Identification of HBXIP and c7orf59 as members of Ragulator

Lawrence D. Schweitzer¹, Liron Bar-Peled¹ and David M. Sabatini^{1,2}

¹ Whitehead Institute for Biomedical Research and Massachusetts Institute of Technology, Department of Biology, Nine Cambridge Center, Cambridge, MA 02142

² Howard Hughes Medical Institute, Department of Biology, Massachusetts Institute of Technology, Cambridge, MA 02139

This work has been published in:

Ragulator is a GEF for the rag GTPases that signal amino acid levels to mTORC1. Bar-Peled L, Schweitzer LD, Zoncu R, Sabatini DM. *Cell*. 2012 Sep 14;150(6):1196-208.

Experiments in Figure 1a and 1b were performed by LDS and Figure 1c by LBP

Experiments in Figure 2a and 2b were performed by LDS and Figure 2c and 2d by LBP

Analysis and illustration in Figure 3 were performed by LDS

Experiments in Figure 4 were performed by LBP except Figure 4e, by LDS

Experiments in Figure 5 were performed by LBP except Figure 5b, by LDS

Experiments in Figure 6 were performed by LBP

INTRODUCTION

mTORC1 regulates a number of important anabolic and catabolic processes promoting cellular growth and proliferation. These processes include mRNA translation, lipid biosynthesis, nucleotide biosynthesis, and mitochondrial biogenesis and function (Zoncu et al., 2011; Laplante and Sabatini, 2012). Because mTORC1 is a central node controlling a myriad of vital cellular functions, the cell tightly controls its activity. The complex responds generally to the health status of a cell; mTORC1 is inhibited by nutrient deprivation and intracellular stress, and is potently activated by growth factors.

In order to be activated, mTORC1 requires the presence of both nutrients (including amino acids and glucose) and growth factors, such as insulin. In the absence of one of these two inputs, mTORC1 is completely inhibited. This is because activation of mTORC1 requires its interaction with two different GTPases: the Rag GTPases and Rheb. When growth factors are present, Rheb is bound to GTP and can potently activate mTOR's kinase. Signaling through the phosphatidylinositol-3-kinase (PI3K)-Akt pathway inactivates the Tuberous Sclerosis Complex proteins (TSC), the GTPase activating protein (GAP) for Rheb, leading to activation of Rheb (Zoncu et al., 2011; Laplante and Sabatini, 2012; Dibble et al., 2015).

However, activated, GTP-bound Rheb is not sufficient to activate mTORC1 alone, due to its subcellular localization. Rheb resides on the cytosolic side of the lysosomal membrane (Menon et al., 2014) and in order for mTORC1 to interact with Rheb, it must localize to the lysosomal membrane. Nutrients, mainly amino acids, control the localization of mTORC1 through activation of the Rag GTPases. The Rag GTPases are obligate heterodimers in which a single RagA or RagB is bound to a single RagC or RagD (Sancak et al., 2008). In the heterodimer, it appears that each GTPase is oppositely-loaded, so when RagA/B is bound to GTP (RagA/B^{GTP}), RagC/D is GDP-bound, and vice-versa. RagA^{GTP}

is sufficient to recruit mTORC1 to the lysosome and activate the pathway when growth factor signaling is present (Sancak et al., 2008).

While the Rag GTPases localize constitutively to the cytosolic side of the lysosomal membrane, no targeting sequences that determine this localization have been found. Instead, they rely on a scaffolding complex named Ragulator, which is composed of five proteins: p18, p14, and MP1 (Sancak et al., 2010) and two others that will be described here. MP1 and p14 form an obligate heterodimer that is maintained at the lysosome by p18, which is docked at the lysosomal membrane by lipid modifications at its N-terminus targeting it to the lysosomal membrane (Wunderlich et al., 2001; Teis et al., 2002; Nada et al., 2008).

Here, we show that HBXIP is a Ragulator-interacting protein and is required for activation of mTORC1 by amino acids and the lysosomal localization of the Rag GTPases as well as mTORC1. In addition, the structure of HBXIP allowed us to make two important conclusions: that HBXIP is very similar to Ragulator components in tertiary structure and that HBXIP must be bound to another small protein. We identified c7orf59 as the binding partner of HBXIP. Because the HBXIP/c7orf59 dimer appears very similar to the p14/MP1 dimer, we concluded that HBXIP and c7orf59 are in fact components of Ragulator. Importantly, this pentameric Ragulator (p18, p14, MP1, HBXIP, c7orf59) is able to bind to the Rag GTPases *in vitro* and also exhibits guanine nucleotide exchange factor (GEF) activity towards RagA and B, activating the amino acid-sensing arm of the mTORC1 pathway.

RESULTS

Following the identification of Rag GTPases and Ragulator as the lysosomal targeting module and scaffold for mTORC1, we aimed to identify whether Ragulator or other Rag-interacting proteins had any regulatory function in addition to scaffolding the Rag GTPases to the lysosome. To address this possibility, we undertook an unbiased, proteomic approach to identify new Ragulator-interacting proteins.

This proteomic approach had been successfully used in the past to identify the other components of the amino acid sensing pathway, as well as the mTORC1 and mTORC2 subunits (Sabatini et al., 1994; Kim et al., 2002; Sarbossov et al., 2004; Sancak et al., 2008; Sancak et al., 2010). We immunopurified p18 or p14 from HEK-293T cells stably expressing epitope-tagged Rag GTPases or Ragulator components and subjected the IP's to mass spectrometry. Among the proteins that had corresponding peptides in the immunopurifications, Hepatitis B X-protein Interacting Protein (HBXIP) was strongly enriched in all Ragulator purifications. We decided to validate it as a Ragulator-interacting protein that may be important for the Rag-Ragulator interaction.

HBXIP is a novel Ragulator-interacting protein

In order to validate the IP/MS data and confirm that HBXIP indeed binds to Rags and Ragulator we transiently expressed the cDNA for FLAG-tagged Ragulator subunits p14 or p18, RagB or Methionine aminopeptidase 2 (Metap2, a control protein) in HEK 293T cells, with HA-tagged HBXIP co-expressed in all samples. HA-HBXIP co-immunopurifies with p14, p18 and RagB (Figure 1A). Transiently-expressed, FLAG-tagged HBXIP also co-immunoprecipitated cellular Ragulator components p14 and p18 in addition to RagA and RagC (Figure 1B).

Figure 1: HBXIP is a Ragulator-interacting protein

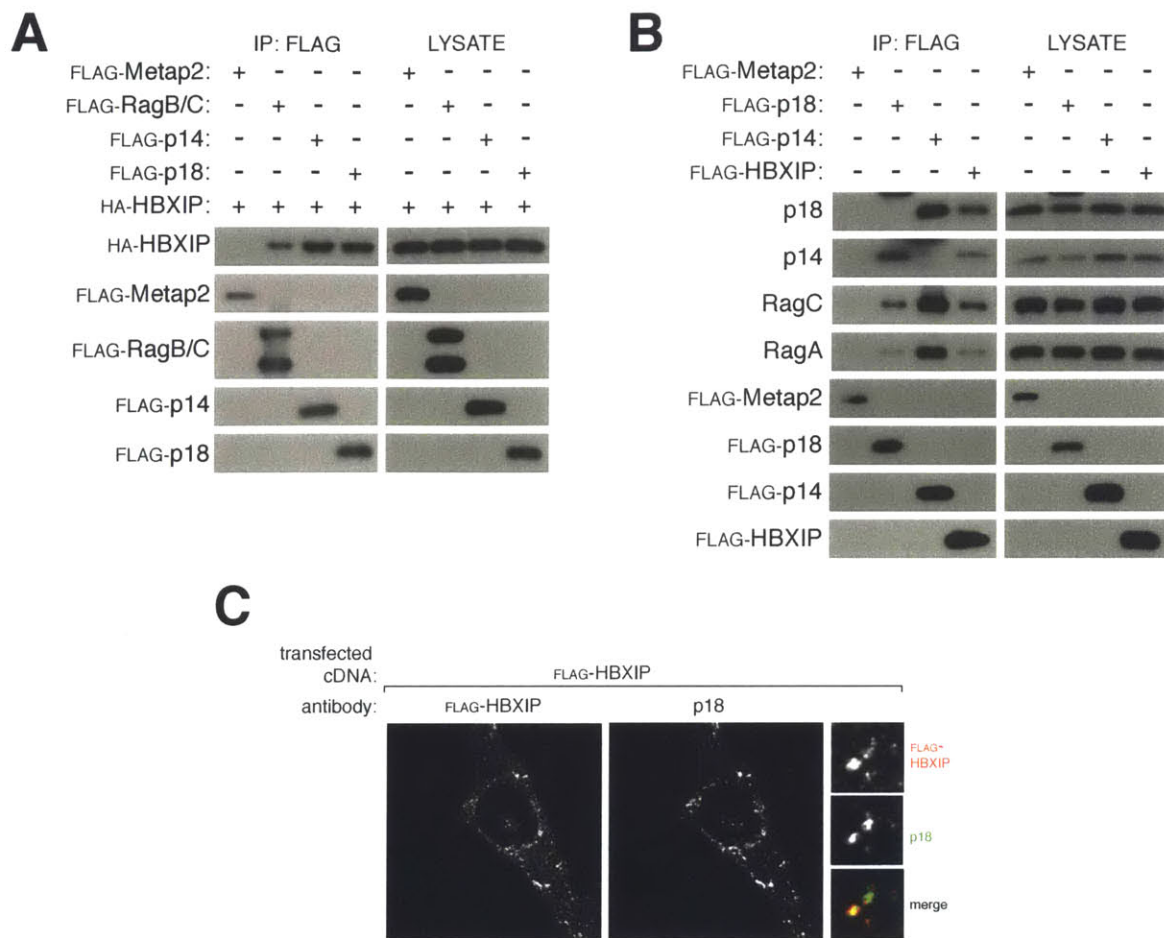


Figure 1: HBXIP is a Ragulator-interacting protein

A) Recombinant Rag GTPases and Ragulator subunits co-immunoprecipitate recombinant HBXIP. Transiently-expressed, FLAG-tagged Rag GTPases, p14, p18 or a control protein (Metap2) were immunoprecipitated from HEK-293T cells that were transiently expressing HA-tagged HBXIP. Immunoprecipitates and whole cell lysates were analyzed by immunoblotting for the indicated proteins.

B) Recombinant HBXIP co-immunoprecipitates Ragulator and Rag GTPases. Transiently-expressed epitope-tagged HBXIP, p14, p18, or a control protein (Metap2) were immunoprecipitated from HEK-293T cells. Immunoprecipitates and whole cell lysates were analyzed by immunoblotting for the indicated proteins.

C) Recombinant HBXIP co-localizes with p18. HEK-293T cells were transfected with the FLAG-HBXIP cDNA, fixed and immunostained with antibodies against the FLAG-epitope tag (pseudo-colored red) and p18 (green) and imaged using confocal microscopy. Insets represent selected fields that have been magnified as well as the overlay of the fields.

Similarly to Ragulator, which localizes to the lysosomal membrane (Sancak et al., 2010), transiently-expressed, epitope-tagged HBXIP co-localizes with p18 at lysosomes in HEK-293T cells (Figure 1C). These data confirm that HBXIP is a Ragulator-interacting protein and that it co-localizes with Ragulator at the lysosome.

Knockdown of HBXIP inhibits mTORC1 activation by amino acids

Next we examined whether HBXIP is required for mTORC1 activation by amino acids. HEK-293T cells expressing two separate short hairpin RNAs (shRNAs) targeting HBXIP were assayed for their mTORC1 activation upon stimulation with amino acids, compared to an shRNA targeting either GFP or p14 (negative and positive controls, respectively), by monitoring the phosphorylation of the mTORC1 substrate S6K1. Cells expressing shRNA targeting HBXIP displayed blunted mTORC1 activation, comparable to mTORC1 inhibition due to p14 knockdown (Figure 2A).

We also tested knockdown of the HBXIP ortholog in *Drosophila melanogaster*, CG14812, which contains 50% similarity to the coding sequence in humans. *Drosophila* S2 cells expressing double stranded RNA (dsRNA) targeting dHBXIP had inhibited dTORC1 activation, as indicated by

phosphorylation of dS6K1 (Figure 2B). Thus, HBXIP is required for mTORC1 activation by amino acids, and this function is conserved to *Drosophila*.

HBXIP is required for both Rag and mTORC1 localization to lysosomes

While knockdown of HBXIP inhibits activation of mTORC1 by amino acids, this does not indicate that HBXIP participates in the amino acid-sensing pathway upstream of mTORC1. The hallmark of the amino acid-sensing arm is the recruitment of mTOR to the lysosome by amino acids; inhibition or modulation of this pathway would prevent mTORC1 from reaching Rheb at the lysosomal membrane. In control cells, mTORC1 is cytoplasmic during amino acid starvation, but translocates to lysosomes upon stimulation with amino acids. RNAi-mediated knockdown of HBXIP, using small interfering RNA (siRNA), prevented the amino acid-mediated recruitment of mTOR to lysosomes (Figure 2C). This indicates that not only does HBXIP bind to the Rag GTPases and Ragulator, but it is required for the Rag GTPases to recruit mTORC1 to lysosomes.

There are two manners in which loss of HBXIP could inhibit the lysosomal recruitment of mTORC1: HBXIP knockdown could alter the Rag nucleotide-bound state such that the Rag GTPases fail to recruit mTORC1 or alternatively could prevent the Rag GTPases from localizing the lysosome. In order to determine which step HBXIP knockdown likely affects, we examined RagA localization in cells expressing the siRNA targeting HBXIP. In control cells, RagA is localized to lysosomes, as expected, but knockdown of HBXIP results in a diffuse, non-lysosomal localization of RagA (Figure 2D).

Figure 2: HBXIP is required for mTORC1 activation by amino acids and Rag GTPase lysosomal localization

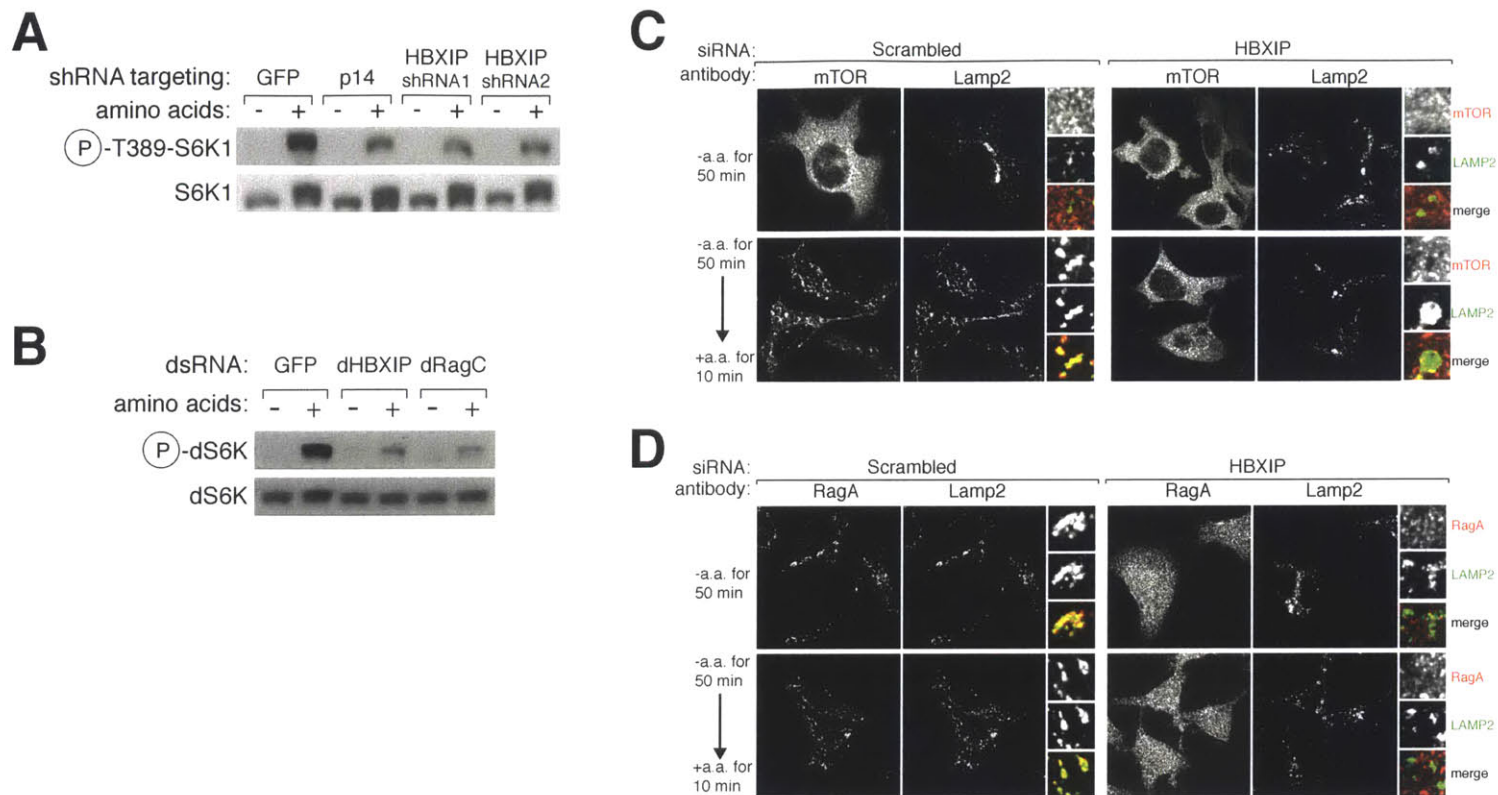


Figure 2: HBXIP is required for mTORC1 activation by amino acids and Rag GTPase lysosomal localization

A) Knockdown of HBXIP inhibits mTORC1 activation by amino acids. HEK-293T cells stably expressing shRNA's targeting HBXIP, p14 or GFP (control) were starved of amino acids for one hour or starved of amino acids for one hour and re-stimulated with amino acids for 10 minutes. Lysates were analyzed by immunoblotting for the indicated proteins.

B) Drosophila homolog of HBXIP is required for TORC1 activity in S2 cells. Drosophila S2 cells were transfected with dsRNAs targeting dHBXIP, dRagC or GFP (control). Cells were starved of amino acids for 90 or starved of amino acids for 90 minutes and re-stimulated with amino acids for 30 minutes. Lysates were analyzed by immunoblotting for the indicated proteins.

C) Knockdown of HBXIP inhibits amino acid-mediated lysosomal localization of mTOR. HEK-293T cells were transfected with a control siRNA or siRNA targeting HBXIP, starved of amino acids for 50 minutes or starved and re-stimulated with amino acids for 10 minutes, stained for mTOR (pseudo-colored red) and LAMP2 (green) and imaged using confocal microscopy. Insets represent selected fields that have been magnified as well as the overlay of the fields.

D) Knockdown of HBXIP leads to cytoplasmic localization of RagA. HEK-293T cells were transfected with a control siRNA or siRNA targeting HBXIP and treated and imaged as in (C), staining for RagA (red) and LAMP2 (green).

HBXIP contains a roadblock domain

We turned to the published crystal structure of HBXIP to potentially uncover the molecular mechanism of its interaction with Ragulator and the Rag GTPases. Interestingly, HBXIP is composed almost entirely of a motif known as a “roadblock domain” (Garcia-Saez et al., 2011). This domain has been associated with modulation of GTPases and NTPases, from bacteria to mammals (Koonin and Aravind, 2000; Levine et al., 2013).

In addition, we considered this fold highly interesting because it is present in the Ragulator subunits p14 and MP1 (Lunin et al., 2004; Kurzbauer et al., 2011). Despite almost no sequence similarity with p14 or MP1, the proteins are very similar in their tertiary structure (Garcia-Saez et al., 2011).

The roadblock domain has a characteristic appearance when modeled in secondary structure prediction tools (Koonin and Aravind, 2000; Figure 3A), which also highlights the similarity between HBXIP, p14 and MP1. Because of the shared motif between different proteins that are important components of the amino acid-sensing machinery, we looked at the predicted secondary structure of

other proteins in that pathway. Surprisingly, the Rag GTPases all contain roadblock domains in their C-termini (Figure 3A), a finding that was confirmed in the crystal structures of the *S. cerevisiae* orthologs (Gong et al., 2011; Jeong et al., 2012). Except for p18, which is predicted to be largely helical or unstructured, all of the known components of the pathway contain roadblock domains.

HBXIP has an unidentified binding partner

The roadblock domain is also notable because many proteins that contain it are obligate dimers (Koonin and Aravind, 2000). In experiments using epitope-tagged versions of HBXIP, we ruled out the possibility that HBXIP homodimerizes (not shown). We therefore hypothesized that HBXIP binds to another roadblock domain-containing protein. In order to find another small roadblock-containing protein that might bind to HBXIP, we carried out a small-scale *in silico* screen for roadblock-containing proteins among the list of proteins corresponding to peptides present in mass spectrometric data from HBXIP immunoprecipitations (Figure 3B).

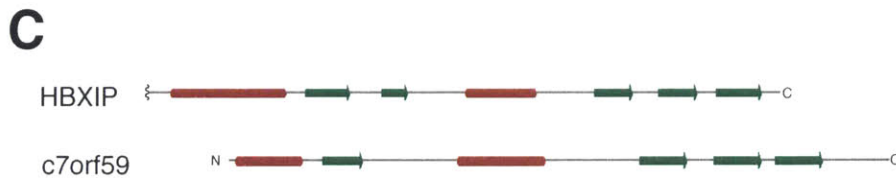
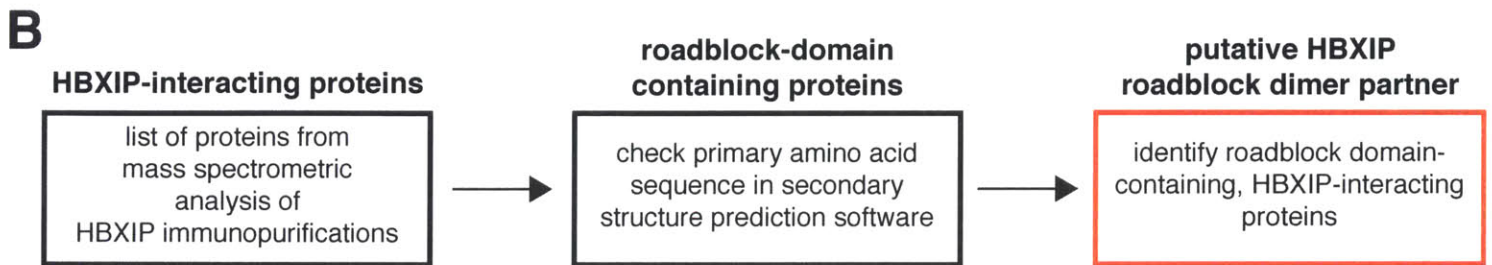
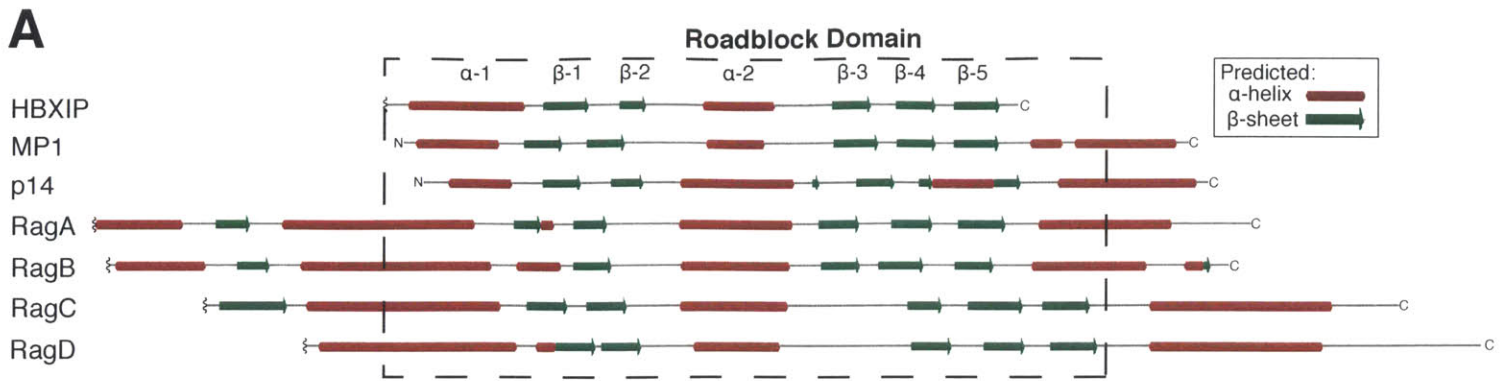
Using this approach, we identified c7orf59. c7orf59 is a small protein composed entirely of a roadblock domain (Figure 3C) that had peptides present in HBXIP IP/MS experiments and has no described functions. We therefore hypothesized that c7orf59 was the binding partner of HBXIP.

Figure 3: HBXIP contains a roadblock domain, allowing for identification of its binding partner
A) HBXIP, Rag GTPases and Ragulator subunits contain roadblock domains. Secondary structure predictions of the indicated proteins using Jpred3 secondary structure prediction software (Cole et al., 2008) are aligned. Predicted helices are indicated in red and beta sheets are indicated with green arrows. The canonical roadblock domain is outlined in the dashed box.

B) Schematic outlining the method used to identify the roadblock domain-containing binding partner of HBXIP.

C) c7orf59 is predicted to contain a roadblock domain. Secondary structure predictions of HBXIP and c7orf59 as in (A) are aligned.

Figure 3: HBXIP contains a roadblock domain, allowing for identification of its binding partner



c7orf59 interacts with HBXIP, Ragulator and Rag GTPases

Peptides corresponding to c7orf59 were found in mass spectrometric analysis of immunoprecipitations of epitope-tagged HBXIP and Ragulator components (not shown). We used co-immunoprecipitation followed by immunoblotting to confirm the IP/MS data. Stably-expressed, FLAG-tagged c7orf59, p14 or Rap2a (a negative control) were immunoprecipitated from HEK-293T cells. Endogenous, cellular RagA, RagC, as well as the Ragulator subunits p18 and MP1 all co-immunoprecipitated with c7orf59 to the same extent that they co-immunoprecipitated with p14 (Figure 4A). Conversely, c7orf59, as well as HBXIP, other Ragulator components and both RagA and RagC co-immunoprecipitated with endogenous, p18 (Figure 4B).

Transiently-expressed, epitope-tagged c7orf59 also co-localizes with p18 at lysosomes (Figure 4C). We concluded that c7orf59 is a roadblock-containing protein that interacts with HBXIP, as well as Ragulator and the Rag GTPases at the lysosome.

c7orf59 and HBXIP dimerization is required for Ragulator-Rag interaction

Binding to HBXIP and containing a roadblock domain are both circumstantial evidence that c7orf59 and HBXIP are a dimer. A requirement for both c7orf59 and HBXIP to be present in order for one to bind to Ragulator, co-regulation of protein levels and effects of mutants that are predicted to alter the roadblock domain interface and disrupt interaction would provide further evidence that the two proteins indeed dimerize.

In HEK-293T cells transiently expressing the cDNAs encoding FLAG-tagged p14, HA-tagged p18, MP1, RagA and RagC, as well as both c7orf59 and HBXIP, p14 co-immunoprecipitates the rest of the Ragulator components, both c7orf59 and HBXIP and the Rag GTPases (Figure 4D). However, if only c7orf59 is removed from the group of expressed cDNAs, p14 no longer co-

Figure 4: c7orf59 interacts with Ragulator and is required for HBXIP and Rag GTPases to bind Ragulator

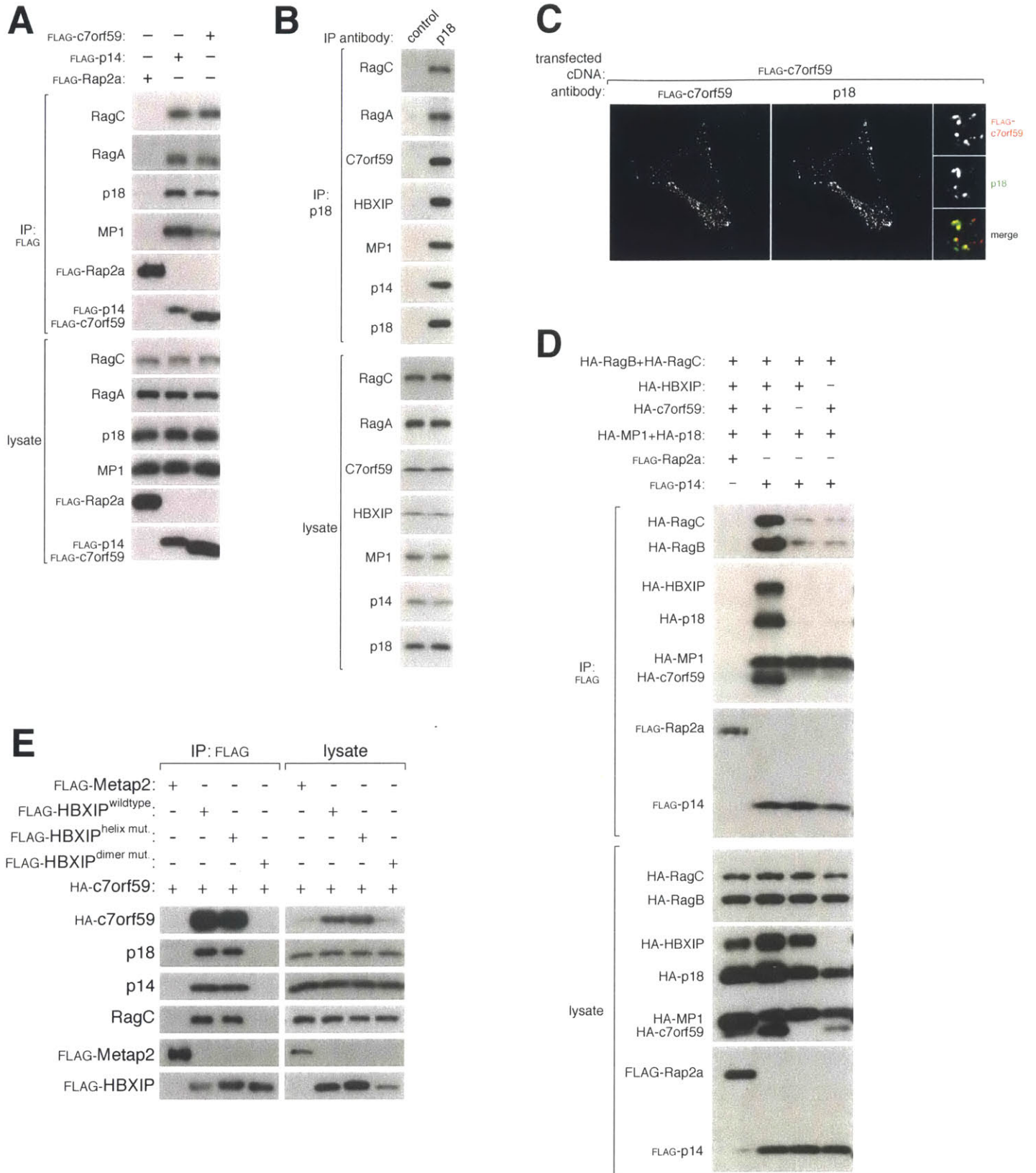


Figure 4: c7orf59 interacts with Ragulator and is required for HBXIP and Rag GTPases to bind Ragulator

A) c7orf59 co-immunopurifies Rag GTPases and Ragulator subunits. Stably-expressed, epitope-tagged c7orf59, p14, or a control protein were immunoprecipitated from HEK-293T cells. Immunoprecipitates and whole cell lysates were analyzed by immunoblotting for the indicated proteins.

B) Ragulator subunit p18 co-immunoprecipitates HBXIP and c7orf59 in addition to Rag GTPases and other Ragulator subunits. p18 or a control protein was immunoprecipitated from HEK-293T cells. Immunoprecipitates and whole cell lysates were analyzed by immunoblotting for the indicated proteins.

C) Recombinant c7orf59 co-localizes with p18. HEK-293T cells were transfected with the FLAG-c7orf59 cDNA, fixed and immunostained with antibodies against the FLAG-epitope tag (pseudo-colored red) and p18 (green) and imaged using confocal microscopy. Insets represent selected fields that have been magnified as well as the overlay of the fields.

D) Recombinant c7orf59 and HBXIP expression increases the amount of recombinant Rag GTPases that interact with recombinant Ragulator. FLAG-tagged p14 or a control protein was immunoprecipitated from HEK-293T cells co-transfected with cDNA encoding HA-tagged MP1, p18, RagB and RagC. In lane 2 both HBXIP and c7orf59 are expressed with Ragulator and Rag GTPases. HBXIP or c7orf59 are removed from the transfections in lanes 3 and 4. Immunoprecipitates and whole cell lysates were analyzed by immunoblotting for the indicated proteins.

E) Mutated recombinant HBXIP that is predicted lack the HBXIP-c7orf59 roadblock dimer interface fails to bind to c7orf59, Rags and Ragulator. cDNA encoding FLAG-tagged, wildtype-, D143A/N153A- ("helix mutant"), or L130A/L137A- ("dimer mutant") HBXIP or a control protein was transfected into HEK-293T cells. HBXIP or the control protein was immunoprecipitated from HEK-293T cells and Immunoprecipitates and whole cell lysates were analyzed by immunoblotting for the indicated proteins.

immunoprecipitates HBXIP, but still co-immunoprecipitates MP1. Importantly, Ragulator expressed with HBXIP but without c7orf59 fails to efficiently co-immunoprecipitate the Rag GTPases. The same results were evident if only HBXIP cDNA is omitted (Figure 4D). Interestingly, not only is HBXIP required for c7orf59 binding to Ragulator, and vice-versa, but without expression of one member of the HBXIP/c7orf59 pair, a drastic reduction in protein levels of the other protein is observed (Figure 4D, lysates).

To confirm the importance of the roadblock domain in HBXIP's binding to c7orf59, we generated mutants in HBXIP that were predicted to disrupt important electrostatic or hydrophobic interactions across the binding interface. These mutants were based upon the binding points in the p14/MP1 dimer crystal structure (Lunin et al., 2004; Kurzbauer et al., 2004). Expression of the cDNA

encoding one of these mutants, which is predicted to disrupt a putative leucine zipper in an important helix of HBXIP (L130A/L137A, “dimer mutant”) in HEK-293T cells strongly reduced that amount of transiently-expressed, epitope-tagged c7orf59 that co-immunoprecipitated with HBXIP (Figure 4E, “dimer mut” lane). Additionally, expression of this mutant strongly reduced the protein level of co-expressed c7orf59 and of HBXIP itself (Figure 4E), indicating that disruption of the HBXIP/c7orf59 dimer destabilizes both proteins, as seen with p14 and MP1 (de Araujo et al., 2013). Another mutant based upon the p14-MP1 interaction (D143A/N153A, “helix mutant”) did not alter HBXIP levels or binding to c7orf59 (Figure 4E), likely because the mutations were not sufficient to disrupt the roadblock domain. These data indicate that c7orf59 binds to Ragulator and the Rag GTPases at the lysosome through its roadblock domain interface with its binding partner, HBXIP.

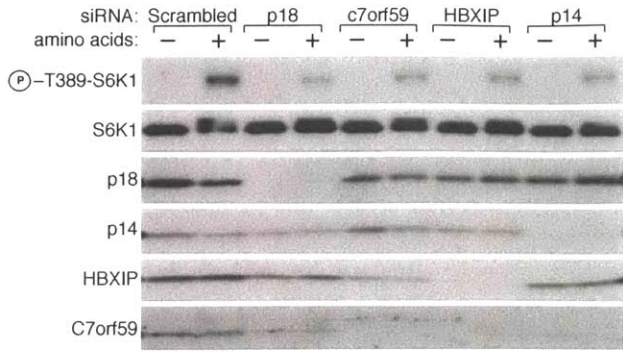
c7orf59 is required for mTORC1 activation and localization by amino acids

Upon characterizing c7orf59 as the roadblock-containing HBXIP binding partner that interacts with Ragulator and the Rag GTPases, we examined the effects of loss of c7orf59. HEK-293T cells expressing siRNA targeting c7orf59 had reduced levels of mTORC1 activation upon stimulation with amino acids comparable to siRNA targeting HBXIP, p14 or p18 (Figure 5A). Additionally, cells expressing siRNA targeting c7orf59 displayed a decrease in HBXIP protein levels while cells expressing siRNA targeting HBXIP displayed decreased c7orf59 levels implying mutual stabilization via binding. Interestingly, knockdown of either p14 or p18 also decreased HBXIP and c7orf59 protein levels (Figure 5A).

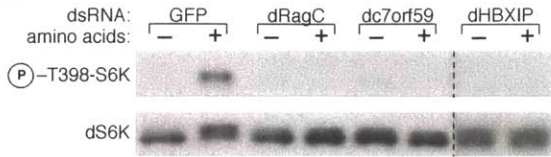
Similarly to HBXIP, c7orf59 has an ortholog present in *Drosophila melanogaster*, CG14977. dsRNA targeting CG14977 in *Drosophila* S2 cells inhibited activation of dTORC1 in response to amino acids to the same extent as knockdown of dRagC or dHBXIP (Figure 5B).

Figure 5: c7orf59 is required for mTORC1 activation and Rag GTPase lysosomal localization

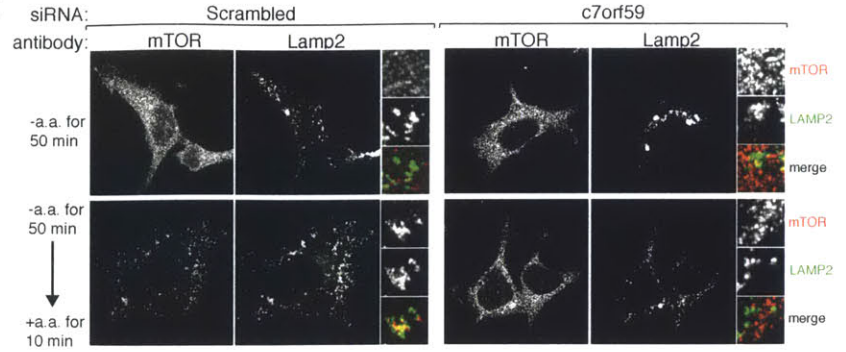
A



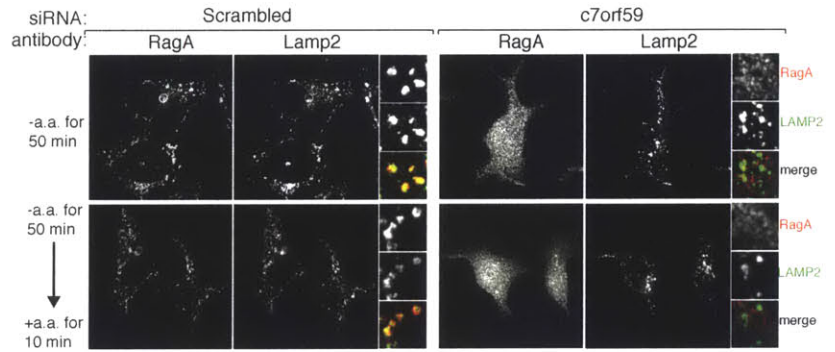
B



C



D



E

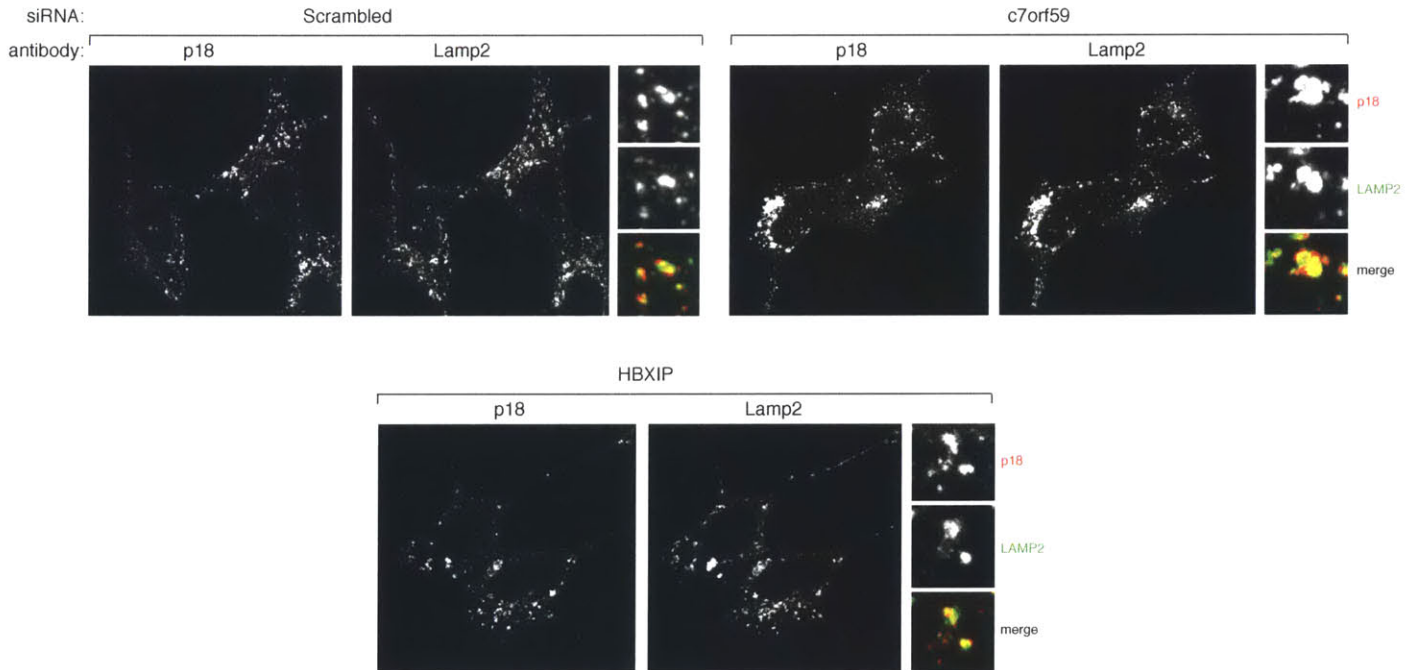


Figure 5: c7orf59 is required for mTORC1 activation by amino acids and Rag GTPase lysosomal localization

A) c7orf59 knockdown inhibits mTORC1 activation by amino acids. HEK-293T cells were transfected with a control siRNA or siRNAs targeting p18, c7orf59, HBXIP, or p14. Cells were starved of amino acids for one hour or starved of amino acids for one hour and re-stimulated with amino acids for 10 minutes. Lysates were analyzed by immunoblotting for the indicated proteins.

B) Knockdown of the Drosophila ortholog of c7orf59 inhibits TORC1 activation. Drosophila S2 cells were transfected with dsRNAs targeting GFP, dRagC dc7orf59 or dHBXIP. Cells were starved of amino acids for 90 or starved of amino acids for 90 minutes and re-stimulated with amino acids for 30 minutes. Lysates were analyzed by immunoblotting for the indicated proteins.

C) Knockdown of c7orf59 inhibits amino acid-mediated lysosomal localization of mTOR. HEK-293T cells were transfected with a control siRNA or siRNA targeting c7orf59, starved of amino acids for 50 minutes or starved and re-stimulated with amino acids for 10 minutes, stained for mTOR (pseudo-colored red) and LAMP2 (green) and imaged using confocal microscopy. Insets represent selected fields that have been magnified as well as the overlay of the fields.

D) Knockdown of c7orf59 leads to cytoplasmic localization of RagA. HEK-293T cells were transfected with a control siRNA or siRNA targeting c7orf59 and treated and imaged as in (C), staining for RagA (red) and LAMP2 (green).

E) Knockdown of c7orf59 or HBXIP does not alter p18 localization. HEK-293T were transfected and imaged as in (C), staining for p18 (red) and LAMP2 (green).

HEK-293T cells expressing siRNA targeting c7orf59 failed to recruit mTOR to lysosomes in response to stimulation with amino acids (Figure 5C). In addition, RagA was no longer lysosomal in these cells (Figure 5D). These data show that loss of c7orf59 phenocopies HBXIP and Ragulator loss (Figure 2C and 2D; Sancak et al., 2010). While RagA is no longer present at lysosomes in cells targeting HBXIP or c7orf59, p18 co-localizes with lysosomal markers in HEK-293T cells expressing siRNAs targeting c7orf59 or HBXIP (Figure 5E), indicating that Ragulator is maintained at lysosomes, but is not sufficient to bind the Rag GTPases when c7orf59 or HBXIP are knocked down.

These data indicate that c7orf59 phenocopies HBXIP and Ragulator loss (Figure 2C and 2D; Sancak et al., 2010).

HBXIP and c7orf59 are Ragulator components

As observed with previously characterized Ragulator subunits, both HBXIP and c7orf59 bind to the Rag GTPases and are required to maintain the Rag GTPases at the lysosome (Figures 1, 2, 4 and 5). In addition to having the same function as Ragulator, HBXIP and c7orf59 have similar structures as Ragulator (Figure 3, Garcia-Saez et al., 2011, Kurzbauer et al., 2004). Because HBXIP and c7orf59 phenocopy Ragulator and appear to have similar structures as Ragulator components, we hypothesized that HBXIP and c7orf59 are bona fide components of Ragulator. Thus, Ragulator is a pentameric complex, composed of p18, p14, MP1 with HBXIP and c7orf59.

Pentameric Ragulator binds the Rag GTPases *in vitro* and is a GEF for RagA/B

In previous work, trimeric Ragulator (p18, p14 and MP1) was unable to efficiently bind to the Rag GTPases *in vitro* (Sancak et al., 2010). While it was hypothesized that in addition to acting as a lysosomal scaffold, Ragulator regulates the Rag GTPases, (Sancak et al., 2010), we were unable to test this possibility using purified proteins without a successful Rag-Ragulator interaction *in vitro*. However, following the identification of HBXIP and c7orf59 as components of the Ragulator, we tested whether the pentameric complex would be sufficient to bind the Rag GTPases *in vitro* and facilitate further study of the regulatory role of Ragulator.

To test this, we purified either pentameric Ragulator from HEK-293T cells transiently expressing cDNA encoding epitope-tagged p18, p14, MP1, HBXIP and c7orf59 or each of the trimeric Ragulator sub-complexes (p18, p14, MP1 or p18, HBXIP, c7orf59) and separately purified GST-tagged Rag dimers composed of RagC and RagB. When the purified trimeric complexes were incubated with immobilized Rag dimers, they failed to co-purify in a glutathione precipitation.

Figure 6: Pentameric Regulator binds Rag GTPases in vitro and has GEF activity towards RagB

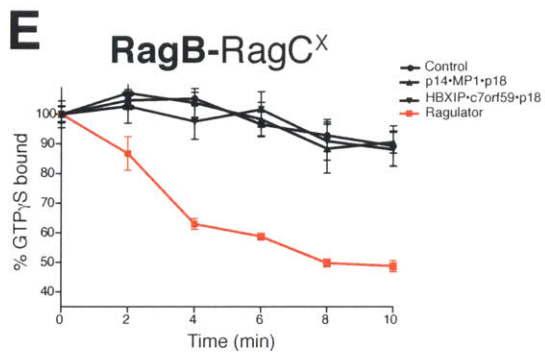
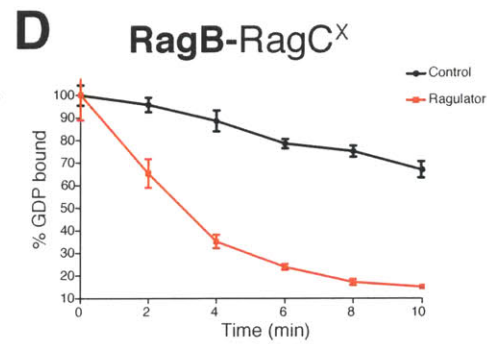
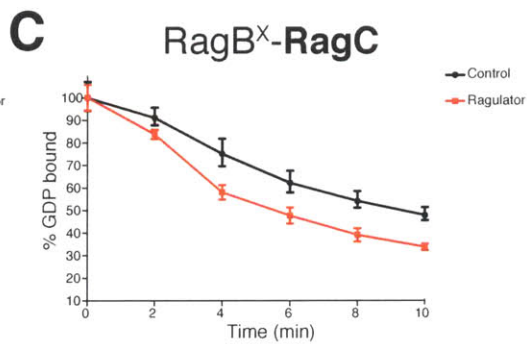
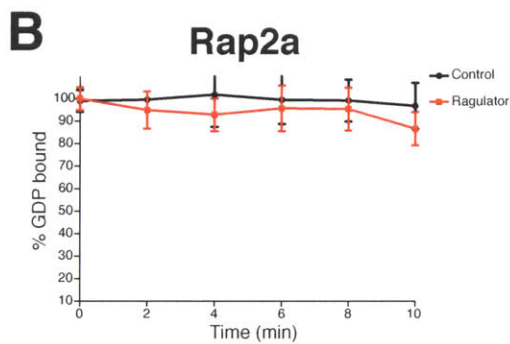
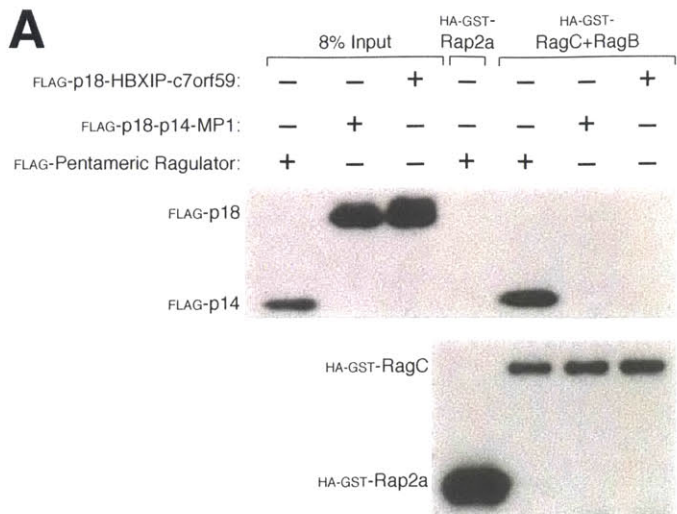


Figure 6: Pentameric Ragulator binds the Rag GTPases *in vitro* and has GEF activity towards RagB.

A) HBXIP and c7orf59 are required for Ragulator to bind the Rag GTPases *in vitro*. Purified, HA-GST-tagged RagC with RagB was incubated with purified, FLAG-tagged Ragulator complexes containing p18, p14, MP1, c7orf59 and HBXIP (lane 5); p18, p14 and MP1 (lane 6); or p18, HBXIP, and c7orf59 (lane 7). Precipitates from glutathione affinity resin were immunoblotted for the indicated epitope tags.

B) Ragulator does not stimulate GDP dissociation from Rap2a. Nucleotide dissociation assay, in which Rap2a was loaded with [³H]GDP and incubated with pentameric Ragulator (p18, p14, MP1, HBXIP and c7orf59). Dissociation was monitored by a filter-binding assay. Each value represents the normalized mean \pm SD for n=4.

C) Ragulator moderately stimulates GDP dissociation from RagC. RagB^{D163N}-RagC was loaded, incubated with Ragulator or a control and analyzed as in (B). Each value represents the normalized mean \pm SD for n=4.

D) Ragulator greatly accelerates GDP dissociation from RagB. RagB-RagC^{D181N} was loaded, incubated with Ragulator or a control and analyzed as in (B). Each value represents the normalized mean \pm SD for n=4.

E) H) Trimeric Ragulator complexes do not increase GTP γ S dissociation from RagB. [³⁵S]GTP γ S bound RagB-C^{D181N} was incubated with Ragulator, p14-MP1-p18, or HBXIP-c7orf59-p18 and dissociation was monitored as in (B). Each value represents the normalized mean \pm SD for n=4.

However, pentameric Ragulator successfully co-purifies with Rag dimers (Figure 6A).

Following successful *in vitro* interaction of the Ragulator with the Rag GTPases, we were able to test the possible regulation of the Rag GTPases by the pentameric Ragulator (referred to as “Ragulator” going forward). We developed a system to examine the nucleotide loading state of individual Rag GTPases *in vitro*, which reflects its activity state. Because the Rags are heterodimers and contain two unique GTP-binding domains, we used a mutation that alters the nucleotide specificity of a small GTPase to reduce guanine binding of one Rag GTPase in the dimer during nucleotide binding assays (Hoffenberg et al., 1995; Schmidt et al., 1996). Mutation of Asp to Asn in the “NKxD motif” of the GTP-binding domain (D163N in RagB or D181N in RagC) increases affinity of the GTPase for xanthosine and decreases the affinity for guanosine (Hoffenberg et al., 1995; Schmidt et al., 1995). Expression and purification of Rag GTPase

dimers consisting of one wildtype Rag and one “x-mutant” Rag allows for examination of the guanine binding of a single GTPase of the dimer.

To test the effects of Ragulator on dissociation of nucleotide from the GTPases, we incubated Rag dimers with one wildtype and one xanthosine-binding mutant with either [³H]GDP or [³⁵S]GTPγS along with cold XDP or XTPγS. Because only the wildtype GTPase binds significant amounts of labeled nucleotide, we could determine rate of nucleotide release of a single Rag GTPase.

Incubating Ragulator with a control small GTPase, Rap2a, resulted in no alterations in release of GDP from the small GTPase (Figure 6B). Similarly, when Ragulator was incubated with a Rag dimer containing wildtype RagC but Rag^x, there was no alteration in the release of GDP from the GTPase (Figure 6C). In contrast, incubation of Ragulator with Rag dimer containing wildtype RagB significantly increased dissociation of GDP from the dimer (Figure 6D). The effect of Ragulator on dissociation of nucleotide from RagB was dependent on the presence of all five Ragulator components, as incubation of p18-p14-MP1 or p18-HBXIP-c7orf59 complexes with RagB^{wt}/RagC^x dimer was not sufficient to increase dissociation of GTPγS from RagB, while incubation of the Rag dimer with the complete Ragulator resulted in increased dissociation of GTPγS (Figure 6E). The increase in dissociation of nucleotide from a GTPase is a characteristic of a guanine nucleotide exchange factor (GEF).

These data indicate that HBXIP and c7orf59 are essential components of Ragulator, and that they are required for both scaffolding the Rag GTPases at the lysosome and for GEF activity upon RagA/B.

DISCUSSION

We found and characterized HBXIP and c7orf59 as new components of the amino acid-dependent mTORC1 activation pathway. We showed that both interact with the Ragulator subunits p18, p14 and MP1 and the Rag GTPases. Our data revealed a requirement for both HBXIP and c7orf59 for activation of mTORC1 by amino acids, as when either gene is knocked down, mTORC1 fails to be recruited to lysosomes and therefore cannot be activated by the lysosomal GTPase Rheb. We showed that mTORC1 failure to localize to lysosomes in amino acid-stimulated cells following knockdown of either HBXIP or c7orf59 is due to the loss of lysosomal localization of the Rag GTPases. Loss of scaffolding the Rag GTPases to the lysosome is similar to the phenotype of loss of function of other Ragulator components.

In addition to having functional similarity to the previously identified Ragulator subunits, HBXIP also shares structural similarities. HBXIP is composed of a roadblock domain, and has a very similar tertiary structure to Ragulator components p14 and MP1. Additionally, based upon secondary structure predictions, c7orf59 is expected to contain the same domain and structure as HBXIP and Ragulator. Because HBXIP and c7orf59 bind to Ragulator components, carry out the same function as Ragulator, and have very similar structures as Ragulator, we hypothesized that they were indeed Ragulator components.

This hypothesis was confirmed when the addition of HBXIP and c7orf59 to the previously trimeric Ragulator allowed for successful binding of Rag GTPases to Ragulator using *in vitro* purified proteins. Additionally, the pentameric, HBXIP- and c7orf59-containing Ragulator, acts as a GEF for RagA and RagB.

The roadblock domain is found in a number of proteins that are associated with NTPases, including in bacteria (Koonin and Aravind, 2000). In particular, the bacterial protein MglB is composed entirely of a roadblock domain, homodimerizes, and acts as a GAP for its cognate GTPase, MglA (Koonin and

Aravind, 2000; Levine et al., 2012). Additionally, another domain with nearly identical tertiary structure but a different permutation of secondary structure, the Longin domain, and is also found in GTPase regulatory proteins, most notably the yeast Rab-GEF complexes MON1/CCZ1 and TRAPP-I, II, III (Levine et al., 2012)

Interestingly, both Npr12 and Npr13 also both contain Longin domains, and these proteins were recently identified as GAPs for RagA and B and responsible for inhibition of mTORC1 in response to amino acid deprivation (Levine et al., 2012; Bar-Peled et al., 2013). Finally, the Rag GTPases themselves contain roadblock domains in their C-termini, indicating that Rag dimers may automodulate nucleotide binding via their roadblock domains. One complicating factor for the concept of cis-regulation of the Rags by roadblock domains is that the C-termini of yeast Rag proteins was shown to remain relatively far away from the GTP-binding domains, and had no contacts with the catalytic portion of the protein, precluding regulatory activity (Gong et al., 2011; Jeong et al., 2012).

The prevalence of roadblock domains (or similar motifs) in the amino acid sensing pathway is striking, and suggests a common mechanism by which proteins can bind and regulate the Rag GTPases.

MATERIALS AND METHODS

Materials

Reagents were obtained from the following sources: antibodies to ATP6V1B2 and LAMP2 from Abcam; antibodies to phospho-T389 S6K1, S6K1, RagA, RagC, p14, p18, MP1, c7orf59, HBXIP mTOR, phospho-T398 dS6K, and the FLAG epitope from Cell Signaling Technology; HRP-labeled anti-mouse, and anti-rabbit secondary antibodies from Santa Cruz Biotechnology; antibody to the HA tag from Bethyl laboratories; RPMI, FLAG M2 affinity gel, GTP γ S, GDP, Chaps, Triton, and amino acids from Sigma Aldrich; [3 H]GDP and [35 S]GTP γ S from Perkin Elmer; protein G-sepharose and immobilized glutathione beads from Pierce; FuGENE 6 and Complete Protease Cocktail from Roche; Alexa 488 and 568-conjugated secondary antibodies, Schneider's media, Express Five Drosophila-SFM, and Inactivated Fetal Calf Serum (IFS) from Invitrogen; amino acid-free RPMI, and amino acid free Schneider's media from US Biological; siRNAs targeting indicated genes and siRNA transfection reagent from Dharmacon; human cDNA encoding HBXIP from Open Biosystems; nitrocellulose membrane filters from Advantec; The dS6K antibody was a generous gift from Mary Stewart (North Dakota State University).

Cell lysis and immunoprecipitation

Cells were rinsed once with ice-cold PBS and lysed with Chaps lysis buffer (0.3% Chaps, 10 mM β -glycerol phosphate, 10 mM pyrophosphate, 40 mM Hepes pH 7.4, 2.5 mM MgCl $_2$ and 1 tablet of EDTA-free protease inhibitor [Roche] per 25 ml). When only cell lysates were required (i.e., no immunoprecipitation was to be performed), 1% Triton X-100 was substituted for Chaps. When the interaction between Regulator and mTORC1 was interrogated, in cell cross-linking with DSP was performed as described in (Sancak et al., 2008) prior to cell lysis. The soluble fractions of cell lysates were isolated by centrifugation at 13,000 rpm in a microcentrifuge for 10 minutes. For immunoprecipitations, primary antibodies were added to the cleared lysates and incubated with rotation for 1.5 hours at 4°C. 60 μ l of a 50% slurry of protein G-sepharose was then added and the incubation continued for an additional 1 hour. Immunoprecipitates were washed three times with lysis buffer containing 150 mM NaCl. Immunoprecipitated proteins were denatured by the addition of 20 μ l of sample buffer and boiling for 5 minutes, resolved by 8%–16% SDS-PAGE, and analyzed by immunoblotting as described (Kim et al., 2002). For anti-FLAG-immunoprecipitations, the FLAG-M2 affinity gel was washed with lysis buffer 3 times. 20 μ l of a 50% slurry of the affinity gel was then added to cleared cell lysates and incubated with rotation for 2 hours at 4°C. The beads were washed 3 times with lysis buffer containing 150 mM NaCl. Immunoprecipitated proteins were denatured by the addition of 50 μ l of sample buffer and boiling for 5 minutes.

For co-transfection experiments, 2,000,000 HEK293T cells were plated in 10 cm culture dishes. Twenty-four hours later, cells were transfected with the pRK5-based cDNA expression plasmids indicated in the figures in the following amounts: 100 ng or 1000 ng FLAG- or HA-HBXIP; 100 ng or 1000 ng FLAG- or HA-HBXIP; 100 ng or 1000 ng FLAG-p14; 100 ng HA-MP1; 100 ng or 1000 ng FLAG- or HA-p18; 100 ng or 1000 ng FLAG-Rap2a; 300 ng Flag-Metap2; 300 ng Flag-VPS39; 100 ng Flag- or HA-RagB and 100 ng HA- or HA-GST-RagC. The total amount of plasmid DNA in each transfection was normalized to 2 μ g with empty pRK5. Thirty-six hours after transfection, cells were lysed as described above.

Identification of HBXIP and c7orf59

Immunoprecipitates from HEK-293T cells stably expressing FLAG-p18, FLAG-p14, FLAG-RagB or FLAG-Metap2 were prepared using Chaps lysis buffer as described above. Proteins were eluted with the FLAG peptide (sequence DYKDDDDK) from the FLAG-M2 affinity gel, resolved on 4-12% NuPage gels (Invitrogen), and stained with simply blue stain (Invitrogen). Each gel lane was sliced into 10-12 pieces and the proteins in each gel slice digested overnight with trypsin. The resulting digests were analyzed by mass spectrometry as described (Sancak et al., 2008). Peptides corresponding to HBXIP and C7orf59 were identified in the FLAG-p14, FLAG-p18 and FLAG-RagB immunoprecipitates, while no peptides were detected in negative control immunoprecipitates of FLAG-Metap2.

Amino acid starvation and stimulation

HEK-293T cells in culture dishes or coated glass cover slips were rinsed with and incubated in amino acid-free RPMI for either 50 minutes, and stimulated with a 10X mixture of total amino acids for 10 minutes. After stimulation, the final concentration of amino acids in the media was the same as in RPMI. The 10X mixture of total amino acids was prepared from individual powders of amino acids.

RNAi in mammalian cells

On day one, 200,000 HEK-293T cells were plated in a 6 well plate. Twenty-four hours later, the cells were transfected with 250 nM of a pool of siRNAs (Dharmacon) targeting HBXIP or C7orf59, a non-targeting pool, or 125 nM of siRNAs targeting p14 or p18. On day four, the cells were transfected again but this time with double the amount of siRNAs. On day five, the cells were either split onto coated glass cover slips or rinsed with ice-cold PBS, lysed and subjected to immunoblotting as described above.

RNAi in Drosophila S2 cells

dsRNAs against Drosophila HBXIP and C7orf59 genes were designed as described in (Sancak et al., 2008). Primer sequences used to amplify DNA templates for dsRNA synthesis for dHBXIP and, dC7orf59 including underlined 5' and 3' T7 promoter sequences, are as follows:

dHBXIP (CG14812)

Forward primer:

GAATTAATACGACTCACTATAGGGAGAGGAGAAAGTCCTAGCGGAAATC

Reverse primer:

GAATTAATACGACTCACTATAGGGAGAGCTTGAAGATAACGCCTGTGAT

dC7orf59 (CG14977)

Forward primer:

GAATTAATACGACTCACTATAGGGAGACTGATACTAAAGGAAGATGGAGCAG

Reverse primer:

GAATTAATACGACTCACTATAGGGAGAGTATATTCTACGGTTGGACATGCAG

dsRNAs targeting GFP and dRagC were used as positive and negative controls, respectively. On day one, 4,000,000 S2 cells were plated in 6-cm culture dishes in 5 ml of Express Five SFM media. Cells were transfected with 1 µg of dsRNA per million cells using Fugene (Roche). Two days later, a second round of dsRNA transfection was performed. On day five, cells were rinsed once with amino acid-free Schneider's medium, and starved for amino acids by replacing the media with amino acid-free Schneider's medium for 1.5 hours. To stimulate with amino acids, the amino acid-free medium was replaced with complete Schneider's medium for 30 minutes. Cells were then washed with ice cold PBS, lysed, and subjected to immunoblotting for phospho-T398 dS6K and total dS6K.

Immunofluorescence assays

Immunofluorescence assays were performed as described in (Sancak et al., 2010). Briefly, 200,000 HEK-293T cells were plated on fibronectin-coated glass coverslips in 12-well tissue culture plates. Twenty-four hours later, the slides were rinsed with PBS once and fixed for 15 min with 4% paraformaldehyde in PBS at room temperature. The slides were rinsed twice with PBS and cells were permeabilized with 0.05% Triton X-100 in PBS for 5 min. After rinsing twice with PBS, the slides were incubated with primary antibody in 5% normal donkey

serum for 1 hr at room temperature, rinsed four times with PBS, and incubated with secondary antibodies produced in donkey (diluted 1:1000 in 5% normal donkey serum) for 45 min at room temperature in the dark and washed four times with PBS. Slides were mounted on glass coverslips using Vectashield (Vector Laboratories) and imaged on a spinning disk confocal system (Perkin Elmer) or a Zeiss Laser Scanning Microscope (LSM) 710.

In immunofluorescence assays where HBXIP or c7orf59 were co-localized with p18, HEK-293T cells were seeded and processed as described above with the following exceptions. Immediately after seeding, cells were transfected with the following constructs (all cDNAs were expressed from pRK5 expression plasmid): 50 ng Flag-HBXIP, 50 ng HA-p14, 50 ng HA-MP1, 50 ng HA-c7orf59 and 50 ng HA-p18; or 50 ng Flag-c7orf59, 50 ng HA-p14, 50 ng HA-MP1, 50 ng HA-HBXIP and 50 ng HA-p18. The cells were processed the following day.

Protein purification of recombinant Rag heterodimers and Ragulator

To produce protein complexes used for GEF or in vitro binding assays, 4,000,000 HEK-293T cells were plated in 15 cm culture dishes. Forty-eight hours later, cells were transfected separately with the following constructs (all cDNAs were expressed from pRK5 expression plasmid). For pentameric Ragulator: 4 µg Flag-p14, 8 µg HA-MP1, 8 µg HA-p18^{G2A} (a lipidation defective mutant), 8 µg HA-HBXIP, and 8 µg HA-C7orf59. For trimeric Ragulator complexes: 8 µg FLAG-p14, 16 µg HA-MP1 and 16 µg HA-p18^{G2A}; or 8 µg FLAG-HBXIP, 16 µg HA-C7orf59 and 16 µg HA-p18^{G2A}. For the Rag dimers: 8 µg FLAG-RagB^{D163N} and 16 µg HA-RagC; 8 µg FLAG-RagC^{D181N} and 16 µg HA-RagB; or 8 µg FLAG-RagB and 16 µg HA-RagC. For individual proteins: 10 µg Flag-p18^{G2A}; 10 µg Flag-Metap2; 15 µg Flag-VPS39; 10 µg HA-GST-HBXIP, 10 µg HA-GST-c7orf59; or 10 µg HAGST-Rap2a

Thirty-six hours post transfection cell lysates were prepared as described above and either 200 µl of a 50% slurry of glutathione affinity beads or 200 µl of a 50% slurry of FLAG-M2 affinity gel were added to lysates from cells expressing HA-GST-tagged or FLAG-tagged proteins, respectively. Recombinant proteins were immunoprecipitated for 3 hours at 4°C. Each sample was washed once with Triton lysis buffer, followed by 3 washes with Triton lysis buffer supplemented with 500 mM NaCl. Samples containing FLAG-tagged proteins were eluted from the FLAG-M2 affinity gel with a competing FLAG peptide as described above.

In vitro binding assays

For the binding reactions, 20 µl of a 50% slurry containing immobilized HA-GST-tagged proteins were incubated in binding buffer (1% Triton X-100, 2.5mM MgCl₂, 40 mM Hepes pH 7.4, 2 mM DTT and 1mg/ml BSA) with 2 µg of FLAG-tagged proteins in a total volume of 50 µl for 1 hour and 30 minutes at 4°C. In

binding assays where HA-GST-Ragulator was used, HA-GST-p14-MP1 was pre-bound to FLAG-HBXIP-HA-C7orf59 and FLAG-p18 for 5 minutes at 4°C prior to the addition of other FLAG-tagged proteins. In experiments where the Flag-RagB-HA-RagC heterodimer was loaded with nucleotides, 2 µg of FLAG-RagB-HA-RagC was incubated at 25°C for 10 minutes in Rag loading buffer (0.3% Chaps, 40 mM Hepes pH 7.4, 5 mM EDTA, 2 mM DTT and 1 mg/ml BSA) supplemented with either 1 mM GTPγS or 1 mM GDP in a total volume of 10 µl. The Rag-nucleotide complex was stabilized by the addition of 20 mM MgCl₂ and incubated for an additional 5 minutes at 25°C. In assays with nucleotide free Rags, 2 µg of FLAG-RagB-HA-RagC was added to the binding assay with 3 µl of Calf-alkaline phosphatase (NEB). Binding assays in which Ragulator was incubated with nucleotide-loaded or -free Rags were conducted at 4°C for 45 minutes. For the nucleotide competition assay, 2 µg FLAG-RagB-HA-RagC was pre-bound to Ragulator proteins for 30 minutes followed by the addition of 1 mM GTPγS and further incubated for 1 hour and 30 minutes at 4°C. To terminate all binding assays, samples were washed 3 times with 1 ml of ice-cold binding buffer supplemented with 150 mM NaCl followed by the addition of 50 µl of sample buffer.

Nucleotide exchange (GEF) assays

40 pmols of FLAG-RagB^{D163N}-HA-RagC, FLAG-RagC^{D181N}-HA-RagB or FLAG-Rap2a were loaded with either 2 µM of [³H]GDP (25-50 Ci/mmol), 10 µCi of [³⁵S]GTPγS (1250 Ci/mmol), 2 mM GDP (for GTP binding assays), or co-loaded with guanine nucleotides and either 50 nM of XTPγS or 50 nM XDP (Ragulator GEF activity was maintained between a range of 5-500 nM xanthine nucleotide) in a total volume of 100 µl of Rag loading buffer as described above. The GTPase-[³H]GDP-XDP/ XTPγS or GTPase-[³⁵S]GTPγS-XDP/ XTPγS and GTPase-GDP complexes were stabilized by addition of 20 mM MgCl₂ followed by a further incubation at 4°C for 12 hours or 25°C for 5 minutes, respectively. To initiate the GEF assay, 40 pmols of pentameric Ragulator, the indicated Ragulator subcomplexes or a control (FLAG-Metap2, FLAG-VPS39, or FLAG-HBXIP-HA-C7orf59) were added along with 200 µM GTPγS or 5 µCi of [³⁵S]GTPγS (for GTP binding assays) and incubated at 25°C. Samples were taken every 2 minutes and spotted on nitrocellulose filters, which were washed with 2 ml of wash buffer (40 mM Hepes pH 7.4, 150 mM NaCl and 5 mM MgCl₂). Filter-associated radioactivity was measured using a TriCarb scintillation counter (Perkin Elmer).

Generating point mutations in HBXIP

The HBXIP cDNA was mutated using QuikChange kit (Stratagene) according to the manufacturer's protocols. The following primers were used to introduce the indicated mutations into HBXIP:

L130A sense: GCTGGAGTGATATCTGTTGCAGCCCAGCAAGCAGCTAAG
L130A antisense: CTTAGCTGCTTGCTGGGCTGCAACAGATATCACTCCAGC

L137A sense: GCCCAGCAAGCAGCTAAGGCAACCTCTGACCCCACTG
L137A antisense: CAGTGGGGTCAGAGGTTGCCTTAGCTGCTTGCTGGGC

D143A sense: GCTAACCTCTGACCCCACTGCTATTCCTGTGGTGTGTCTAG
D143A antisense:
CTAGACACACCACAGGAATAGCAGTGGGGTCAGAGGTTAGC

N153A sense: GGTGTGTCTAGAATCAGATGCTGGGAACATTATGATCCAG
N153A antisense: CTGGATCATAATGTTCCCAGCATCTGATTCTAGACACACC

ACKNOWLEDGEMENTS

We thank all members of the Sabatini Lab for helpful suggestions and Eric Spooner for mass spectrometric analyses of samples. This work was supported by grants from the NIH (CA103866 and AI47389) and Department of Defense (W81XWH-07-0448) to D.M.S., awards from the LAM Foundation to D.M.S, and fellowship support from the LAM Foundation and from the Jane Coffin Childs Memorial Fund for Medical Research to R.Z. D.M.S. is an investigator of the Howard Hughes Medical Institute.

REFERENCES

de Araújo ME, Stasyk T, Taub N, Ebner HL, Fürst B, Filipek P, Weys SR, Hess MW, Lindner H, Kremser L, Huber LA. Stability of the endosomal scaffold protein LAMTOR3 depends on heterodimer assembly and proteasomal degradation. *J Biol Chem*. 2013 Jun 21;288(25):18228-42.

Bar-Peled L, Chantranupong L, Cherniack AD, Chen WW, Ottina KA, Grabiner BC, Spear ED, Carter SL, Meyerson M, Sabatini DM. A Tumor suppressor complex with GAP activity for the Rag GTPases that signal amino acid sufficiency to mTORC1. *Science*. 2013 May 31;340(6136):1100-6.

Dibble CC, Cantley LC. Regulation of mTORC1 by PI3K signaling. *Trends Cell Biol*. 2015 Sep;25(9):545-55.

Garcia-Saez I, Lacroix FB, Blot D, Gabel F, Skoufias DA. Structural characterization of HBXIP: the protein that interacts with the anti-apoptotic protein survivin and the oncogenic viral protein HBx. *J Mol Biol*. 2011 Jan 14;405(2):331-40.

Gong R, Li L, Liu Y, Wang P, Yang H, Wang L, Cheng J, Guan KL, Xu Y. Crystal structure of the Gtr1p-Gtr2p complex reveals new insights into the amino acid-induced TORC1 activation. *Genes Dev*. 2011 Aug 15;25(16):1668-73.

Hoffenberg S, Nikolova L, Pan JY, Daniel DS, Wessling-Resnick M, Knoll BJ, Dickey BF. Functional and structural interactions of the Rab5 D136N mutant with xanthine nucleotides. *Biochem Biophys Res Commun*. 1995 Oct 4;215(1):241-9.

Jeong JH, Lee KH, Kim YM, Kim DH, Oh BH, Kim YG. Crystal structure of the Gtr1p(GTP)-Gtr2p(GDP) protein complex reveals large structural rearrangements triggered by GTP-to-GDP conversion. *J Biol Chem*. 2012 Aug 24;287(35):29648-53.

Kim DH, Sarbassov DD, Ali SM, King JE, Latek RR, Erdjument-Bromage H, Tempst P, Sabatini DM. mTOR interacts with raptor to form a nutrient-sensitive complex that signals to the cell growth machinery. *Cell*. 2002 Jul 26;110(2):163-75.

Koonin EV, Aravind L. Dynein light chains of the Roadblock/LC7 group belong to an ancient protein superfamily implicated in NTPase regulation. *Curr Biol*. 2000 Nov 2;10(21):R774-6.

Kurzbauer R, Teis D, de Araujo ME, Maurer-Stroh S, Eisenhaber F, Bourenkov GP, Bartunik HD, Hekman M, Rapp UR, Huber LA, Clausen T. Crystal structure

of the p14/MP1 scaffolding complex: how a twin couple attaches mitogen-activated protein kinase signaling to late endosomes. *Proc Natl Acad Sci U S A*. 2004 Jul 27;101(30):10984-9.

Laplante M, Sabatini DM. mTOR signaling in growth control and disease. *Cell*. 2012 Apr 13;149(2):274-93.

Levine TP, Daniels RD, Wong LH, Gatta AT, Gerondopoulos A, Barr FA. Discovery of new Longin and Roadblock domains that form platforms for small GTPases in Ragulator and TRAPP-II. *Small GTPases*. 2013 Apr-Jun;4(2):62-9.

Lunin VV, Munger C, Wagner J, Ye Z, Cygler M, Sacher M. The structure of the MAPK scaffold, MP1, bound to its partner, p14. A complex with a critical role in endosomal map kinase signaling. *J Biol Chem*. 2004 May 28;279(22):23422-30.

Menon S, Dibble CC, Talbott G, Hoxhaj G, Valvezan AJ, Takahashi H, Cantley LC, Manning BD. Spatial control of the TSC complex integrates insulin and nutrient regulation of mTORC1 at the lysosome. *Cell*. 2014 Feb 13;156(4):771-85.

Nada S, Hondo A, Kasai A, Koike M, Saito K, Uchiyama Y, Okada M. The novel lipid raft adaptor p18 controls endosome dynamics by anchoring the MEK-ERK pathway to late endosomes. *EMBO J*. 2009 Mar 4;28(5):477-89.

Sabatini DM, Erdjument-Bromage H, Lui M, Tempst P, Snyder SH. RAFT1: a mammalian protein that binds to FKBP12 in a rapamycin-dependent fashion and is homologous to yeast TORs. *Cell*. 1994 Jul 15;78(1):35-43.

Sancak Y, Thoreen CC, Peterson TR, Lindquist RA, Kang SA, Spooner E, Carr SA, Sabatini DM. PRAS40 is an insulin-regulated inhibitor of the mTORC1 protein kinase. *Mol Cell*. 2007 Mar 23;25(6):903-15.

Sancak Y, Peterson TR, Shaul YD, Lindquist RA, Thoreen CC, Bar-Peled L, Sabatini DM. The Rag GTPases bind raptor and mediate amino acid signaling to mTORC1. *Science*. 2008 Jun 13;320(5882):1496-501.

Sancak Y, Bar-Peled L, Zoncu R, Markhard AL, Nada S, Sabatini DM. Ragulator-Rag complex targets mTORC1 to the lysosomal surface and is necessary for its activation by amino acids. *Cell*. 2010 Apr 16;141(2):290-303.

Sarbassov DD, Ali SM, Kim DH, Guertin DA, Latek RR, Erdjument-Bromage H, Tempst P, Sabatini DM. Rictor, a novel binding partner of mTOR, defines a rapamycin-insensitive and raptor-independent pathway that regulates the cytoskeleton. *Curr Biol*. 2004 Jul 27;14(14):1296-302.

Schmidt G, Lenzen C, Simon I, Deuter R, Cool RH, Goody RS, Wittinghofer A. Biochemical and biological consequences of changing the specificity of p21ras from guanosine to xanthosine nucleotides. *ncogene*. 1996 Jan 4;12(1):87-96.

Teis D, Wunderlich W, Huber LA. Localization of the MP1-MAPK scaffold complex to endosomes is mediated by p14 and required for signal transduction. *Dev Cell*. 2002 Dec;3(6):803-14.

Wunderlich W, Fialka I, Teis D, Alpi A, Pfeifer A, Parton RG, Lottspeich F, Huber LA. A novel 14-kilodalton protein interacts with the mitogen-activated protein kinase scaffold mp1 on a late endosomal/lysosomal compartment. *J Cell Biol*. 2001 Feb 19;152(4):765-76.

Zoncu R, Efeyan A, Sabatini DM. mTOR: from growth signal integration to cancer, diabetes and ageing. *Nat Rev Mol Cell Biol*. 2011 Jan;12(1):21-35.

CHAPTER 3

RagA deletion in the mouse

Lawrence D. Schweitzer¹, Alejo Efeyan¹, Angelina M. Bilate², and David M. Sabatini^{1,3}

¹ Whitehead Institute for Biomedical Research and Massachusetts Institute of Technology, Department of Biology, Nine Cambridge Center, Cambridge, MA 02142

² Whitehead Institute for Biomedical Research and Massachusetts Institute of Technology, Nine Cambridge Center, Cambridge, MA 02142

³ Howard Hughes Medical Institute, Department of Biology, Massachusetts Institute of Technology, Cambridge, MA 02139

This work has been published in:

RagA, but not RagB, is essential for embryonic development and adult mice. Efeyan A, Schweitzer LD, Bilate AM, Chang S, Kirak O, Lamming DW, Sabatini DM. *Dev Cell*. 2014 May 12;29(3):321-9.

Experiments and analysis in Table 1 were performed by AE

Experiments in Figure 1 were performed by AE

Experiments in Figure 2a, 2d, and 2g were performed by AE and experiments in Figure 2b, 2c, and 2f were carried out by LDS and AE. Experiments in Figure 2e were performed by LDS

Experiments in Figure 3 were performed by AE except 3d by LDS

Experiments and analysis in Figure 4a, 4b, 4c and 4g were performed by AE. Experiments and analysis in Figure 4d, 4e, and 4f were carried out by AE and AMB. Experiments in Figure 4h were performed by LDS.

INTRODUCTION

mTORC1 is an important regulator of cell growth and metabolism in cell culture and in animals (Zoncu et al., 2011; Laplante and Sabatini, 2012). Because the serine threonine kinase regulates a wide variety of processes, it is tightly regulated by inputs that signal the nutritional and health status of a cell or organism. The major signals include growth factors and nutrients.

Growth factors act through phosphoinositide 3-kinase (PI3K) signaling to activate a small GTPase, Rheb, by inactivating its cognate GTPase activating protein (GAP), the TSC complex. When Rheb is bound to GTP, it potently activates the kinase activity of mTORC1. However, in order for mTORC1 to interact with Rheb and be activated downstream of growth factors, mTOR must translocate from the cytosol to the surface of the lysosomal membrane, where Rheb resides. This translocation is induced by nutrients. When amino acids and glucose are present, mTORC1 is lysosomal and can be activated by Rheb. If there are not sufficient nutrients available, mTORC1 remains cytoplasmic and cannot interact with Rheb (Zoncu et al., 2011; Laplante and Sabatini, 2012).

Nutrients induce the lysosomal localization of mTORC1 through the Rag GTPases. The Rag GTPases are obligate heterodimers in which a RagA or RagB protein is paired with a RagC or RagD protein. When nutrients are present, RagA or RagB becomes GTP-bound and recruits mTORC1 to the lysosome (Sancak et al., 2008). Thus, both growth factors and nutrients are required to activate mTORC1, because mTORC1 must translocate to the lysosome in response to nutrients, where it can be activated by Rheb in response to growth factors.

Different mouse models depleted of several components of the mTORC1 pathway proved essential for mouse. Mice lacking mTOR or Raptor (the defining component of mTORC1) succumb very early in development, prior to day E7 (Gangloff et al., 2004; Murakami et al., 2004; Guertin et al, 2006). Similarly, loss

of Rheb leads to embryonic lethality, and no Rheb-null embryos are present by day E12.5 (Goorden et al, 2011).

Interestingly, over-activation of the growth factor signaling to mTORC1 is also lethal. Loss of the Rheb-GAP components TSC1 or TSC2 leads to embryonic lethality within day E10.5-E11.5 (Kobayashi et al., 1999; Onda et al., 1999). In contrast, mice expressing a constitutively active RagA mutant that mimics the GTP-bound state survive to birth, but die from energetic crisis after birth due to defects in autophagy (Efeyan et al., 2013). Thus, unlike growth factor-dependent activation of mTORC1, constitutive activation of the nutrient-responsive arm of mTORC1 is dispensable during embryonic development. However, it remained unknown whether the amino acid-sensing arm alone essential for mouse development.

In order to determine the requirement of amino acid sensing by the mTORC1 pathway in mouse development, we generated mice that lack expression of RagA. RagA is expressed in all tissues and during embryonic development, while its paralog RagB is expressed at low levels during development and is restricted to few tissues in the adult mouse (Efeyan et al., 2013). Here we show that loss of RagA is embryonic lethal, indicating that lysosomal localization of mTORC1 is required during development. Mouse embryonic fibroblasts (MEFs) derived from RagA-null embryos display aberrant mTORC1 activity that is not regulated by nutrients. When RagA is deleted in adult mice, individuals that survive intestinal atrophy succumb to an expansion of myeloid cells that resemble the mouse version of myeloid leukemia.

RESULTS

To uncover the role of RagA in early development, we utilized two genetic models of RagA. The first was the previously published constitutively-active RagA^{GTP} allele that is preceded by a STOP codon flanked by LoxP sites (RagA^{STOP}; Efeyan et al., 2013). In the absence of Cre recombinase, the allele is not expressed due to the STOP codon. The other model used is a traditional conditional knockout allele in which the RagA gene is flanked by LoxP sites (RagA^{fl/fl}). RagA^{fl/fl} were crossed with CMV-Cre lines to generate pan-tissue null alleles.

RagA is required for embryonic development

RagA deletion is lethal, as indicated by the lack of RagA^{-/-} mice after weaning in both genetic models (Table 1). We next sought to define the embryonic day in which lethality occurs due to RagA deletion. We studied embryos at days E13.5 and before and were able to detect RagA-null embryos in near-Mendelian ratios at day E10.5 and E11.5, but no RagA-null embryos were present at day E13.5 (Table 1). At these timepoints all RagA^{-/-} embryos were markedly smaller than heterozygous or wildtype littermates or were reabsorbed embryos, presented developmental defects such as open neural tubes, or were partially reabsorbed embryos (Figure 1A, Table 1).

Extracts from day E10.5 embryos showed that RagA^{-/-} mice that were not being reabsorbed displayed loss of mTORC1 activity, as determined by phosphorylation of S6 kinase 1 (S6K1) and eIF4E-binding protein 1 (4E-BP1), two mTORC1 substrates (Figure 1B and 1C). Coincident with downregulation of mTORC1, RagA-deficient embryos also demonstrated increased phosphorylation of Akt (Figure 1B and 1C), indicating that they were alive and that other signaling pathways were still responsive to inputs; it has been well established that mTORC1 acts as a negative feedback loop to inhibit Akt (Harrington et al., 2004;

Table 1: Embryonic lethality of RagA^{-/-} mice

Crosses*	Time	RagA ^{+/+}	RagA ^{+/-}	RagA ^{-/-}
RagA ^{+/-} x RagA ^{+/-}	adult mice	51	121	0
	E13.5	5	6	0
	E11.5	7	13	5 (3 ^s +2 ^r)
	E10.5	26	60	31 (23 ^s +8 ^r)

*: Parental mice were either RagA^{STOP/+} or RagA^{Δ/+}; results were similar and added to the present Table

“s” indicates that the embryo was smaller, but still with identifiable embryonic structures and generally heart beating was detected

“r” indicates that the embryo was reabsorbed

Figure 1: RagA-null embryos die at day E10.5 with inhibited mTORC1 activity

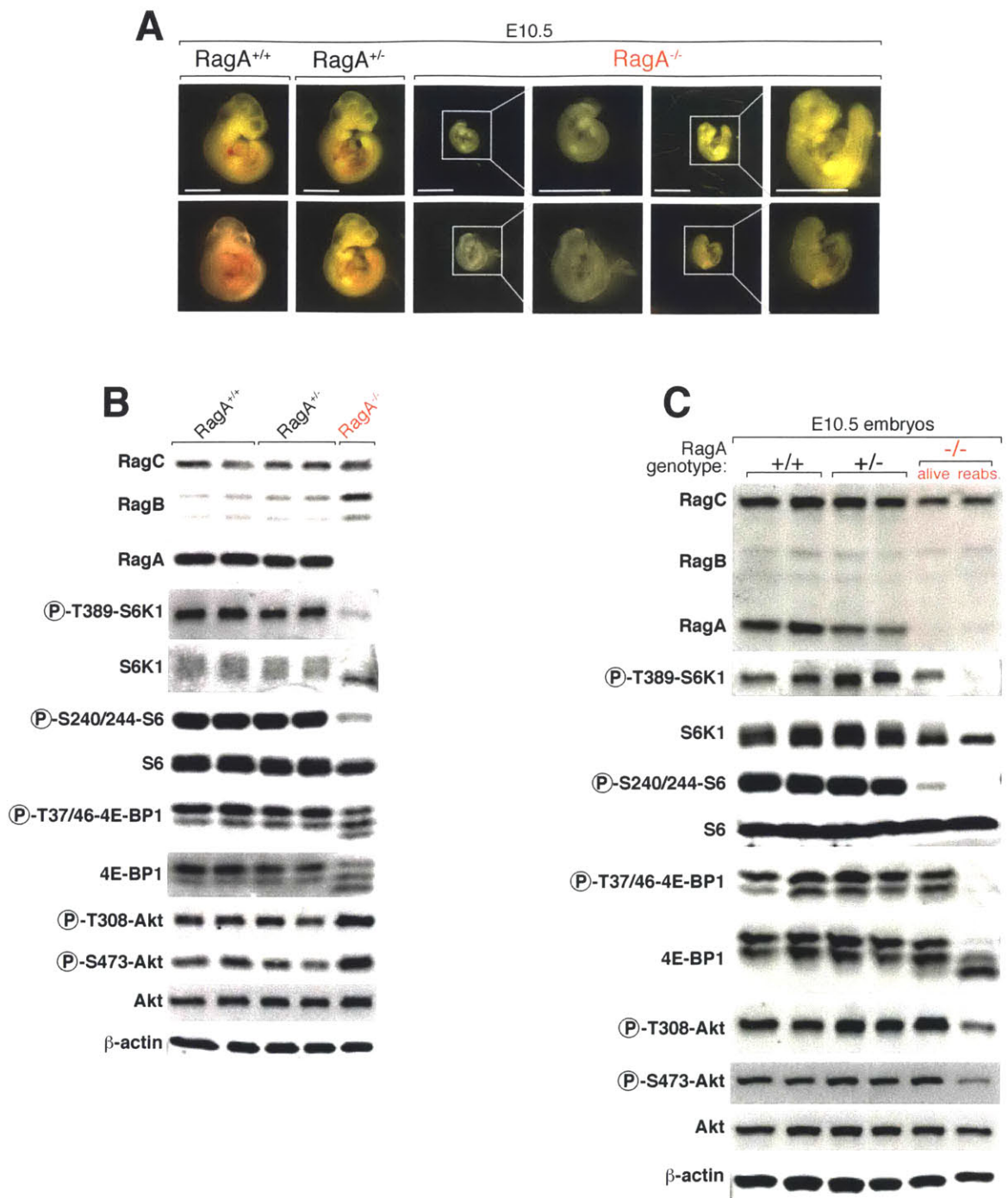


Figure 1: Deletion of RagA leads to embryonic lethality

A) RagA-null embryos are smaller than wildtype, contain defects and die at day E10.5. Representative images Rag^{+/+}, Rag^{+/-} and Rag^{-/-} embryos at day E10.5.

B) RagA-null embryos display inhibited mTORC1. Whole-embryo protein extracts from RagA^{+/+}, RagA^{+/-} and RagA^{-/-} littermates were analyzed by immunoblotting for the indicated proteins.

C) Additional RagA-null embryos display inhibited mTORC1. Whole-embryo protein extracts from RagA^{+/+}, RagA^{+/-} and RagA^{-/-} littermates were analyzed by immunoblotting for the indicated proteins.

Haruta et al., 2000; Um et al., 2004). Interestingly, some RagA-deficient embryos have increased levels of RagB (Figure 1B and 1C), but this increase of RagB is not sufficient to rescue the effects of RagA deletion and only represents a fraction of the wildtype RagA levels.

RagA-null mouse embryonic fibroblasts are insensitive to amino acid deprivation

To better characterize the signaling aberrations in when RagA-null embryos, we derived mouse embryonic fibroblasts (MEFs) from day E10.5 embryos. We were able to generate cell lines from RagA^{-/-} embryos, however the cell lines were established at a much lower rate than wildtype or heterozygous littermates (not shown).

Lysates from representative RagA^{+/+}, RagA^{+/-}, and RagA^{-/-} cells were produced and analyzed by immunoblotting (Figure 2A). Wildtype MEFs express both RagA and RagC, but not RagB. RagA^{+/-} MEFs maintain full expression of both RagA and RagC as well, but have slight elevations in RagB protein. As expected, RagA^{-/-} do not express RagA and, as observed in the corresponding embryos, have a noticeable increase in RagB protein level. Interestingly, the RagA-deficient MEFs also have a marked decrease in RagC, indicating that RagA expression is important for the stability of RagC (Figure 2A).

mTORC1 is regulated normally by growth factor signaling in Rag-deficient MEFs, as S6K1 and 4E-BP phosphorylation are both inhibited by serum

withdrawal and activated by stimulation with insulin (Figure 2B). Interestingly, despite the apparently normal regulation of mTORC1 by growth factors, RagA-deficient cells have increased sensitivity to insulin stimulation downstream of other growth factor receptor-responsive pathways; phosphorylation of Akt as well as ERK is strongly elevated in RagA^{-/-} cells (Figure 2B).

In contrast to the normal regulation of mTORC1 in response to growth factors in RagA-deficient MEFs, cells lacking RagA display altered mTORC1 signaling in response to nutrients. When RagA heterozygous MEFs are starved of either glucose or amino acids for one hour, mTORC1 is inhibited as expected and mTORC1 is fully re-activated upon stimulation with either amino acids or glucose. Surprisingly, RagA^{-/-} MEFs that have been starved of either amino acids or glucose for one hour display no decrease in phosphorylation of either S6K1 or 4E-BP1 (Figure 2C). When amino acids or glucose were added back to starved cells, there was no increase in S6K1 or 4E-BP1 phosphorylation, indicating that the nutrient sensing pathway that activates mTORC1 is constitutively active in RagA-deficient cells (Figure 2C).

RagA-deficient cells in full growth media that have not been starved or re-stimulated with amino acids display reduced levels of S6K1 and 4E-BP1 phosphorylation compared to heterozygous cells (Figure 2D untreated lanes). While regulation of mTORC1 by amino acids is constitutively active, basal mTORC1 activity is reduced by the loss of RagA. Importantly, the phosphorylation of S6K1 and 4E-BP is completely inhibited by treatment with rapamycin in RagA^{-/-} MEFs (Figure 2D), indicating that mTORC1 is still the kinase responsible for these phosphorylation events.

As expected, RagA^{-/-} cells expressing shRNA targeting Rheb are unable to phosphorylate S6K1 (Figure 2E), consistent with maintained regulation of mTORC1 by growth factor signaling in RagA-deficient MEFs (Figure 2B).

We aimed to determine if the insensitivity to amino acid deprivation evident in RagA-deficient MEFs was reversible. To address this, we stably expressed RagB in RagA^{+/-} and RagA^{-/-} MEFs. Expression of RagB in RagA-

Figure 2: RagA-null MEFs exhibit nutrient-independent mTORC1 activity

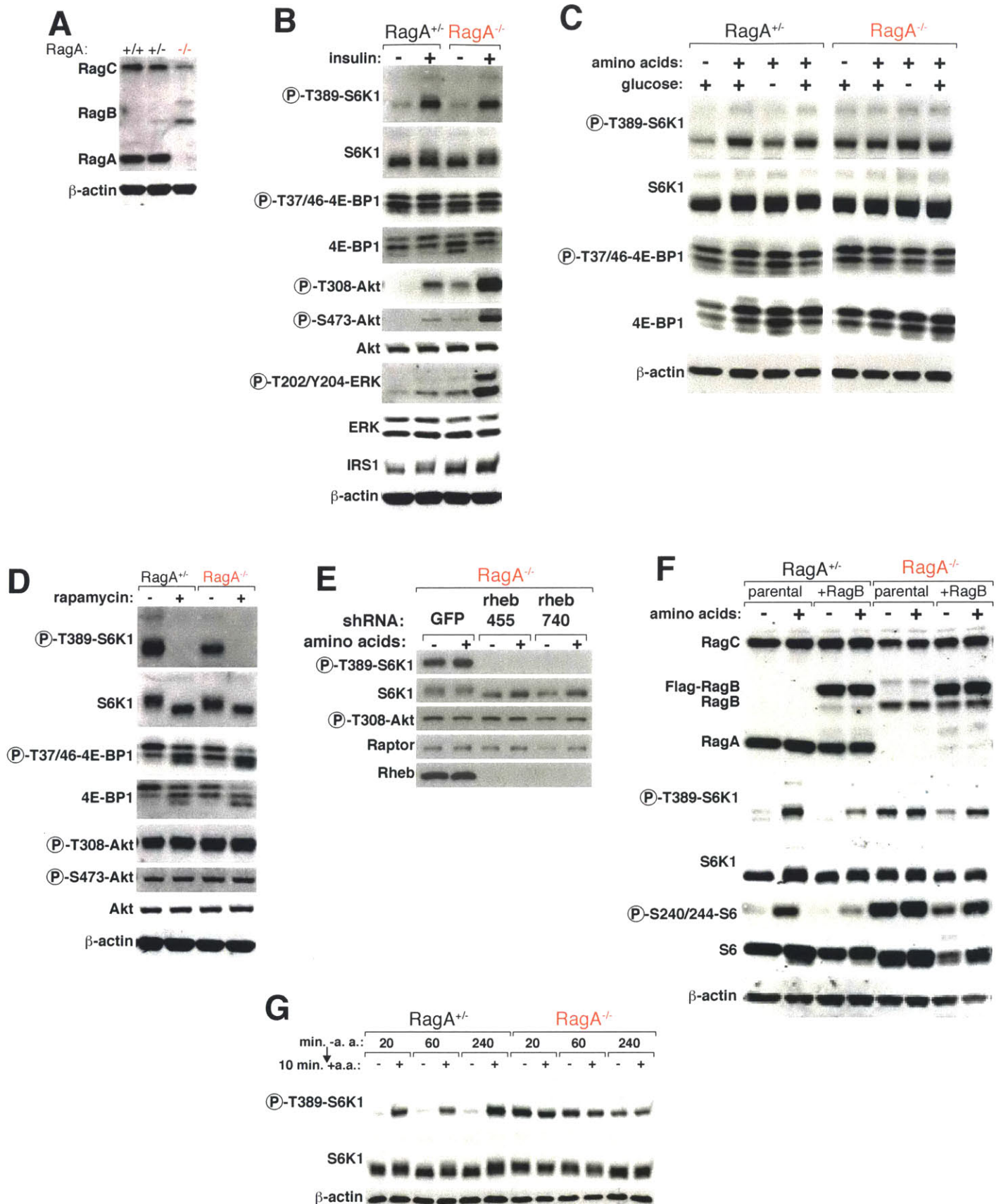


Figure 2: RagA-null MEFs exhibit nutrient-independent mTORC1 activity

A) MEFs derived from RagA-null embryos have decreased levels of RagC and increased levels of RagB. Cell lines were generated from RagA-deficient embryos and whole cell lysates were analyzed by immunoblotting for the indicated proteins.

B) RagA-null MEFs maintain normal regulation of mTORC1 by insulin. MEFs of the indicated genotypes were incubated for one hour without serum or incubated without serum for one hour and re-stimulated with insulin (100 nM) for 10 minutes. Lysates were analyzed by immunoblotting for the indicated proteins.

C) RagA^{-/-} cells exhibit constitutive mTORC1 activity regardless of nutrient (amino acid or glucose) availability. MEFs of the indicated genotypes were starved of glucose or amino acids for one hour or starved of glucose or amino acids for one hour and re-stimulated with either glucose or amino acids, respectively, for 10 minutes. Lysates were analyzed by immunoblotting for the indicated proteins.

D) S6K and 4E-BP phosphorylation in RagA-null cells is rapamycin sensitive. MEFs of the indicated genotypes were treated with rapamycin (10 nM). Lysates were analyzed by immunoblotting for the indicated proteins.

E) Knockdown of Rheb in RagA-null cells inhibits mTORC1. RagA-null MEFs expressing a control shRNA or shRNA targeting the Rheb GTPase were starved of amino acids and re-stimulated with amino acids as in (C). Lysates were analyzed by immunoblotting for the indicated proteins.

F) Expression of RagB in RagA-null cells restores regulation of mTORC1 activity by amino acids. MEFs of the indicated genotypes, stably expressing RagB or the parental cells, were starved of amino acids and re-stimulated with amino acids as in (C). Lysates were analyzed by immunoblotting for the indicated proteins.

G) RagA-null cells maintain lack of regulation by amino acids even under long-term amino acid deprivation. MEFs of the indicated genotypes were starved of amino acids for the indicated lengths of time and re-stimulated with amino acids for 10 minutes. Lysates were analyzed by immunoblotting for the indicated proteins.

deficient cells restored some level of regulation by amino acids; when RagB-expressing cells were starved of amino acids for one hour, phosphorylation of S6K1 was decreased (Figure 2F). RagA-null cells expressing RagB also displayed slightly higher levels of RagC, indicating that increasing the amounts of RagB can stabilize the RagB/C dimer, re-establishing regulation of mTORC1 activity by amino acids.

Because we were able to restore regulation of amino acid signaling, we were curious if the lack of inhibition of mTORC1 upon amino acid starvation was due to a delay in responding to amino deprivation. In RagA^{+/-} MEFs, starvation of amino acids for as short as 20 minutes or as long as two hours resulted in

inhibition of S6K1 phosphorylation by mTORC1, which was reversed by stimulation with amino acids for 10 minutes (Figure 2G). In contrast, RagA-deficient cells had altered kinetics and response to amino acid deprivation. With increasing starvation times, RagA^{-/-} displayed decreasing phosphorylation of S6K1. However, when the cells were re-stimulated with amino acids, there was no discernable activation of mTORC1; S6K1 phosphorylation is decreased upon prolonged amino acid deprivation, but mTORC1 is no longer activated by 10 minute stimulation with amino acids (Figure 2G). RagA^{-/-} MEFs no longer maintain canonical regulation of mTORC1 activation by amino acids.

mTORC1 does not localize to lysosomes in RagA-deficient MEFs

In RagA-heterozygous cells, mTOR is recruited to lysosomes upon amino acid stimulation via the Rag GTPases and is cytoplasmic upon amino acid deprivation. In RagA^{-/-} MEFs that are starved of amino acids, mTOR remains cytoplasmic and fails to localize to lysosomes after re-stimulation with amino acids, (Figure 3A). mTOR remains cytoplasmic regardless of the levels of amino acids in RagA-deficient MEFs, despite the constitutive activity of the pathway during the starvation and re-stimulation. Surprisingly, mTOR is activated in a growth factor- and Rheb-dependent manner, but not at lysosomes in RagA-null MEFs.

The lysosomal localization of mTORC1 by amino acid signaling can be restored upon re-expression of RagB. RagA-null cells that stably express an epitope-tagged RagB recruit mTOR to discrete puncta, likely lysosomes, upon stimulation with amino acids (Figure 3B). This indicates that the defects associated with loss of RagA are reversible, similar to the re-establishment of amino acid-regulated phosphorylation of S6K1 in RagB-expressing cells (Figure 2F). Importantly, lysosomal morphology is not grossly altered in RagA-deficient cells, as indicated by staining LAMP1 in RagA^{-/-} or RagA^{+/-} cells fixed using methanol (Figure 3C), which better preserves membrane-bound organelles for

Figure 3: RagA-null MEFs display non-lysosomal activation of mTORC1

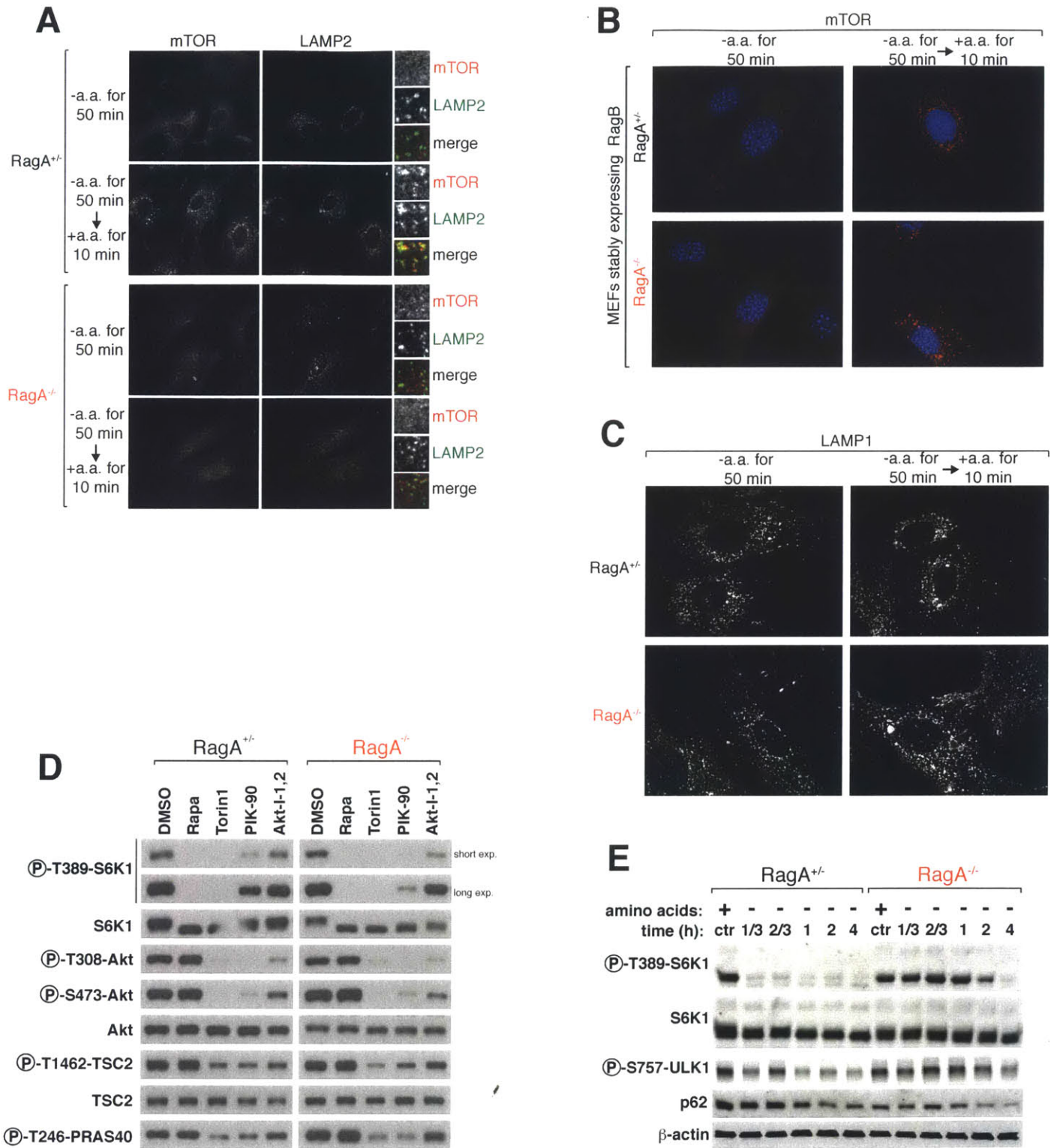


Figure 3: RagA-null MEFs display non-lysosomal activation of mTORC1

A) RagA-null MEFs show constitutively diffuse cytoplasmic localization, regardless of the presence of amino acids. MEFs of the indicated genotypes were starved of amino acids for one hour or starved of amino acids for one hour and re-stimulated with amino acids for 10 minutes. Cells were stained for mTOR (pseudo-colored red) and LAMP2 (green) and imaged using confocal microscopy. Insets represent selected fields that have been magnified as well as the overlay of the fields.

B) Expression of RagB in RagA-null cells restores lysosomal localization of mTOR. Cells of the indicated genotypes stably expressing RagB were treated and imaged as in (A). mTOR is pseudocolored red.

C) Lysosomal morphology is unaffected by loss of RagA. MEFs of the indicated genotypes were starved of amino acids for one hour or starved of amino acids for one hour and re-stimulated with amino acids for 10 minutes. Cells were fixed in methanol for improved visualization of membrane-bound organelles, stained for LAMP1 and imaged using confocal microscopy.

D) RagA-null MEFs are hypersensitive to PI3K and Akt inhibition. MEFs of the indicated genotypes were treated with the indicated inhibitors for one hour. Lysates were analyzed by immunoblotting for the indicated proteins.

E) Regulation of autophagy is altered in RagA-null MEFs. MEFs of the indicated genotypes were starved of amino acids for the indicated lengths of time. Lysates were analyzed by immunoblotting for the indicated proteins.

imaging. The diffuse staining of mTOR in RagA-deficient cells does not represent an alteration in lysosomal morphology, which could complicate our interpretation of the mTOR localization images.

In RagA^{-/-} MEFs, mTORC1 fails to localize to lysosomes, but this phenotype can be rescued by re-addition of RagB, suggesting that the surprising, non-lysosomal activation of mTORC1 by Rheb is reversible.

RagA-deficient MEFs are hypersensitive to inhibition of the PI3K pathway and delay autophagy induction

In order to determine the physiological consequences of the aberrant regulation of mTORC1 activity in RagA-null MEFs, we examined mTORC1 and PI3K activity in response to drugs that inhibit PI3K or Akt by analyzing phosphorylation of S6K1 at Thr389, Akt at Thr308 and Ser473, TSC2 at Thr1462 and PRAS40 at Thr246. These sites are readouts for mTORC1 activation

(S6K1), PI3K activation (Akt T308 and S473 are phosphorylated by PDK1 and mTORC2, respectively), and Akt activation (TSC2 and PRAS40 are both phosphorylated by Akt). RagA^{-/-} cells treated with rapamycin or Torin1 (an ATP-competitive inhibitor of mTOR, inhibiting both mTORC1 and mTORC2 [Thoreen et al., 2009]) had similar inhibition of mTORC1 as RagA^{+/-} cells and displayed no defects in growth factor signaling. In contrast, mTORC1 activity was hypersensitive to inhibitors of PI3K and Akt in RagA-deficient cells (Figure 3D).

RagA-deficient MEFs also displayed defects in activation of autophagy upon amino acid deprivation. mTORC1 phosphorylates and inactivates ULK1, an early regulator of autophagy (Kim and Guan, 2015). In wildtype cells, ULK1 phosphorylation decreases within 20-40 minutes after amino deprivation, resulting in degradation of p62, an autophagy adaptor and substrate, within an hour of starvation (Figure 3E). In contrast, RagA-null MEFs maintain phosphorylation of ULK1 up to two hours of amino acid deprivation (Figure 3E), indicating that other mTORC1 substrates have altered phosphorylation kinetics.

These data indicate that RagA-null MEFs have an increased dependence on growth factor signaling to maintain mTORC1 activity, suggesting the possibility that hyperactive Akt could play a role in the non-canonical mTORC1 activation in these cells. Interestingly, the inability of the mTORC1 pathway to recognize nutrient deprivation in RagA-null cells alters the initiation of autophagy in response to amino acid starvation.

Deletion of RagA in adult mice induces an expansion of monocytes

To better examine the physiological effects of RagA loss, we returned to mouse models. We used tamoxifen-inducible Cre-recombinase driven by a ubiquitous promoter (UBC-CreER; Ruzankina et al., 2007), to achieve full-body acute deletion of RagA in adult RagA^{fl/fl} mice. In all experiments below, mice were treated with tamoxifen to delete RagA, generating “RagA-iKO” mice, and compared to RagA^{fl/fl} or RagA^{fl/+} mice that lacked the UBC-CreER allele.

More than 50 percent of all RagA-iKO mice die within three weeks of tamoxifen injections (Figure 4A). These mice displayed increased apoptotic bodies in their small intestines (Figure 4B), indicating that the mice may be succumbing to atrophy of the small intestine similarly to that observed in acute deletion of Raptor in adult mice (Hoshii et al., 2012). In addition to increased apoptosis in the small intestine, within two weeks of tamoxifen injections, RagA-iKO mice had accumulation of cells that morphologically appeared to be monocytes in their bone marrow and spleen (Figure 4C). Immunostaining of bone marrow cells with markers of monocytes revealed a drastic increase in the number of monocytes in RagA-iKO mice compared to wildtype (Figure 4D). The population of CD11b⁺ Gr1^{low} resident or patrolling macrophages was strongly upregulated in RagA-iKO mice (Figure 4D).

In addition, these cells exhibited increased proliferation, as assayed by BrdU incorporation (Figure 4E). CD11b^{low} Gr-1⁺ CD115⁻ cells from bone marrow of RagA-iKO incorporated nearly twice as much BrdU as did the corresponding cells in control mice, indicated an increase in proliferation. Coincident with the increase in monocytes in the bone marrow, there was a reduction in the number of B lymphocytes and progenitors, as determined by immunostaining for B220 and CD-3 (Figure 4F). This reduction in B lymphocytes has also been observed with acute deletion of Raptor (Hosii et al., 2012; Kalaitzidis et al., 2012).

A subset of RagA-iKO mice succumb rapidly after RagA deletion, likely due to intestinal atrophy and the most striking phenotype in RagA-iKO mice is the proliferation and accumulation of a myeloid cell population and the depletion of B lymphocytes and their progenitors.

Figure 4: Acute deletion of RagA in adult mice causes a malignant expansion of monocytes

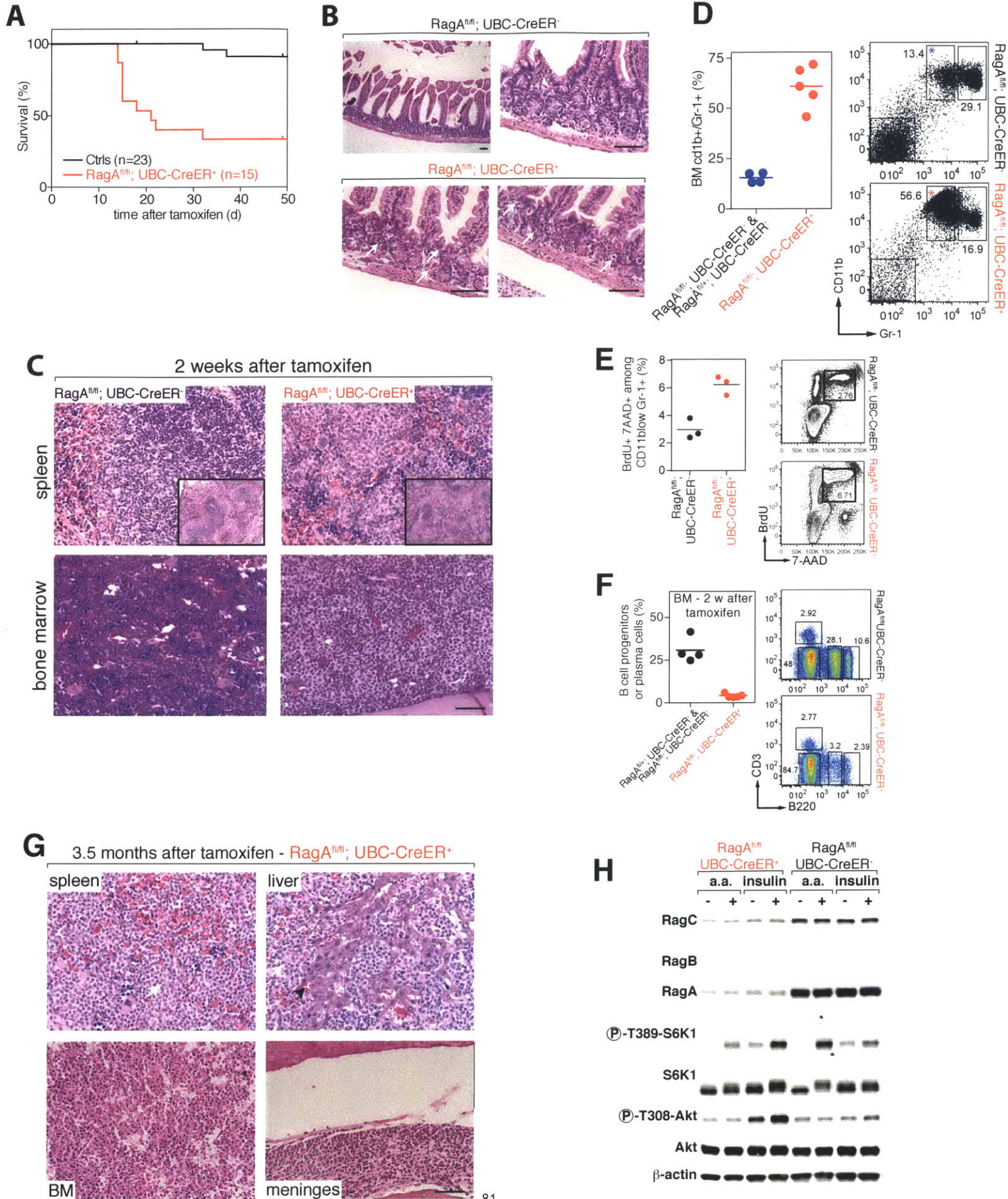


Figure 4: Acute deletion of RagA in adult mice causes malignant expansion of monocytes

A) Depletion of RagA in adult mice is lethal within two weeks in a partially penetrant manner. Kaplan-Meier survival curves after tamoxifen injection of Control (RagA^{fl/+}; UBC-CreER⁻, RagA^{fl/+}; UBC-CreER⁺, RagA^{fl/fl}; UBC-CreER⁻) versus RagA^{fl/fl}; UBC-CreER⁺ mice.

B) Deletion of RagA in adult mice increases apoptosis in the small intestine. Representative H&E sections of small intestine from RagA^{fl/fl}; UBC-CreER⁻ mice and RagA^{fl/fl}; UBC-CreER⁺ mice 2 weeks after start of tamoxifen injections. Arrowhead indicates apoptotic figures.

C) Expansion of a monocytic cell population in spleen and bone marrow two weeks after deletion of RagA. Representative H&E sections of spleen and bone marrow from RagA^{fl/fl}; UBC-CreER⁻ mice and RagA^{fl/fl}; UBC-CreER⁺ mice 2 weeks after start of tamoxifen injections.

D) Expansion of a bone marrow monocytic cell type in RagA-depleted mice. Bone marrow cells were harvested, immune-stained and analyzed by flow cytometry. Dot plots show the cells gated on Lin⁻ (CD3/CD19/Ter119/NK1.1) and are representative of one mouse out of 4–5. Gr-1 and CD11b staining was used to identify monocytes. Graph shows the quantification of the proportion of resident (or patrolling) BM monocytes (determined by CD11b⁺ Gr-1^{low}). CD11b⁺ Gr-1^{high} corresponds to inflammatory monocytes.

E) Monocytic population from RagA-deleted mice displays increased proliferation. Proliferation determined by in vivo BrdU incorporation and 7-AAD staining in bone marrow samples of tamoxifen-treated mice of the indicated genotypes on CD11b^{low} Gr-1⁺ CD115⁻ cells, and 2 representative examples of the FACS plots.

F) Depletion of B-cell progenitors in RagA-deleted mice. Bone-marrow derived cells were purified and B cell progenitors and plasma cells were quantified by B220 and CD-3 staining followed by FACS (mean and scatter plot, n=4 and n=5, respectively), and 2 representative examples of the FACS plots.

G) Monocytic cell expansion in liver, meninges, spleen and bone marrow 3.5 months after deletion of RagA. Representative H&E sections of spleen, liver, bone marrow (BM) and meninges from RagA^{fl/fl}; UBC-CreER⁺ mice 3.5 weeks after start of tamoxifen injections. Black arrowheads indicate normal tissue; white arrows indicate monocytic population.

H) Macrophages isolated from RagA-deleted mice have depleted mTORC1 activation in response to amino acids but hyperactive response to insulin. Macrophages, after tamoxifen injections, were purified and cultured. Cells were then deprived of serum or amino acids, and re-stimulated with insulin or amino acids, and lysates were analyzed by immunoblotting for the indicated proteins.

RagA-iKO mice die of malignant expansion of myeloid cells after 3-4 months

Subsequent to the rapid death of approximately 60 percent of RagA-iKO mice due to intestinal atrophy, the remaining 40 percent of mice all succumbed to a continued expansion of the monocytes within 3-4 months. Increases in myeloid cell numbers were evident in multiple organs, including the spleen, liver, bone marrow and meninges (Figure 4G). This disease was histopathologically similar to histiocytic sarcoma, the murine equivalent of monocytic leukemia.

Macrophages were purified from bone marrow and spleen of RagA-iKO mice with advanced disease (2-3 months after tamoxifen injections) and examined for mTORC1 activity. Unlike MEFs derived from CMV-Cre⁺/RagA^{fl/fl} mice, macrophages from RagA-iKO maintained regulation of amino acid-mediated mTORC1 signaling. RagA-iKO macrophages displayed a marked decrease in phosphorylation of S6K1 upon amino acid stimulation, but did have further inhibition of the phosphorylation when cells were deprived of amino acids (Figure 4H).

While S6K1 regulation by amino acids was strongly blunted in RagA-iKO macrophages, mTORC1 and PI3K pathways were both hyper-activated by growth factors. Stimulation of serum-starved macrophages by insulin led to an increase in phosphorylation of S6K1 and an even stronger increase in phosphorylation of Akt. This indicates that growth factor signaling was hyperactive in RagA-iKO cells, likely due to the release of the mTORC1-mediated negative feedback loop on PI3K and Akt activity (Harrington et al., 2004; Haruta et al., 2000; Um et al., 2004).

RagA-iKO mice that survive the initial insult of RagA deletion develop a lethal expansion of monocytes, which accumulate in a number of tissues. These monocytes display hyper-active growth factor signaling, which likely drives their proliferation.

DISCUSSION

Our work provided data supporting the essentiality of RagA during embryonic development and in adult mice. Comparing the effect of deleting different components of the mTORC1 pathway may offer insight into mTORC1 activation during embryonic development. Deletion of RagA caused embryonic lethality at day E11.5, which is similar to the embryonic lethality kinetics observed in Rheb knockout animals (Goorden et al., 2011). However, loss of p14, a member of the Ragulator scaffolding complex that is required for Rag GTPase and mTORC1 activity, leads to embryonic lethality prior to day E10.5, earlier than either Rheb or RagA loss (Teis et al., 2006). Even earlier lethality (prior to day E7) is observed following the deletion of mTOR or the mTORC1 component Raptor (Gangloff et al., 2004; Murakami et al., 2004; Guertin et al., 2006). This implies that very early in development, mTORC1 can function independently of its activating stimuli, or alternatively that there are other proteins that fulfill the functions of Rheb and RagA in the early embryo. This possibility is also enticing considering that cells in culture that lack RagA no longer inhibit mTORC1 in response to nutrient deprivation.

mTORC1 activity in MEFs derived from Rheb- and RagA-null embryos also suggests that there are mechanisms by which mTORC1 can be active in the absence of canonical signals. Rheb-deficient MEFs are responsive to serum stimulation, but not to insulin alone, indicating that there are stimuli present in serum that activate mTORC1 independently of Rheb (Groenewoud et al., 2013), but the molecular mechanism facilitating this is still unknown. It is also unclear what how mTORC1 is activated in absence of RagA.

Unlike the differences in embryonic deletion of components of the mTORC1 pathway, deleting RagA acutely in the adult animal is phenotypically similar to deletion of Raptor (Hoshii et al., 2012). In adult tissues, loss of mTORC1 activity due to Raptor deletion leads to atrophy of the small intestine and death within two weeks (Hoshii et al., 2012). This phenotype was also

observed in the RagA-null mice. However, the rapid lethality associated with intestinal atrophy was only partially penetrant, and approximately 40 percent of RagA-iKO mice survived the intestinal atrophy-induced lethality at two weeks. Eventually, all RagA-iKO mice succumbed to a monocytic leukemia within months of RagA deletion.

The expansion of myeloid cells observed in RagA-iKO mice coincided with an increase in Akt activity. This is reminiscent of the effects of hematopoietic-specific PTEN loss, which activates Akt and can lead to the development of myeloproliferative disease with increased numbers of CD11b⁺ Gr1⁺ cells (Tesio et al., 2013). In this model, the mice upregulated expression of G-CSF, inducing the mobilization of hematopoietic stem cells and an expansion of myeloid cells. It remains to be seen if a similar mechanism underlies the disease in Rag-iKO mice.

MATERIALS AND METHODS

Generation of RagA knock out mice

All animal studies and procedures were approved by the MIT Institutional Animal Care and Use Committee. RagA locus was targeted by introducing LoxP sites and frt-neomycin- frt cassette flanking RagA exon. Homology arms were 1500 bp and 3000 bp for 5' and 3', respectively. LoxP sites were inserted 300 bp upstream and 500 bp downstream of the RagA exon. The frt-neomycin-frt cassette was inserted next to the 3' LoxP site. RagASTOP allele was previously described (Efeyan et al., 2013). Linearized constructs were electroporated into male v6.5 ES cells of mixed 129Sv/C57B6 background (v6.5). ES colonies were picked and identified by Southern blot and confirmed by PCR amplification of specific insertion products.

Positive ES cells clones were then injected into blastocysts and transferred into pseudo-pregnant females to obtain chimeric mice. Pure C57B6 transgenic Cre strains of mice were then bred with RagA floxed mice.

Treatments of mice

Tamoxifen was dissolved in corn oil (Sigma) at 10 mg/ml and 200 μ ml per 25 g was injected i.p. for 7 consecutive days. For bone marrow reconstitution, host mice were lethally irradiated with 1200 rad divided in two irradiation sessions 4 h apart, and purified 1×10^6 bone marrow cells from either RagAfl/fl ; UBC-CreER⁺ or RagAfl/fl ; UBC-CreER⁻ were injected retro-orbitally 1 h after the last irradiation.

Preparation of MEFs

MEFs from E10.5 embryos were prepared by chemical digestion with trypsin, followed by serial passage when cells reached confluence. MEFs from E13.5 embryos were prepared by chemical digestion with trypsin for 15 min, followed by mechanical disaggregation.

Treatments of MEFs

For amino acids and glucose deprivation in MEFs, sub-confluent cells were rinsed twice and incubated in RPMI without amino acids and/or glucose, and supplemented with 10% dialyzed FBS, as described (Sancak et al., 2008). Stimulation with glucose (5 mM) or amino acids (concentration as in RPMI) was performed for 10 min. For serum withdrawal, cells were rinsed twice in serum-free DMEM and incubated in serum-free DMEM for the indicated times; 100 nM was used for insulin stimulation. Rapamycin was used at 10 nM.

For introducing RagB and RagA in RagA E10.5 MEFs, MEFs were infected with the pLJM1 lentivirus encoding for Metap2 (control protein), Flag-RagA or Flag-RagB and selected for stable integration.

For treatments with kinase inhibitors, 300,000 MEF of the indicated genotypes were seeded in 6-well plates. The following day, media was changed to fresh DMEM+IFS. Four hours after media change, cells were incubated in the following concentrations of inhibitors for one hour, prior to lysing. Cells were treated with rapamycin (LC Laboratories) at 100nM, Torin1 at 100nM, PIK-90 (Selleck) at 500nM, and Akt1/2 inhibitor (SignaGen Laboratories) at 1 μ m.

Treatments of macrophages

Bone marrow-derived macrophages were isolated as described (Weischenfeldt and Porse, 2008). Briefly, bone marrow from femurs and tibias was plated on 10 cm bacterial grade petri dishes in macrophage media (RPMI containing 10% fetal bovine serum, penicillin and streptomycin, 2 mM glutamine and 30 % v/v L929-conditioned media).

Media was replaced two days after isolation. Every two or three days, cells were passaged by scraping with a cell lifter or media was replaced. Five hundred thousand macrophages were seeded in 6-well tissue culture dishes and treated 48 h later. Cells were washed with PBS and incubated for one hour with RPMI lacking amino acids supplemented with dialyzed FBS or DMEM without serum and stimulated with amino acids or 100 nM insulin for 30 minutes.

Immunoblotting

Reagents were obtained from the following sources: anti phospho-T389 S6K1, phospho-S2240/244 S6, phospho-S235/236 S6, phospho-T37/T46 4E-BP1, phospho-T308 Akt, phospho-S473 Akt, phospho-S9 GSK3-b, phospho-T24/T32 FoxO1/3a, phospho-ERK1/2, phospho-ULK1; total Akt, S6, S6K1, 4E-BP1, GSK3-b, FoxO1/3a, RagA, RagC, ERK1/2, IRS1, p62, from Cell Signaling Technology (CST); anti RagB from Abnova; anti β -actin (clone AC-15) from Sigma. Cells were rinsed once with ice-cold PBS and lysed in ice-cold lysis buffer (50 mM HEPES [pH 7.4], 40 mM NaCl, 2 mM EDTA, 1.5 mM sodium orthovanadate, 50 mM NaF, 10 mM pyrophosphate, 10 mM glycerophosphate, and 1% Triton X-100, and one tablet of EDTA-free complete protease inhibitors [Roche] per 25 ml). Cell lysates were cleared by centrifugation at 13,000 rpm for 10 min. Protein extracts were denatured by the addition of sample buffer, boiled for 5 min, resolved by SDS-PAGE, and analyzed by immunoblotting.

Immunofluorescence and immunohistochemistry

MEFs were plated on fibronectin-coated glass coverslips at a sub-confluent density of 50-100,000 cells/coverslip. The following day, cells were transferred to amino acid-free RPMI, starved for 60 min or starved for 50 min and re-stimulated for 10 min with amino acids, rinsed with cold PBS once and fixed for 15 min with 4% paraformaldehyde, or with -20C methanol for 10 min. PFA-fixed coverslips were permeabilized with 0.05% Triton X-100 in PBS and then all coverslips were incubated with primary antibodies in 5 % normal donkey serum for 1 h, rinsed, and incubated with Alexa fluor-conjugated secondary antibodies (Invitrogen) diluted 1:400, for 45 min. Coverslips were mounted on glass slides using Vectashield (Vector Laboratories) and imaged on a spinning disk confocal system (Perkin Elmer) equipped with 405 nm, 488 nm and 561 nm laser lines, through a 63X objective.

Flow Cytometry

Total bone marrow and spleen cells were stained with the following conjugated monoclonal antibodies: CD3, CD19, B220, NK1.1, Ter119, CD11c, CD11b, Gr-1 (Ebioscience). Stained cells were analyzed on a LSR cytometer (BD Biosciences) and data analyzed on FloJo software (TreeStar). For BrdU incorporation, 1.5mg of BrdU was injected intraperitoneally into mice previously treated with tamoxifen 10-12 days before.

After 6h, mice were sacrificed and BrdU incorporation was analyzed by flow cytometry by standard nuclear staining following manufacturer's instruction (BD Pharmingen).

Statistical analyses

For Kaplan-Meier survival curves, comparisons were made with the Log-rank Mantel-Cox method. For qtPCR analyses and other comparison between pairs, non-parametric t-tests were performed.

ACKNOWLEDGEMENTS

We thank members of the Sabatini Lab for helpful suggestions, and Amanda Hutchins and Samantha Murphy for technical assistance. Supported by grants from the National Institutes of Health (R01 CA129105, CA103866 and AI047389; R21 AG042876) and awards from the American Federation for Aging, Starr Foundation, Koch Institute Frontier Research Program, and the Ellison Medical Foundation to D.M.S., and fellowships from the Human Frontiers Science Program and Charles King's Trust Foundation / Fortin Fellowship to A.E. L.D.S is a recipient of the NCI Fellowship F31CA167872. D.W.L. is supported by an NIH K99/R00 Pathway to Independence Award (AG041765). D.M.S. is an investigator of Howard Hughes Medical Institute.

REFERENCES

Efeyan A, Zoncu R, Chang S, Gumper I, Snitkin H, Wolfson RL, Kirak O, Sabatini DD, Sabatini DM. Regulation of mTORC1 by the Rag GTPases is necessary for neonatal autophagy and survival. *Nature*. 2013 Jan 31;493(7434):679-83.

Gangloff YG, Mueller M, Dann SG, Svoboda P, Sticker M, Spetz JF, Um SH, Brown EJ, Cereghini S, Thomas G, Kozma SC. Disruption of the mouse mTOR gene leads to early postimplantation lethality and prohibits embryonic stem cell development. *Mol Cell Biol*. 2004 Nov;24(21):9508-16.

Goorden SM, Hoogeveen-Westerveld M, Cheng C, van Woerden GM, Mozaffari M, Post L, Duckers HJ, Nellist M, Elgersma Y. Rheb is essential for murine development. *Mol Cell Biol*. 2011 Apr;31(8):1672-8.

Groenewoud MJ, Goorden SM, Kassies J, Pellis-van Berkel W, Lamb RF, Elgersma Y, Zwartkruis FJ. Mammalian target of rapamycin complex I (mTORC1) activity in ras homologue enriched in brain (Rheb)-deficient mouse embryonic fibroblasts. *PLoS One*. 2013 Nov 26;8(11):e81649.

Guertin DA, Stevens DM, Thoreen CC, Burds AA, Kalaany NY, Moffat J, Brown M, Fitzgerald KJ, Sabatini DM. Ablation in mice of the mTORC components raptor, rictor, or mLST8 reveals that mTORC2 is required for signaling to Akt-FOXO and PKCalpha, but not S6K1. *Dev Cell*. 2006 Dec;11(6):859-71.

Harrington LS, Findlay GM, Gray A, Tolkacheva T, Wigfield S, Rebholz H, Barnett J, Leslie NR, Cheng S, Shepherd PR, Gout I, Downes CP, Lamb RF. The TSC1-2 tumor suppressor controls insulin-PI3K signaling via regulation of IRS proteins. *J Cell Biol*. 2004 Jul 19;166(2):213-23.

Haruta T, Uno T, Kawahara J, Takano A, Egawa K, Sharma PM, Olefsky JM, Kobayashi M. A rapamycin-sensitive pathway down-regulates insulin signaling via phosphorylation and proteasomal degradation of insulin receptor substrate-1. *Mol Endocrinol*. 2000 Jun;14(6):783-94.

Hoshii T, Tadokoro Y, Naka K, Ooshio T, Muraguchi T, Sugiyama N, Soga T, Araki K, Yamamura K, Hirao A. mTORC1 is essential for leukemia propagation but not stem cell self-renewal. *J Clin Invest*. 2012 Jun;122(6):2114-29.

Kalaitzidis D, Sykes SM, Wang Z, Punt N, Tang Y, Ragu C, Sinha AU, Lane SW, Souza AL, Clish CB, Anastasiou D, Gilliland DG, Scadden DT, Guertin DA, Armstrong SA. mTOR complex 1 plays critical roles in hematopoiesis and Pten-loss-evoked leukemogenesis. *Cell Stem Cell*. 2012 Sep 7;11(3):429-39.

Kim YC, Guan KL. mTOR: a pharmacologic target for autophagy regulation. *J Clin Invest.* 2015 Jan;125(1):25-32.

Kobayashi T, Minowa O, Kuno J, Mitani H, Hino O, Noda T. Renal carcinogenesis, hepatic hemangiomas, and embryonic lethality caused by a germ-line Tsc2 mutation in mice. *Cancer Res.* 1999 Mar 15;59(6):1206-11

Laplante M, Sabatini DM. mTOR signaling in growth control and disease. *Cell.* 2012 Apr 13;149(2):274-93.

Murakami M, Ichisaka T, Maeda M, Oshiro N, Hara K, Edenhofer F, Kiyama H, Yonezawa K, Yamanaka S. mTOR is essential for growth and proliferation in early mouse embryos and embryonic stem cells. *Mol Cell Biol.* 2004 Aug;24(15):6710-8.

Onda H, Lueck A, Marks PW, Warren HB, Kwiatkowski DJ. Tsc2(+/-) mice develop tumors in multiple sites that express p130Cas and are influenced by genetic background. *J Clin Invest.* 1999 Sep;104(6):687-95.

Ruzankina Y, Pinzon-Guzman C, Asare A, Ong T, Pontano L, Cotsarelis G, Zediak VP, Velez M, Bhandoola A, Brown EJ. Deletion of the developmentally essential gene ATR in adult mice leads to age-related phenotypes and stem cell loss. *Cell Stem Cell.* 2007 Jun 7;1(1):113-26.

Sancak Y, Peterson TR, Shaul YD, Lindquist RA, Thoreen CC, Bar-Peled L, Sabatini DM. The Rag GTPases bind raptor and mediate amino acid signaling to mTORC1. *Science.* 2008 Jun 13;320(5882):1496-501.

Teis D, Taub N, Kurzbauer R, Hilber D, de Araujo ME, Erlacher M, Offterdinger M, Villunger A, Geley S, Bohn G, Klein C, Hess MW, Huber LA. p14-MP1-MEK1 signaling regulates endosomal traffic and cellular proliferation during tissue homeostasis. *J Cell Biol.* 2006 Dec 18;175(6):861-8.

Tesio M, Oser GM, Baccelli I, Blanco-Bose W, Wu H, Göthert JR, Kogan SC, Trumpp A. Pten loss in the bone marrow leads to G-CSF-mediated HSC mobilization. *J Exp Med.* 2013 Oct 21;210(11):2337-49.

Thoreen CC, Kang SA, Chang JW, Liu Q, Zhang J, Gao Y, Reichling LJ, Sim T, Sabatini DM, Gray NS. An ATP-competitive mammalian target of rapamycin inhibitor reveals rapamycin-resistant functions of mTORC1. *J Biol Chem.* 2009 Mar 20;284(12):8023-32.

Um SH, Frigerio F, Watanabe M, Picard F, Joaquin M, Sticker M, Fumagalli S, Allegrini PR, Kozma SC, Auwerx J, Thomas G. Absence of S6K1 protects

against age- and diet-induced obesity while enhancing insulin sensitivity. *Nature*. 2004 Sep 9;431(7005):200-5.

Zoncu R, Efeyan A, Sabatini DM. mTOR: from growth signal integration to cancer, diabetes and ageing. *Nat Rev Mol Cell Biol*. 2011 Jan;12(1):21-35.

CHAPTER 4

Disruption of the Rag-Ragulator complex by c17orf59 inhibits mTORC1

Lawrence D. Schweitzer¹, William C. Comb¹, Naama Kanarek^{1,2}, Tim Wang¹,
Liron Bar-Peled¹, and David M. Sabatini^{1,2}

¹ Whitehead Institute for Biomedical Research and Massachusetts Institute of Technology, Department of Biology, Nine Cambridge Center, Cambridge, MA 02142

² Howard Hughes Medical Institute, Department of Biology, Massachusetts Institute of Technology, Cambridge, MA 02139

This work has been published in:

Schweitzer LD, Comb WC, Bar-Peled L, Sabatini DM. Disruption of the Rag-Ragulator Complex by c17orf59 Inhibits mTORC1. *Cell Rep.* 2015 Sep 1;12(9):1445-55.

All experiments and analysis in experiments in all Figures were performed by LDS with the following exceptions:

Experiments in Figure 2b, 2c, and 2e were performed by WCC with LDS.

Analysis in Figure 2d was carried out by WCC

Experiments in Figure 6 were performed by WCC with LDS

Experiments in Figure 7b were performed by WCC with LDS

Analysis in Figure 9b was performed by TW.

Experiments and analysis in Figure 9d were performed by NK

INTRODUCTION

As described in detail in Chapter 1, mTORC1 represents the convergence of the systemic and local environment of a cell with its anabolism and growth. mTORC1 activation requires the presence of both growth factors and nutrients. Growth factor signaling, through the small GTPase Rheb, directly activates the kinase, while nutrients, particularly amino acids, regulate the interaction between mTORC1 and Rheb by allowing mTORC1 to localize to the lysosomal surface in close proximity to Rheb.

Previously, we used immunoprecipitation followed by mass spectrometry (IP/MS) to identify proteins that control activation of mTORC1 by amino acids. Initially, this allowed us to show that the Rag GTPases are mTORC1-interacting proteins that are responsible for recruiting mTORC1 to the lysosome in response to the presence of amino acids (Sancak et al., 2008). Immunoprecipitations of the Rag GTPases contained peptides corresponding to p18, p14, and MP1, HBXIP and c7orf59 which compose the complex we termed Ragulator (Sancak et al., 2010; Bar-Peled et al., 2012; described in Chapter 2).

Ragulator maintains the Rag GTPases at the lysosome, and acts as a scaffold, allowing mTORC1 recruitment to the lysosome. Upon identification of the complete Ragulator (including HBXIP and c7orf59) we showed that the complex acts as a guanine nucleotide exchange factor (GEF) for RagA, inducing the formation of active conformation of the Rag GTPases and recruiting mTORC1 to the lysosome (Bar-Peled et al., 2012).

As Ragulator is not just a scaffolding molecule, but also a GEF for RagA, we began a search for proteins that interact with Ragulator and regulate its GEF activity. Once again, we turned to IP/MS to identify Ragulator-interacting proteins. With this approach, we identified the previously un-described protein c17orf59 as a novel Ragulator-binding protein. c17orf59 binds Ragulator but not the Rag GTPases and induces a mTORC1- and Rag-independent Ragulator complex. Overexpression of c17orf59 disrupts the Rag-Ragulator interaction and

inhibits mTORC1 by preventing its recruitment to lysosomes. This represents a new cellular mechanism to inhibit mTORC1 and we have investigated how c17orf59 might be regulated at the transcriptional and post-translational levels to inhibit mTORC1.

RESULTS

Identification of c17orf59 as a new Ragulator interacting protein

To identify proteins that may play a role in the amino sensing pathway upstream of mTORC1, we immunoprecipitated epitope-tagged Ragulator components and subjected the precipitate to mass spectrometry. Immunoprecipitation of the FLAG-tagged, stably-expressed Ragulator subunit HBXIP specifically yielded peptides corresponding to c17orf59 in addition to the Rag GTPases and other known members of Ragulator complex (Figure 1A). Consistent with this finding, mass spectrometric analysis of immunoprecipitates of stably-expressed, epitope-tagged c17orf59 contained peptides corresponding to all Ragulator subunits, including p18, p14, MP1, HBXIP, and c7orf59. Interestingly, no peptides were identified corresponding to any Rag protein, suggesting that c17orf59 only interacts with Ragulator (Figure 1A).

To confirm the mass spectrometry data, we analyzed immunoprecipitates of c17orf59, Ragulator, and the Rags by western blotting. Stably-expressed, epitope-tagged c17orf59 co-immunoprecipitated all subunits of Ragulator, to levels comparable with epitope-tagged p14 (Figure 1B). While, as expected, p14 interacted with RagA and RagC, c17orf59 did not co-immunoprecipitate either Rag GTPase (Figure 1B). In reciprocal immunoprecipitations, epitope-tagged RagB co-immunoprecipitated Ragulator subunits, but not c17orf59 (Figure 1C).

We used in vitro binding assays to test whether c17orf59 binds directly to Ragulator, as opposed to an indirect interaction that depends on other proteins or components of the cell. In these assays, purified Ragulator bound c17orf59 (Figure 1D). Purified Rags failed to interact with purified c17orf59, even when Ragulator was present (Figure 1D). This confirms that c17orf59 likely interacts directly with members of Ragulator and that the Rags do not interact with c17orf59.

Figure 1: c17orf59 is a Ragulator-interacting protein

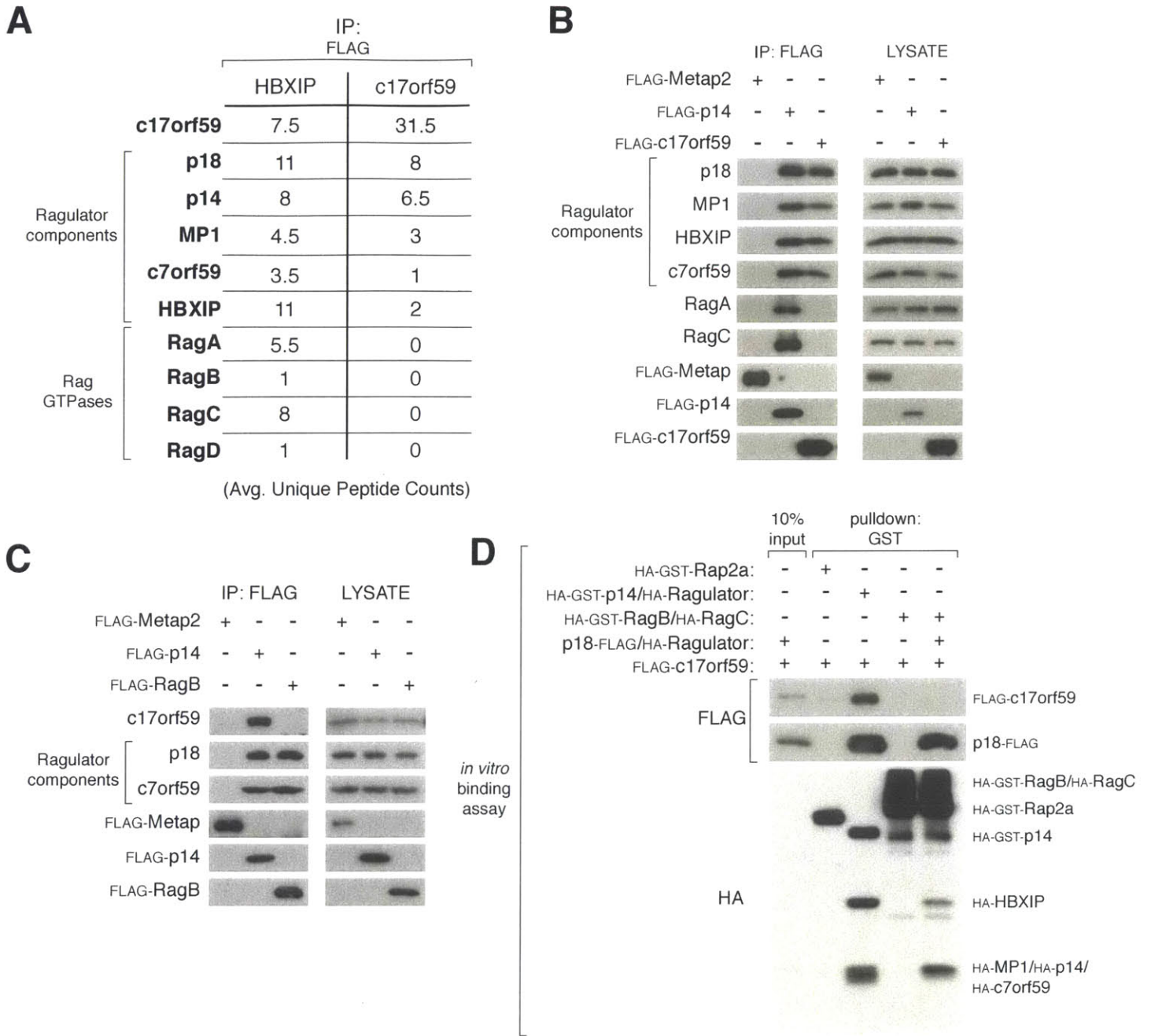


Figure 1: c17orf59 is a Ragulator-interacting protein

A) c17orf59 binds Ragulator. Mass spectrometric analysis of anti-FLAG-immunoprecipitates from HEK-293T cells stably-expressing FLAG-tagged HBXIP, a Ragulator subunit, or c17orf59. Data are presented as average unique peptide counts from two independent immunoprecipitations of HBXIP or c17orf59.

B) Recombinant c17orf59 co-immunoprecipitates Ragulator but not the Rag GTPases. Stably-expressed Ragulator subunit p14, c17orf59, or a control protein (Metap2) were immunoprecipitated from HEK-293T cells. Immunoprecipitates and whole cell lysates were analyzed by immunoblotting for the indicated proteins.

C) Recombinant Rag GTPases co-immunoprecipitate Ragulator, but not c17orf59. Anti-FLAG immunoprecipitates and whole cell lysates from HEK-293T cells transiently expressing the indicated FLAG-tagged cDNA were analyzed by immunoblotting for the indicated proteins.

D) Ragulator, but not the Rag GTPases, binds c17orf59 in in vitro assays. Recombinant, HA-GST-tagged Ragulator, Rag dimer, or Rap2a (a control protein) were incubated with 20pmol purified, FLAG-tagged c17orf59. In lane 5, HA-GST-tagged Rag dimer was incubated with 20pmol FLAG-tagged Ragulator in addition to 20pmol FLAG-tagged c17orf59. Precipitates from glutathione affinity resin were immunoblotted for the indicated epitope tags. GST-Ragulator was expressed as HA-GST-p14, HA-MP1, -HBXIP, -c7orf59 and p18-FLAG. FLAG-Ragulator was expressed as p18-FLAG, HA-p14, -MP1, -HBXIP, and -c7orf59.

c17orf59 localizes to the lysosome along with Ragulator

Ragulator localizes to lysosomes and late endosomes by virtue of lipid modifications and targeting sequences on the N-terminus of p18 (Sancak et al., 2010, Nada et al., 2009). Consistent with its interaction with Ragulator, HA-tagged c17orf59 co-localizes with the lysosomal marker LAMP2 (Figure 2A) indicating its presence at lysosomes. To determine the extent of co-localization between c17orf59 and Ragulator, we re-expressed the cDNA for p18 in p18-null MEFs and examined the localization of c17orf59 and p18. Cells expressing HA-tagged c17orf59 display a highly significant co-localization with p18 (Figure 2B, 2C and 2D). c17orf59 also co-localizes with another Ragulator subunit, LAMTOR4, in a p18-dependent manner (2E), further supporting the existence of a c17orf59-Ragulator interaction.

The subcellular localization of c17orf59 was unaffected by the presence or absence of amino acids or insulin (Figure 3A and 3B), indicating that under the conditions tested, c17orf59 is constitutively localized to the lysosome and bound to Ragulator.

Figure 2: C17orf59 localizes to the lysosome with Ragulator

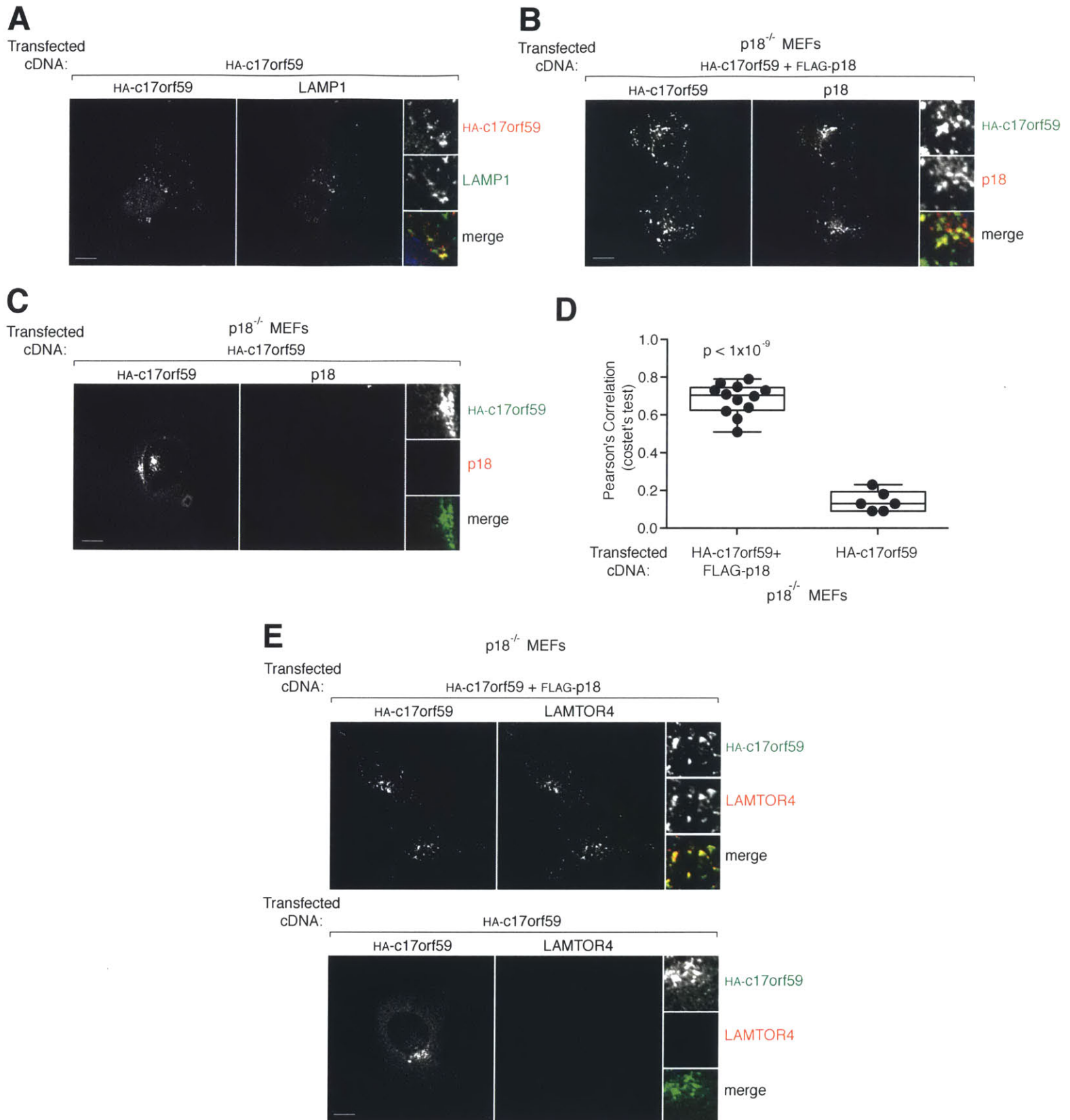


Figure 2: c17orf59 localizes to lysosomes with Ragulator

A) Recombinant c17orf59 localizes to lysosomes. p53-null MEFs were transfected with the HA-c17orf59 cDNA, immunostained with antibodies against LAMP1 (pseudocolored green) and the HA epitope tag (red), and imaged using confocal microscopy. Insets represent selected fields that have been magnified as well as the overlay of the fields. Scale bar represents 10 micrometers.

B) Recombinant c17orf59 co-localizes with p18. p18-null MEFs were transfected with the HA-c17orf59 and FLAG-p18 cDNA and processed and imaged as in (A), with p18 pseudocolored red and the HA epitope tag pseudocolored green. Insets represent selected fields that have been magnified as well as the overlay of the fields. Scale bar represents 10 micrometers.

C) Recombinant c17orf59 localization in p18-null MEFs and validation of the anti-p18 antibody. p18-null MEFs were transfected with the HA-c17orf59 cDNA. Cells were processed and imaged as in (A), with antibodies against the HA epitope tag (green) and against p18 (red). Insets represent selected fields that have been magnified as well as the overlay of the fields. Scale bar represents 10 micrometers.

D) Recombinant c17orf59 has a highly significant correlation in signal distribution and intensity with p18. Correlation of p18 and c17orf59 signal distribution and intensity was compared between p18-null MEFs expressing the cDNA for HA-c17orf59 with or without expression of the cDNA coding for FLAG-p18. Pearson's correlation between HA-c17orf59 and p18 from 12 images in FLAG-p18 expressing cells and 6 images in null cells was quantified and statistical significance was calculated using Student's two-tailed t-test.

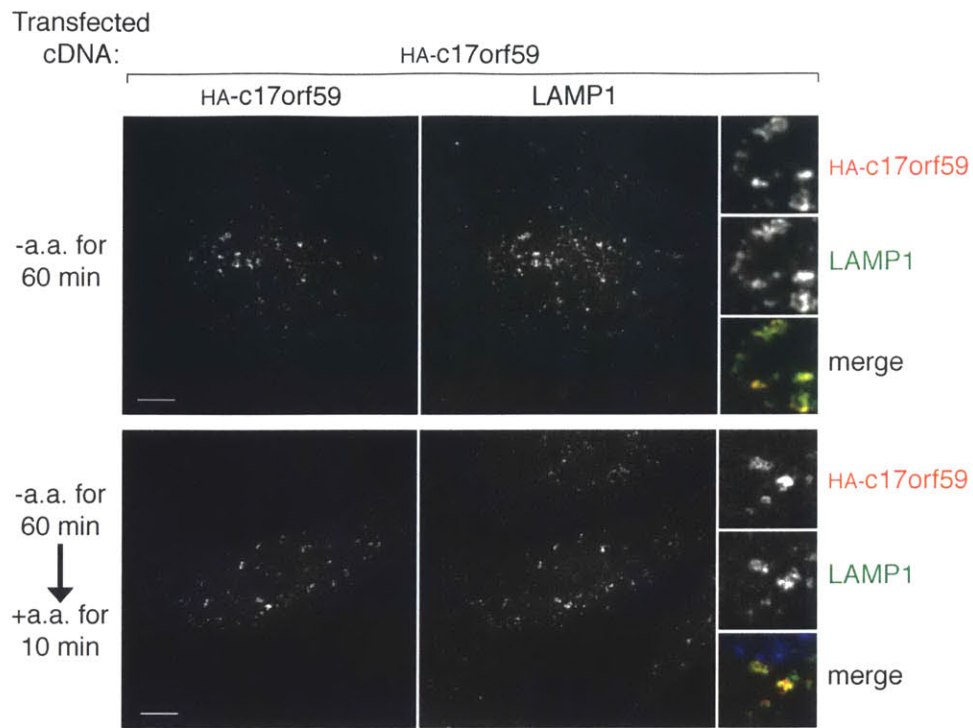
E) Recombinant c17orf59 co-localizes with LAMTOR4 in a p18-dependent manner. p18-null MEFs were transfected with the HA-c17orf59 cDNA alone (bottom panels) or with the FLAG-p18 cDNA (top panels). Cells were processed and imaged as in (A). Insets represent selected fields that have been magnified as well as the overlay of the fields. Scale bar represents 10 micrometers.

c17orf59 loss does not alter mTORC1 activity in response to amino acids or insulin

To examine the effects of loss of c17orf59 on mTORC1 activation, we generated c17orf59-null HEK-293E and HeLa cells using the gRNA/Cas9 system and reconstituted c17orf59 with expression of its cDNA driven by the c17orf59 promoter. The c17orf59-null HEK-293E cells showed no signaling defects in response to amino acid or serum starvation and re-stimulation, as compared to non-targeting gRNA or c17orf59-null cells reconstituted with c17orf59 (Figure 4A, and 4B). HeLa cells in which c17orf59 has been knocked out also show no defects in mTORC1 signaling upon amino acid or serum starvation and re-stimulation (Figure 4C and 4D). c17orf59-null cells displayed no alterations in

Figure 3: c17orf59 localizes to the lysosome regardless of amino acid or serum levels

A



B

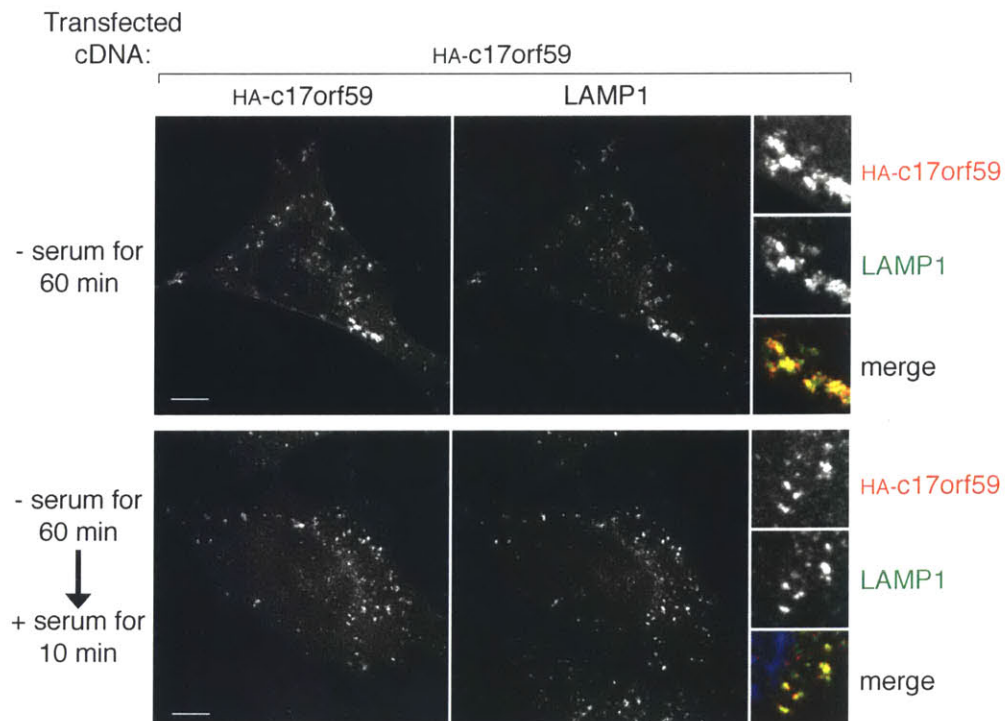


Figure 3: c17orf59 localizes to lysosomes regardless of amino acid or serum levels

A) Recombinant c17orf59 co-localizes with lysosomes in an amino acid-insensitive manner. p53-null MEFs were transfected with the HA-c17orf59 cDNA, starved for amino acids for 60 minutes and stimulated with amino acids for 10 minutes. Cells were immunostained with antibodies against LAMP1 (pseudocolored green) and the HA epitope tag (red), and imaged using confocal microscopy. Insets represent selected fields that have been magnified as well as the overlay of the fields. Scale bar represents 10 micrometers.

B) Recombinant c17orf59 co-localizes with lysosomes in serum-insensitive manner. p53-null MEFs were transfected with the HA-c17orf59 cDNA, starved for amino acids for 60 minutes and stimulated with amino acids for 10 minutes. Cells were processed and imaged as in (A). Insets represent selected fields that have been magnified as well as the overlay of the fields. Scale bar represents 10 micrometers.

mTORC1 activity even when intermediate doses of either amino acids or insulin were added back to cells (Figure 4E and F).

Despite its interaction with Ragulator, loss of c17orf59 does not cause alterations in mTORC1 activation by amino acids or insulin. This lack of signaling phenotype was consistent across multiple clones of c17orf59-null cells using multiple guides in both HEK-293E and HeLa cells, as well as using shRNA-mediated knockdown of c17orf59 (data not shown), so we are confident that the results are not the product of re-wiring in the single cell clones that became the c17orf59-null cells. Based on these results, we tested the effects of c17orf59 overexpression on Ragulator function and mTORC1 activity.

c17orf59 disrupts the Rag-Ragulator interaction in cells and in vitro

The interaction between c17orf59 and Ragulator, but not the Rags, implies that there is a subset of the cellular pool of Ragulator that does not interact with the Rags. As some of this pool interacts with c17orf59, it is possible that increasing the amount of the c17orf59-Ragulator complex could lead to the loss of the Rag-Ragulator interaction by titrating away Ragulator from the Rags. We tested this hypothesis by overexpressing c17orf59 transiently in cells expressing either FLAG-tagged p14 or RagB.

As expected, Ragulator subunits p18 and p14 both co-immunoprecipitated with purified FLAG-tagged RagA when a control protein (Methionine

Figure 4: Loss of c17orf59 does not alter mTORC1 signaling in response to amino acids or insulin

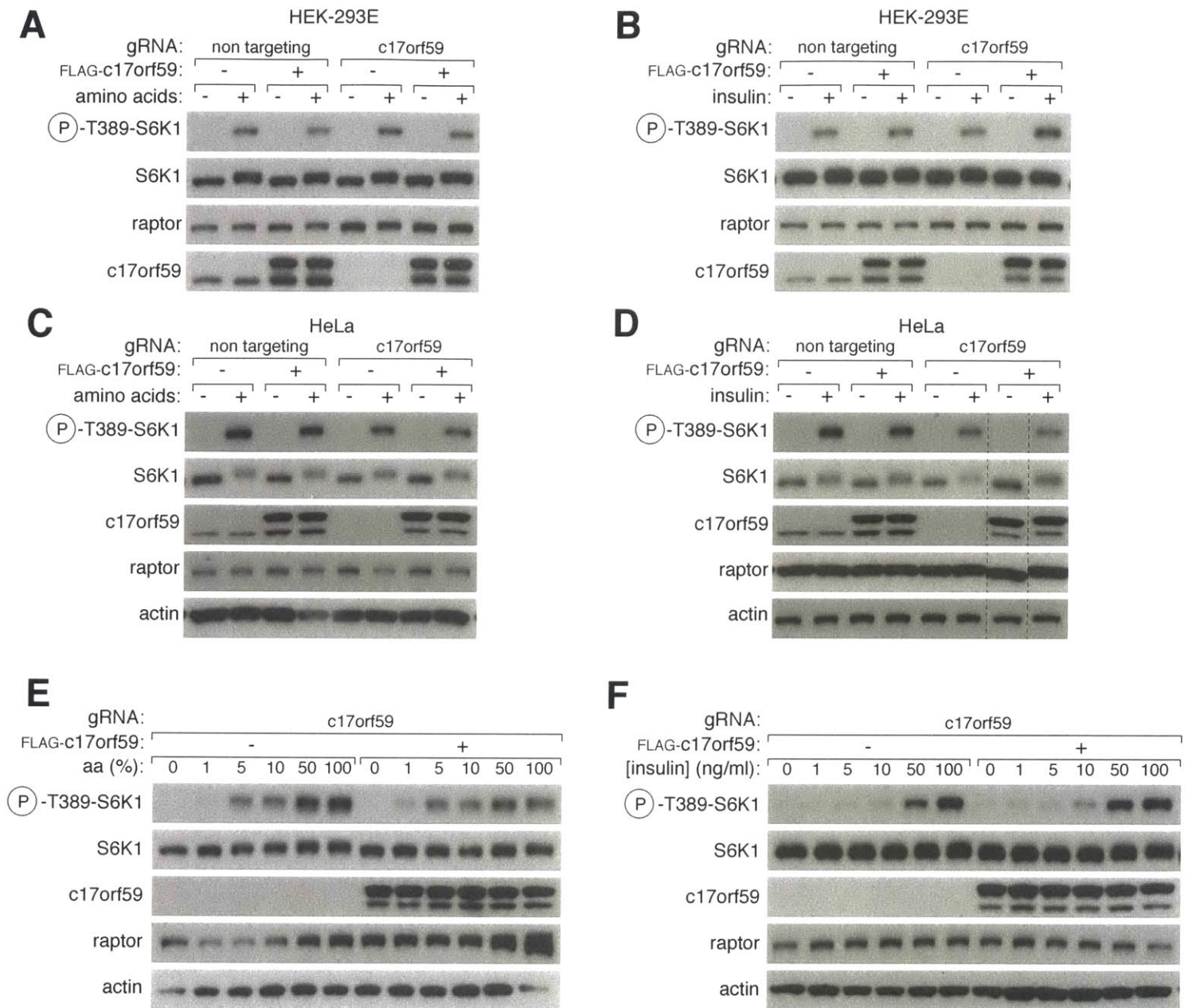


Figure 4: Loss of c17orf59 does not alter mTORC1 signaling in response to amino acids or insulin

A) c17orf59-null HEK-293E cells do not have alterations in amino acid-sensitive mTORC1 activity. c17orf59-null HEK-293E cells were generated by CRISPR/Cas9 technology. Cells were starved of amino acids for one hour and re-stimulated with amino acids for 10 minutes. Lysates were analyzed by immunoblotting for the indicated proteins.

B) c17orf59-null HEK-293E cells do not have alterations in growth factor-sensitive mTORC1 activity. c17orf59-null HEK-293E cells were starved of serum for three hours and re-stimulated with insulin for 10 minutes. Lysates were analyzed as in (A)

C) c17orf59-null HeLa cells do not have alterations in amino acid-sensitive mTORC1 activity. c17orf59-null HeLa cells were generated by CRISPR/Cas9 technology. Cells were starved of amino acids for one hour and re-stimulated with amino acids for 10 minutes. Lysates were analyzed as in (A).

D) c17orf59-null HeLa cells do not have alterations in growth factor-sensitive mTORC1 activity. c17orf59-null HeLa cells were starved of serum for three hours and re-stimulated with 100ng/ml insulin for 10 minutes. Lysates were analyzed as in (A).

E) c17orf59-null cells do not have altered mTORC1 activity in response to lower doses of amino acids. c17orf59-null HeLa cells were starved of amino acids for one hour and re-stimulated with the indicated dilution of all amino acids for 10 minutes. 100 percent amino acid stimulation represents the concentration in full RPMI and the concentration used in other experiments. Lysates were analyzed as in (A).

F) c17orf59-null cells do not have altered mTORC1 activity in response to lower doses of insulin. c17orf59-null HeLa cells were starved of serum for one hour and re-stimulated with the indicated concentration of insulin for 10 minutes. The highest dose (100ng/ml) represents that concentration of insulin used to stimulate cells in previous experiments. Lysates were analyzed as in (A).

aminopeptidase 2, Metap2) was overexpressed. As expected, Raptor, the defining subunit of mTORC1, also co-immunoprecipitated with FLAG-RagA. However, overexpression of c17orf59 disrupted the Rag-Ragulator complex so that RagA no longer co-immunoprecipitated p18, p14, or Raptor to the same extent, indicating a loss of binding to both Ragulator and mTORC1 (Figure 5A). Conversely, immunoprecipitated Ragulator interacted with RagA and RagC, as well as Raptor, but these interactions diminished upon c17orf59 overexpression (Figure 5B).

To examine if c17orf59 can alter the Rag-Ragulator interaction in a cell-free setting, we used in vitro binding assays with purified proteins. Much like in cells, when purified c17orf59 was pre-incubated with the GST-Ragulator, there was a dose-dependent decrease in the amount of purified Rags that bound to

Figure 5: c17orf59 disrupts the Rag-Ragulator interaction

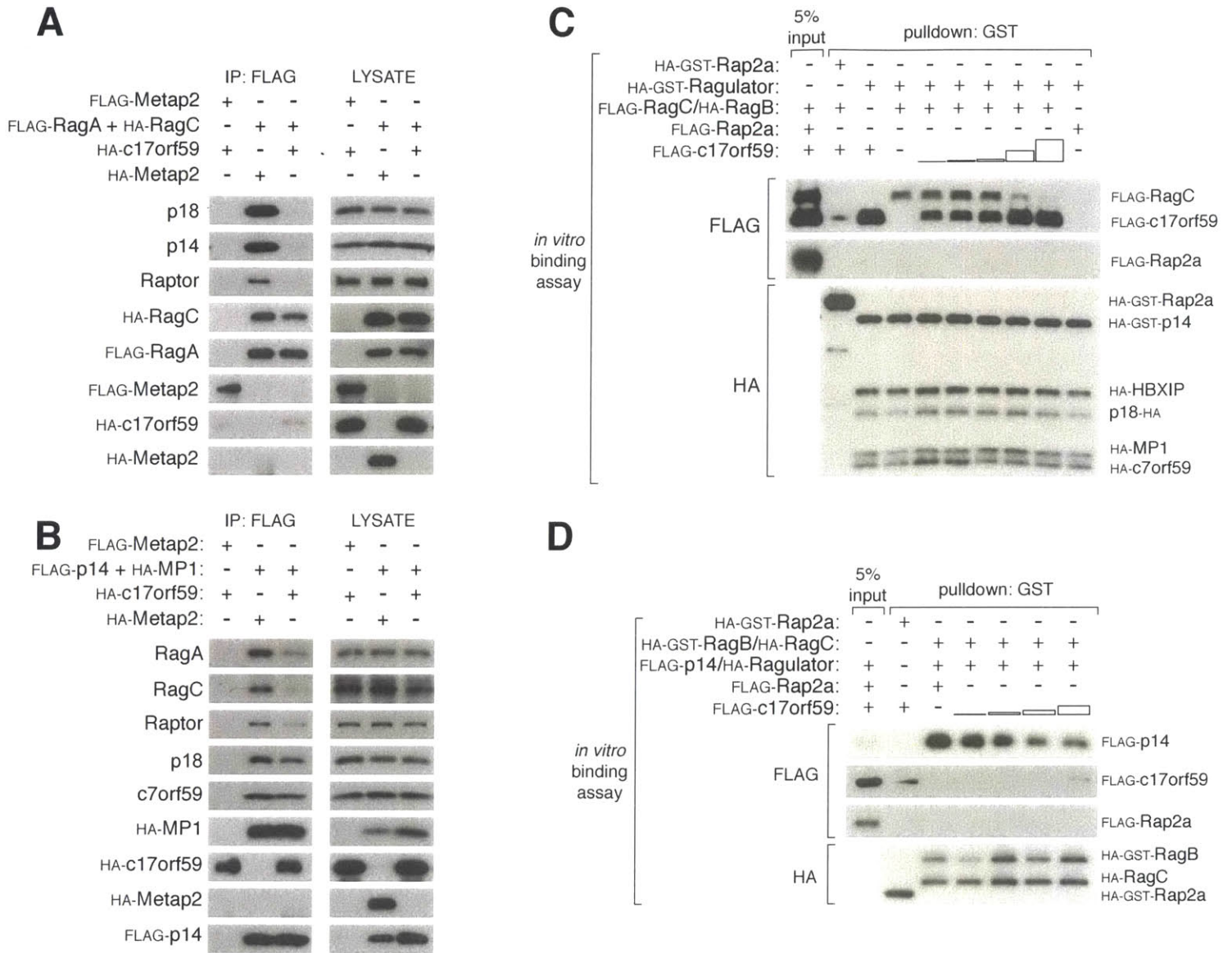


Figure 5: c17orf59 disrupts the Rag-Ragulator interaction

A) c17orf59 overexpression decreases the amount of Ragulator and Raptor recovered with immunoprecipitated Rags. Anti-FLAG immunoprecipitates and whole cell lysates from HEK-293T cells transfected with 100ng of the cDNAs encoding a FLAG-RagA/HA-RagC dimer or a control protein along with 1 µg of HA-c17orf59 or a control protein were analyzed by immunoblotting for the indicated proteins.

B) c17orf59 overexpression decreases the amount of Rag and Raptor, but not Ragulator subunits, that interact with p14. Anti-FLAG immunoprecipitates and whole cell lysates from HEK-293T cells transfected with 100ng of the cDNAs encoding FLAG-p14 and HA-MP1 or a control protein along with 1 µg HA-c17orf59 or a control protein were analyzed as in (A).

C) Purified c17orf59 binds Ragulator in vitro and inhibits the Rag-Ragulator interaction. In vitro binding assay in which recombinant HA-GST Ragulator was pre-incubated with increasing quantities of purified FLAG-c17orf59 and followed by an incubation with purified FLAG-RagB/HA-RagC. For all samples in which FLAG-RagC/HA-RagB were used, 2 µg (25 pmol) of Rag protein was added (lane 2, lanes 4-9). Similarly, 2 µg of FLAG-Rap2a protein as added in each marked sample (lane 10). The amount of FLAG-c17orf59 protein added was as follows: 100ng (2.7 pmol, lane 5), 500ng (13.5 pmol, lane 6), 1 µg (27 pmol, lane 7), 5 µg (135 pmol, lane 8), and 10 µg (270 pmol, lane 9 and all lanes marked with a "+"). The bar above each lane is to scale for c17orf59 protein added. Precipitates using glutathione affinity resin were analyzed by immunoblotting for indicated tagged proteins.

D) c17orf59 decreases the amount of Ragulator bound to Rags in vitro. In vitro binding assay in which purified HA-GST-RagB/HA-RagC was incubated with purified FLAG-Ragulator and increasing amounts of purified FLAG-c17orf59. For all samples in which FLAG-Ragulator were used, 1 µg (14 pmol) of Ragulator protein was added (lanes 3-7). Similarly, 2 µg of FLAG-Rap2a protein as added in each marked sample (lane 3). The amount of FLAG-c17orf59 protein added was as follows: 100ng (2.7 pmol, lane 5), 500ng (13.5 pmol, lane 6), 1 µg (27 pmol, lane 7), 2 µg (135 pmol, lane 8 and all lanes marked with a "+"). The bar above each lane is to scale for c17orf59 protein added. Precipitates using glutathione affinity resin precipitates were analyzed as in (C).

immobilized Ragulator (Figure 5C). In a similar experiment using immobilized, GST-tagged RagB with RagC, increasing amounts of purified c17orf59 decreased Ragulator binding to the Rags (Figure 5D).

Because Ragulator is required for the lysosomal localization of the Rag GTPases, it is possible that the disruption of the Rag-Ragulator interaction due to c17orf59 overexpression results in a mis-localization of the Rag GTPases away from the lysosome. To test this, we transiently expressed FLAG-tagged c17orf59 in HEK-293T cells, marking cells that were transfected using GFP driven by an internal ribosome entry sequence (IRES) downstream of the c17orf59 cDNA. The amount of RagC that co-localizes with the lysosomal marker LAMP1 decreases in cells that overexpress c17orf59, but not FLAG-tagged GFP alone

Figure 6: c17orf59 prevents Rag GTPase lysosomal localization

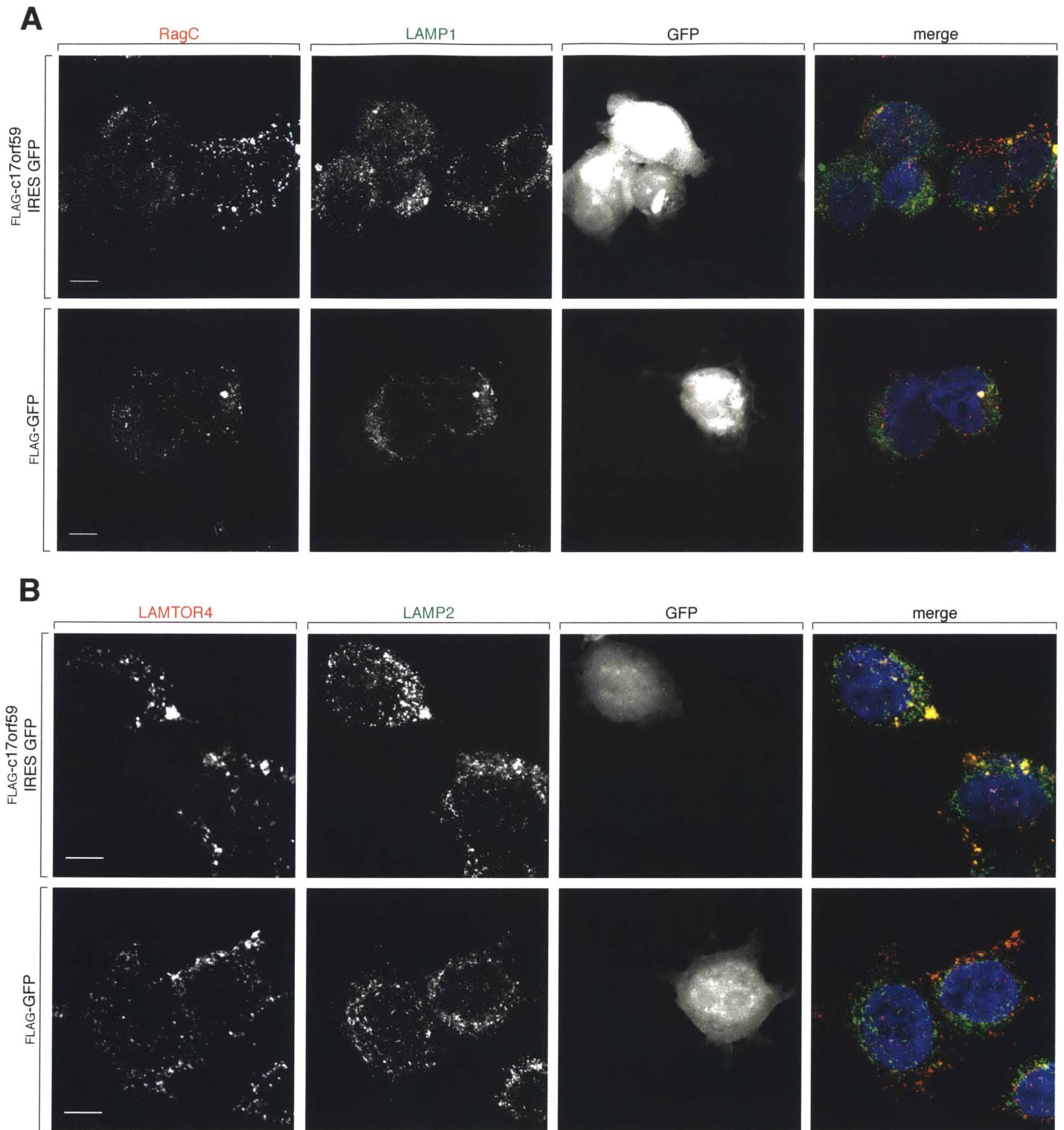


Figure 6: c17orf59 overexpression prevents Rag GTPase lysosomal localization

A) c17orf59 overexpression decreases the amount of lysosomal RagC. HEK-293T cells were transfected with 1 µg of the cDNA encoding FLAG-c17orf59-IRES-GFP (top panels) or FLAG-GFP controls (bottom panels). Cells were starved of amino acids for one hour and re-stimulated with amino acids for 10 minutes, and immunostained with antibodies against RagC (pseudocolored red) and the LAMP1 (green) and imaged for GFP (white) using confocal microscopy. GFP-positive cells (third column) represent transfected cells.

B) c17orf59 overexpression does not alter the localization of LAMTOR4. HEK-293T cells were transfected with 1 µg of the cDNA encoding FLAG-c17orf59-IRES-GFP (top panels) or FLAG-GFP controls (bottom panels). Cells were starved of amino acids for one hour and re-stimulated with amino acids for 10 minutes, and immunostained with antibodies against LAMTOR4 (pseudocolored red) and the LAMP1 (green) and imaged for GFP (white) using confocal microscopy. GFP-positive cells (third column) represent transfected cells.

(Figure 6A, GFP-positive cells). Importantly, overexpression of c17orf59 does not alter the localization of Ragulator component LAMTOR4 (Figure 6B) indicating that Ragulator is still intact and present at lysosomes.

In summary, c17orf59 disrupts the Rag-Ragulator complex in cells as well as in vitro resulting in a reduction in the lysosomal localization of the Rag GTPases. C17orf59 binding to Ragulator does not alter Ragulator stability or lysosomal localization, as evident from maintained intra-Ragulator interactions and LAMTOR4 localization upon c17orf59 overexpression in cells and in vitro binding experiments. In vitro binding of either Rags or c17orf59 to Ragulator implies that c17orf59 has the ability to directly compete with the Rags for binding to Ragulator, producing a Rag- and mTORC1-free Ragulator-c17orf59 complex.

c17orf59 overexpression inhibits mTORC1

We hypothesized that because c17orf59 can disrupt the Rag-Ragulator interaction and RagC localization, c17orf59 overexpression would inhibit mTORC1 activation by amino acids. Indeed, overexpression of c17orf59 produced a dose-dependent inhibition of mTORC1 activation in response to amino acid stimulation, to a level comparable to the inhibition produced by dominant-negative RagB^{GDP} expression (Figure 7A).

Figure 7: c17orf59 overexpression inhibits mTORC1

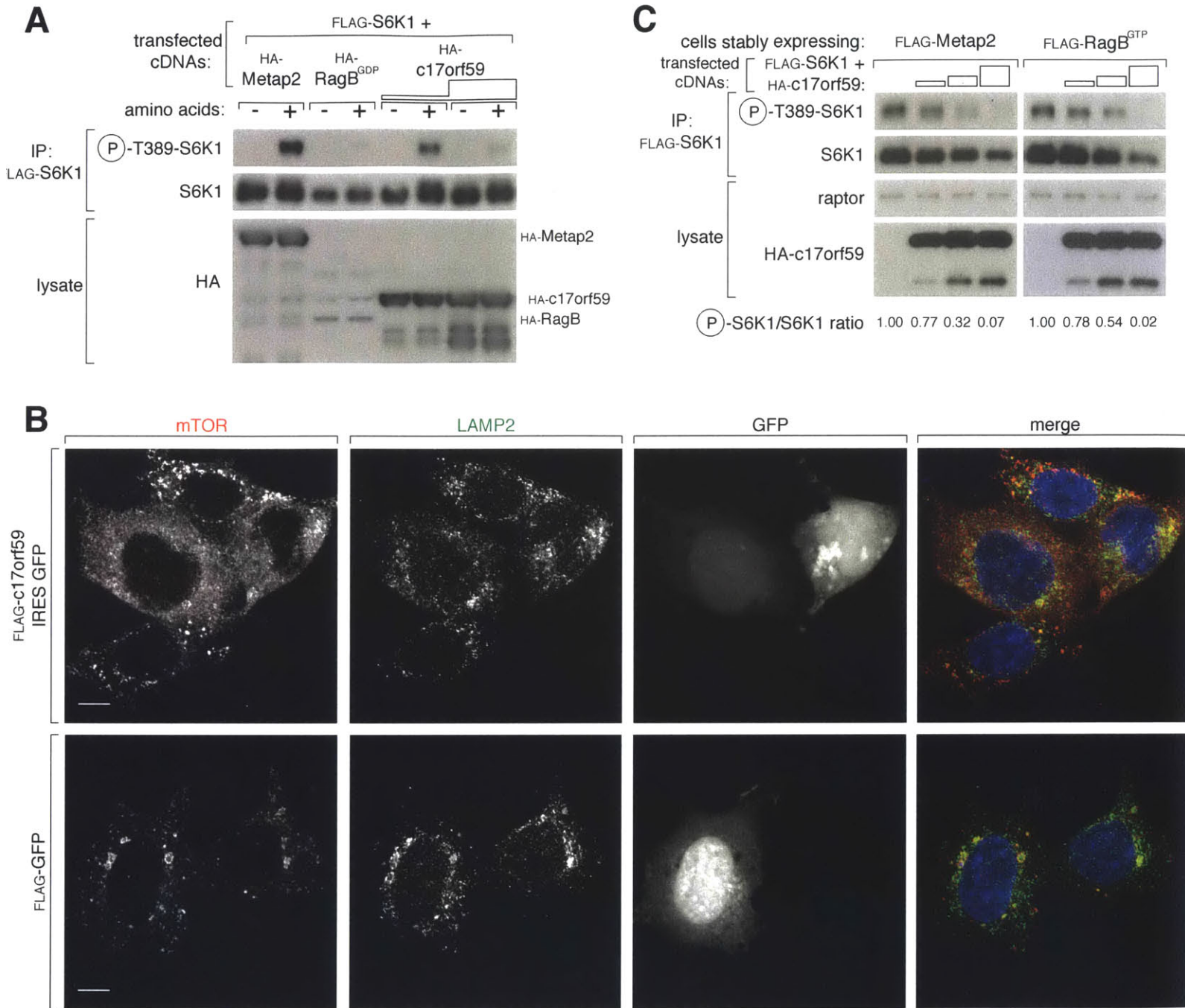


Figure 7: Overexpression of c17orf59 inhibits mTORC1

A) Overexpression of c17orf59 inhibits mTORC1 activity in cells. HEK-293T cells were transfected with 2 ng of the cDNA for FLAG-S6K1 as well as the increasing amounts of HA-c17orf59, HA-RagB-54L (GDP-bound mimetic), or control protein cDNAs. The amounts of HA-c17orf59 cDNA transfected are as follows: 500ng (lanes 5 and 6), and 2 μ g (lanes 7 and 8). FLAG immunoprecipitates and whole cell lysates were analyzed by immunoblotting for the indicated proteins.

B) c17orf59 overexpression decreases the amount of lysosomal mTOR. HEK-293T cells were transfected with 1 μ g of the cDNA encoding FLAG-c17orf59-IRES-GFP (top panels) or FLAG-GFP controls (bottom panels). Cells were starved of amino acids for one hour and re-stimulated with amino acids for 10 minutes, and immunostained with antibodies against mTOR (pseudocolored red) and the LAMP1 (green) and imaged for GFP (white) using confocal microscopy. GFP-positive cells (third column) represent transfected cells.

C) c17orf59 inhibits mTORC1 in cells with amino acid-insensitive mTORC1 signaling. HEK-293T cells stably expressing the RagB Q99L mutant (GTPase deficient; GTP-bound) or a control protein were transfected with a cDNA for FLAG-S6K1 and increasing amounts of the cDNA for HA-c17orf59 as in (A). The amounts of HA-c17orf59 cDNA transfected are as follows: 500ng (lane 2), 1 μ g (lane 3) and 2 μ g (lane 4). The bar above each lane is to scale for c17orf59 cDNA added. Samples were analyzed as in (A).

To confirm that overexpression of c17orf59 inhibits mTORC1 through the nutrient sensing machinery and through the disruption of the Rag-Ragulator interaction, we examined mTOR localization in cells that overexpress c17orf59. Using the FLAG-c17orf59-IRES-GFP construct described above, mTOR remained largely diffuse upon stimulation with amino acids in c17orf59-expressing HEK-293T cells (Figure 7B, GFP-positive cells in the top panel). mTOR localizes to lysosomes in control cells that either were not transfected or expressed FLAG-GFP alone (Figure 7B, GFP-negative cells in the top panel or GFP-positive cells in the bottom panel).

If the c17orf59 overexpression-mediated disruption of the Rag-Ragulator interaction represents the mechanism of mTORC1 inhibition by c17orf59, overexpression of c17orf59 should inhibit mTORC1 even in cells that express the dominant-active RagB^{GTP} mutant. Under normal conditions, dominant-active RagB^{GTP} constitutively recruits mTORC1 to the lysosome. The interaction between Rags and Ragulator is required to bring mTORC1 to the lysosome; disruption of the Rag-Ragulator complex by c17orf59 would act in an epistatic

nature to the normally activating effect of RagB^{GTP}. Without Rag binding to Ragulator, the Rag mTORC1 will not be recruited to the lysosome.

We overexpressed c17orf59 in cells stably expressing RagB^{Q99L}, the RagB^{GTP} mutant, or a control protein, Metap2. Overexpression of c17orf59 diminished phosphorylation of S6K1 in a dose-dependent manner in both constitutively active, RagB^{GTP}-expressing and control cells (Figure 7C), indicating that c17orf59 overexpression inhibits mTORC1 signaling even in the presence of the active Rags, likely due to the loss of lysosomal Rag localization.

What regulates c17orf59 to inhibit mTORC1?

While c17orf59 inhibits mTORC1 by disrupting the Rag-Ragulator interaction, loss of the protein does not alter mTORC1 activity in response to amino acid or insulin deprivation or stimulation. It is possible that, if c17orf59 is a cellular mTORC1 inhibitor, these inputs into mTORC1 signaling do not regulate c17orf59. Another stimulus that either inhibits or activates mTORC1 could do so through its regulation of c17orf59.

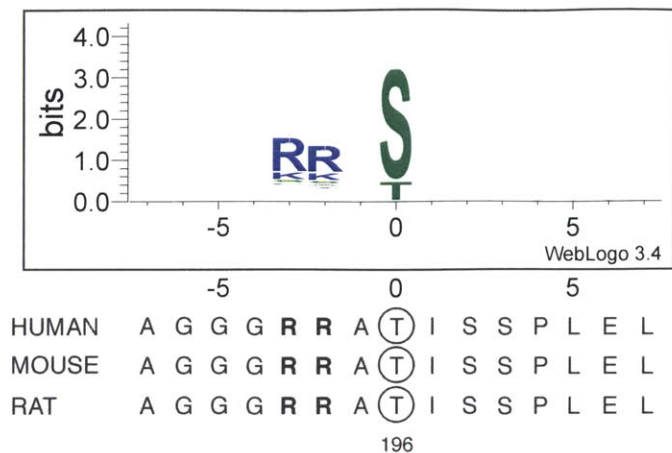
There are two potential modes by which c17orf59 could be regulated: by modulating expression level or by post-translational modification. In HEK-293T cells and *in vitro*, overexpression or excess of c17orf59 is required to disrupt the Rag-Ragulator interaction and inhibit mTORC1. It is also possible that there are ways that cells naturally overexpress c17orf59 to inhibit mTORC1 in a chronic setting or that a modification on c17orf59 would make it a more potent Ragulator-binding protein. We will address these possibilities below.

c17orf59 is a PKA substrate

It is possible that c17orf59 protein could be modified to increase its affinity for Ragulator, considering that in order for c17orf59 to inhibit the Rag-Ragulator interaction, c17orf59 levels must drastically increase (Figure 5 and 6). If a post-

Figure 8: c17orf59 is a PKA substrate

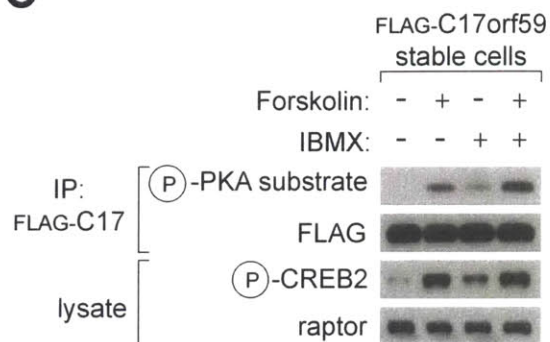
A



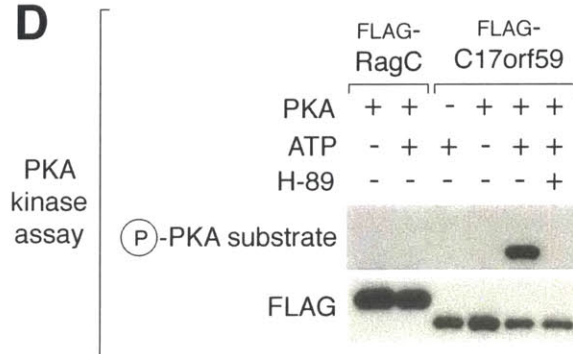
B

	DMSO	Forskolin
(P)-T196	1/24	8/36
(P)-S198	0/24	1/36
(P)-S199	4/24	5/36

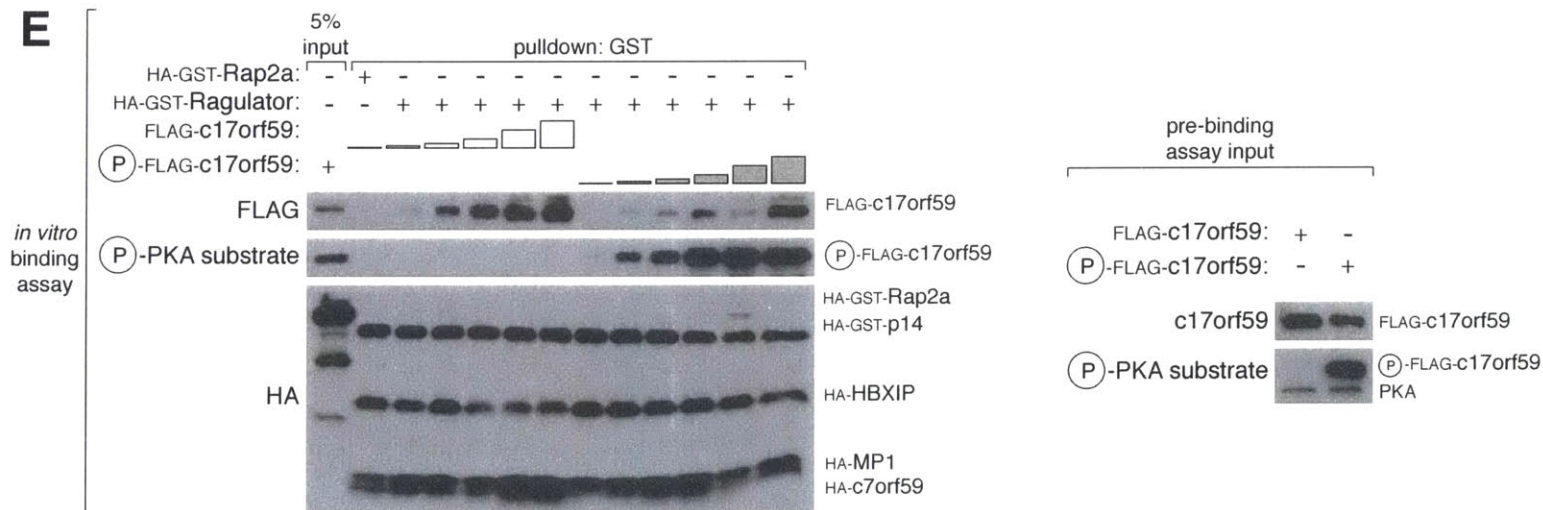
C



D



E



F

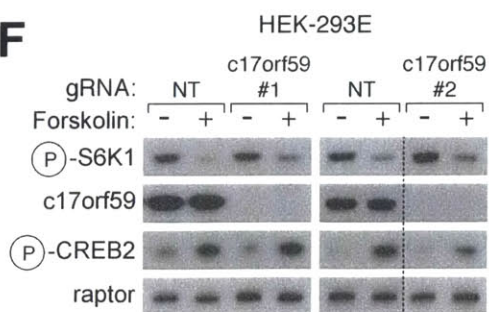


Figure 8: c17orf59 is a PKA substrate

A) Threonine 196 on c17orf59 fits the PKA-substrate motif. The seven residues up- and downstream of threonine 196 from three species (bottom of panel) are aligned to a logo of the annotated PKA phosphorylation sites (top of panel; made using WebLogo 3.4).

B) Threonine 196 on c17orf59 is phosphorylated upon treatment with a PKA agonist. Mass spectrometric analysis of anti-FLAG-immunoprecipitates from HEK-293T cells stably-expressing FLAG-tagged c17orf59 that were treated with forskolin or DMSO for one hour. Data are presented as the fraction of peptides containing a phosphorylation at indicated residue over the total number of peptides containing the indicated residue. Data are from a single experiment.

C) c17orf59 is phosphorylated upon PKA agonism in cells. Stably-expressed, epitope-tagged c17orf59 was immunoprecipitated from HEK-293T cells that had been treated with DMSO or the PKA agonists forskolin, IBMX or both together for one hour. Immunoprecipitates and whole cell lysates were analyzed by immunoblotting for the indicated proteins. Phosphorylation of c17orf59 was examined by reactivity with an anti-phospho-PKA substrate antibody.

D) c17orf59 is phosphorylated by PKA in vitro. Purified, recombinant Rag GTPases or c17orf59 was incubated with recombinant PKA catalytic subunit in the presence or absence of ATP or in the presence of both ATP and H-89, a PKA inhibitor. Samples were analyzed by immunoblotting for the indicated proteins. Phosphorylation of c17orf59 was examined by reactivity with an anti-phospho-PKA substrate antibody.

E) Phosphorylation of c17orf59 by PKA reduces the amount of c17orf59 bound to Ragulator in vitro. Purified, recombinant c17orf59 that had been phosphorylated by PKA or unphosphorylated, as in (A), was incubated at increasing concentrations with purified, immobilized GST-tagged Ragulator. Input samples from the in vitro phosphorylation reaction (right) or precipitates from glutathione affinity resin (left) were immunoblotted for the indicated epitope tags.

F) Loss of c17orf59 does not alter the inhibition of mTORC1 by PKA agonism. c17orf59-null HEK-293E cells were treated with forskolin or DMSO for one hour. Lysates were analyzed by immunoblotting for the indicated proteins.

translational modification such as phosphorylation made c17orf59 a better Ragulator-interacting protein, it would be a more potent inhibitor of the Rag-Ragulator complex and mTORC1 signaling. A publicly available database of post-translational modifications identified a number of phosphopeptides corresponding to threonine 196 in c17orf59 ("c17orf59," PhosphoSite Plus, <http://www.phosphosite.org>, curated by Cell Signaling Technology). The primary sequence surrounding threonine 196 is similar to the motif that is preferred by Protein Kinase A (PKA), particularly the presence of a pair of arginines that are a single residue upstream of the putative phosphorylation site (Figure 8A).

To experimentally determine if c17orf59 is phosphorylated at Thr 196 we turned to unbiased phospho-proteomics. Stably-expressed, epitope tagged

c17orf59 was immunoprecipitated from HEK-293T cells that had been treated with forskolin, a potent PKA agonist. Mass spectrometry of the immunoprecipitation yielded numerous peptides corresponding to c17orf59 that contained Thr 196. Upon PKA agonism by forskolin, there was a marked increase in the number of peptides that contained phosphorylation at Thr 196, but not other potentially phosphorylated residues in the same region (Figure 8B).

Because this proteomic approach is not quantitative, we wanted to validate that stably-expressed c17orf59 is phosphorylated upon PKA agonism. We immunoprecipitated epitope-tagged c17orf59 from HEK-293T cells that had been treated with various PKA agonists or vehicle and examined the precipitated proteins by western blot using a phosphorylated PKA substrate-specific antibody. The anti-phospho-PKA-substrate antibody reacted with immunoprecipitated c17orf59 in a manner that recapitulated PKA activity, comparable to phosphorylation of a bona-fide PKA substrate, CREB2 (Figure 8C). This indicates that c17orf59 can be phosphorylated upon PKA agonism in cells, but does not confirm that c17orf59 is indeed a PKA substrate.

In order to prove direct phosphorylation of c17orf59 by PKA, we tested the phosphorylation *in vitro*. We observed that purified c17orf59, but not the Rag GTPases, is indeed phosphorylated by recombinant PKA in a manner that is sensitive to an ATP-competitive PKA inhibitor (Figure 8D).

One hypothesis is that phosphorylation of c17orf59 can alter its binding to Ragulator. We tested whether c17orf59 that had been phosphorylated *in vitro* by PKA displayed altered binding to Ragulator using *in vitro* binding assays and detected reduced binding of phosphorylated c17orf59 to immobilized, epitope-tagged Ragulator (Figure 8E). These results suggest a PKA-mediated regulation of mTORC1 activity through alterations in the binding affinity of c17orf59 for Ragulator.

Despite the apparent difference for affinity of phosphorylated c17orf59 for Ragulator *in vitro*, loss of c17orf59 did not alter the effect of PKA agonism on mTORC1 activity. Treatment with PKA agonists forskolin and IBMX inhibits

mTORC1 in HEK-293E cells, similar to published reports that cAMP and PKA can inhibit mTORC1 (Xie et al., 2011; Okunishi et al., 2014). However, PKA agonists still inhibited mTORC1 to the same extent in c17orf59-null cells (Figure 8F). These data indicate that in the cells used there appears to be no significant role of c17orf59 in the PKA-mediated inhibition of mTORC1.

c17orf59 expression is regulated by cholesterol levels

We moved on to study the transcriptional regulation of c17orf59. The only reported stimulus that alters c17orf59 expression is cholesterol deprivation (Bartz et al., 2009). The c17orf59 promoter contains an SREBP binding site. SREBP responds to cholesterol deprivation (Brown and Goldstein, 1997), and SREBP might represent a mechanism to upregulate c17orf59 and inhibit mTORC1 in low cholesterol conditions.

Upon deprivation of cholesterol using lipid-depleted serum, c17orf59 protein levels increase slightly, indicating that SREBP likely does regulate its transcription (Figure 9A). This increase in c17orf59 protein levels is not further enhanced by treatment with hydroxypropyl- β -cyclodextrin (HPCD), which depletes cholesterol from membranes. Cholesterol starvation inhibits mTORC1, and HPCD treatment further abrogates S6K1 phosphorylation (Figure 9A). However, this inhibition of mTORC1 was not altered in c17orf59-null cells (Figure 9A), ruling out the speculated role of c17orf59 in mTORC1 inhibition following cholesterol deprivation.

Plasma cell myeloma cell lines are enriched for c17orf59 expression

Because the regulation of c17orf59 protein levels by cholesterol was relatively weak and loss of c17orf59 did not alter the effect of cholesterol deprivation on mTORC1 activity, we determined what cell lines had highest levels

Figure 9: c17orf59 levels are regulated by cholesterol deprivation and are higher in plasma cell myeloma cell lines

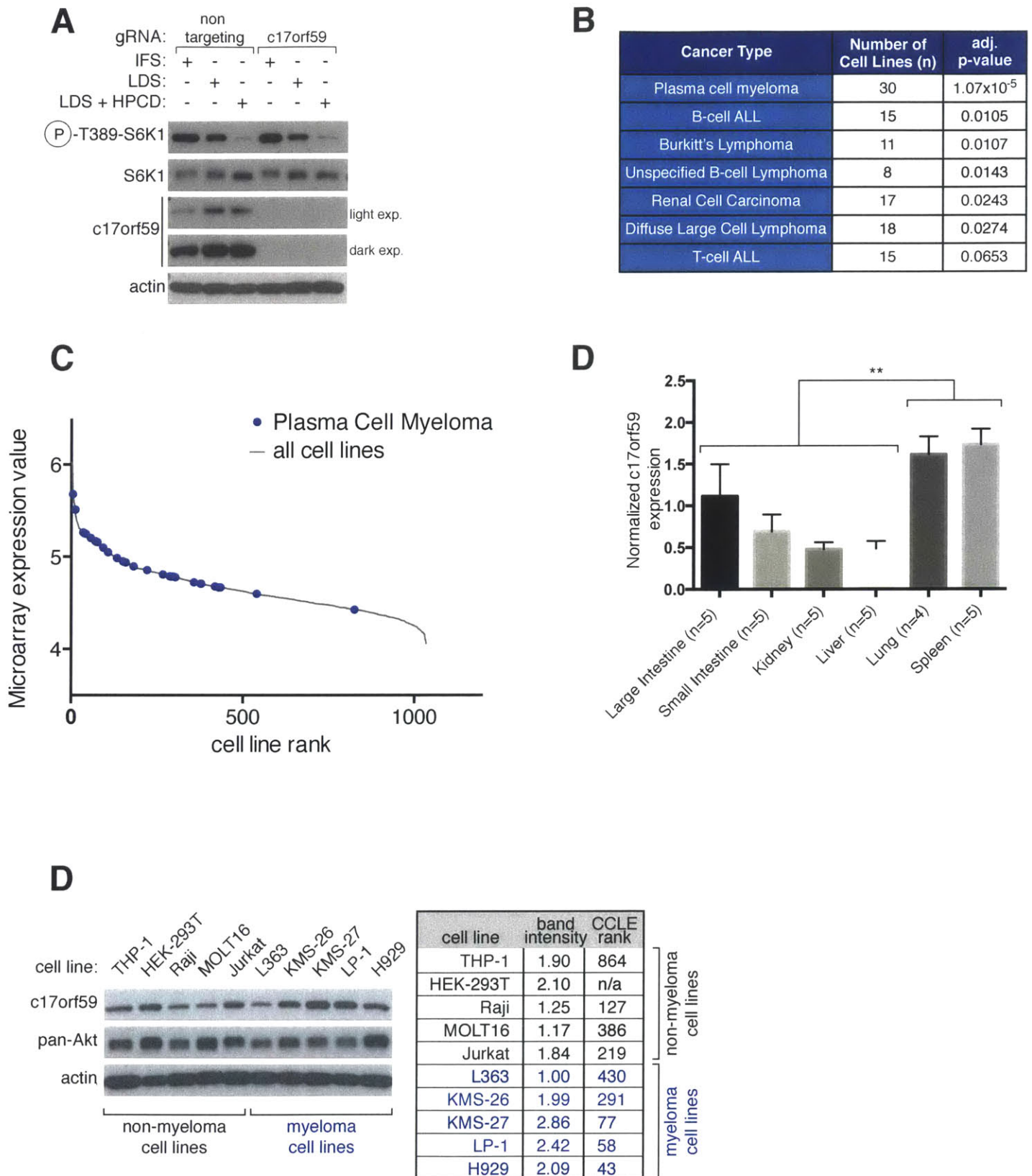


Figure 9: c17orf59 levels are regulated by cholesterol deprivation are higher in plasma cell myeloma cell lines

A) c17orf59-null HeLa cells do not have alterations in mTORC1 signaling in response to cholesterol deprivation. c17orf59-null HeLa were incubated in media containing 10% FCS ("IFS" lanes), 0.5% lipid-depleted serum overnight ("LDS" lanes), or 0.5% lipid-depleted serum overnight followed by 5 hours in 2% hydroxypropyl-beta-cyclodextrin ("LDS + HPCD" lanes). Lysates were analyzed by immunoblotting for the indicated proteins.

B) Plasma cell myeloma cell lines are enriched among cell lines with higher c17orf59 expression. Left panel: One-sided Kolmogorov-Smirnov test was used to analyze cell lines for the distribution of ranks of c17orf59 expression using microarray data available from CCLE. Right panel: Plasma cell myeloma cell lines are indicated with blue dots in a plot of all cell lines in the CCLE microarray data.

C) c17orf59 is expressed higher in mouse spleen and lung. qPCR analysis of c17orf59 levels in 6 tissues collected from mice. Lung and spleen had statistically significantly higher levels than other tissues tested ($p < 0.01$; Tukey's multiple comparison's test).

D) c17orf59 protein is mildly elevated in plasma cell myeloma cell lines. The indicated cell lines were lysed and lysates were analyzed by immunoblotting for the indicated proteins. Right panel: band intensity of the c17orf59 immunoblot was quantified using ImageJ and compared to the microarray-based rank in CCLE.

of c17orf59 expression. Identification of cell lines that express the highest amount of c17orf59 could potentially uncover a loss-of-function phenotype.

Using microarray data from the publicly-available Cancer Cell Line Encyclopedia (CCLE; <http://www.broadinstitute.org/ccle/home>), we determined what cell type was enriched among cell lines that expressed higher amounts of c17orf59. The most significantly enriched cell type was plasma cell myeloma cells ($p=1.07 \times 10^{-5}$; Figure 9B). Other B-lymphocyte malignancies were also enriched among the highest c17orf59-expressing cells (Figure 9B). The vast majority of plasma cell myeloma cell lines found in the CCLE express higher amounts of c17orf59; when cell lines were ranked by c17orf59 expression, 28 of 30 plasma cell myeloma cell lines were above the median expression level (Figure 9C).

We also examine what mouse tissues had the highest expression of c17orf59 by qPCR. From several tissues, the spleen and lung displayed the highest expression of c17orf59 RNA (Figure 9D). High expression of c17orf59 in the spleen correlates with the CCLE microarray data, as the spleen contains the

highest proportion of B-lymphocytes of the tissues that we examined (as determined by B220 expression; not shown).

Despite the apparent elevation in c17orf59 levels in B-lymphocytes and plasma cell myeloma in particular, we did not observe a significant increase in c17orf59 protein level in plasma cell myeloma cell lines (Figure 9E). While the plasma cell myeloma cell lines did tend to have higher amounts of c17orf59, the increase in protein level were not over the c17orf59 levels observed in HEK-293T cells. While c17orf59 is likely upregulated in plasma cell myeloma cell lines, this upregulation likely does not alter mTORC1 activation.

DISCUSSION

We find that c17orf59 is a Ragulator-interacting protein. c17orf59 interacts with Ragulator in a manner that competes with the Rag GTPases for binding, both in cells and in vitro. Loss of the Rag-Ragulator interaction due to c17orf59 overexpression decreases binding between the Rags and mTORC1 as well as Ragulator and mTORC1 and prevents both the Rags and mTORC1 from binding to the lysosomal membrane. Concomitant to the loss of the Ragulator-Rag-mTORC1 interactions, overexpression of c17orf59 inhibits mTORC1 activity in response to amino acid availability. RagA^{GTP} expression, which normally induces constitutively active amino acid signaling by maintaining mTORC1 on the lysosome, is not sufficient to rescue the signaling defect downstream of c17orf59 overexpression, indicating that high levels of c17orf59 prevent productive interactions between the Rags, Ragulator and mTORC1 in a Rag nucleotide state-independent manner, likely by preventing the Rags from localizing to the lysosome. c17orf59 is a PKA substrate and this phosphorylation slightly alter the affinity of c17orf59 for Ragulator, but loss of c17orf59 does not alter the effects of PKA agonism on mTORC1 activity.

Identifying and characterizing proteins that interact with Ragulator or other components of the amino acid-sensitive mTORC1 signaling pathway is important for understanding how eukaryotic cells sense amino acids and other nutrients that regulate mTORC1. Ragulator was originally described as the lysosomal scaffold for the Rags (Sancak et al., 2010) and upon identification of additional components of the Ragulator (HBXIP and c7orf59) we found that the scaffold also acts as a GEF for the Rags (Bar-Peled et al., 2012). It is likely that as more Ragulator-interacting proteins are uncovered, additional ways that Ragulator can control mTORC1 will be found; here c17orf59 competes with the Rags to bind Ragulator.

c17orf59-mediated inhibition of the Rag-Ragulator interaction represents an alternative mechanism of mTORC1 inhibition. Potential negative regulators of

the amino acid sensing pathway have been reported to act directly upon the Rag GTPases or their regulatory proteins to alter their nucleotide-bound state (e.g. GATOR [Bar-Peled et al., 2013; Panchaud et al., 2013], Sestrins [Parmigiani et al., 2014; Chantranupong et al., 2014; Peng et al., 2014], Leucyl-tRNA synthetase [Han et al., 2012; Bonfils et al., 2012], SH3BP4 [Kim et al., 2012]). Interestingly, the mechanism of mTORC1 inhibition by c17orf59 is independent of the Rag nucleotide-bound state, implying that regardless of the presence of nutrients, c17orf59 can inhibit the Rag-mTORC1 interaction and prevent mTORC1 from being activated by Rheb.

The binding of c17orf59 to the Ragulator in a Rag-independent manner and the inhibition of mTORC1 activity by c17orf59 overexpression suggest that c17orf59 is a negative regulator of the nutrient-sensing pathway. However, loss of c17orf59 did not result in detectable defects in mTORC1 signaling in response to starvation or re-stimulation by amino acids or insulin in HEK-293E and HeLa cell lines and did not alter the inhibition of mTORC1 by PKA agonism. c17orf59-null cells also displayed no alterations in the inhibition of mTORC1 by cholesterol deprivation, the only reported regulator of c17orf59 expression. It is possible that other conditions may inhibit mTORC1 in a manner that depends on either an increase in c17orf59 expression or promotes c17orf59 binding to Ragulator.

It is possible, however, that c17orf59 is not a negative regulator of the mTORC1 pathway, but rather that the c17orf59-Ragulator complex has mTORC1-independent functions. c17orf59 could have a role in a different, unidentified pathway that also utilizes Ragulator. If this were the case, Ragulator would have mTORC1-independent functions when bound to c17orf59 and not the Rags. This would not be completely unprecedented, as other components of the nutrient-sensing pathway serve other functions in the cell. We have previously shown that the v-ATPase is a Ragulator-binding complex that regulates mTORC1 signaling but also functions as a major proton pump to maintain the acidic nature of the lysosome as well as other organelles, and that the maintenance of pH may be de-coupled from the role of the v-ATPase in mTORC1 activation (Zoncu et al.,

2011). Similarly, GATOR2, which acts upstream of the GAP for RagA and B (GATOR1) and is required for amino acid signaling to mTORC1, includes Sec13 and Seh1L (Bar-Peled et al., 2013), which serve multiple other functions in the cell. Sec13 is a COPII component required for the generation of vesicles that traffic from the endoplasmic reticulum and Golgi and also participates in the nuclear pore complex (Devos et al., 2004; Gurkan et al., 2006; Brohawn et al., 2009). Seh1L is also a component of the nuclear pore complex, where it binds directly to Sec13 (Brohawn et al., 2009).

One potential function for the c17orf59-Ragulator complex could be the recently described BLOC-1-related complex (BORC), which contains c17orf59 and controls lysosomal positioning (Pu et al., 2015). It is unclear how the assembly of BORC is regulated within the cell or if this complex regulates mTORC1, but the authors imply that Ragulator interacts with BORC subunits (Pu et al., 2015), which would indicate a role for the c17orf59-Ragulator complex in lysosomal positioning as a part of BORC. This is consistent with literature that Ragulator components are important for maintaining endolysosomal morphology and biogenesis (Teis et al., 2006; Nada et al., 2009; Takahashi et al., 2012; Vogel et al., 2015) and consistent with our observed alterations in lysosomal staining in cells that overexpress c17orf59 (Figure 4E and Figure 5B). It is possible that Ragulator binds to c17orf59 and BORC in a Rag- and mTORC1-independent manner to control endosome and lysosome morphology.

It remains to be determined if c17orf59 is indeed a negative regulator of the nutrient-sensing pathway, or if it is a component of a Ragulator-containing pathway that acts independently of mTORC1. Regardless of the physiological role of c17orf59 in the cell, we have uncovered an additional cellular mechanism for mTORC1-specific inhibition, namely by altering the Rag-Ragulator interaction.

MATERIALS AND METHODS

Reagents

The following antibodies were obtained from Cell Signaling Technologies (CST): antibodies against Phospho-T389-S6K (#9206 and #9205), S6K1 (9202 and 2708), mTOR (#293), c7orf59/LAMTOR4 (#12284 for blotting; #13140 for immunofluorescence), p18 (#8975), MP1 (#8168), p14 (#8145), HBXIP (#14633), RagA (#4357), RagC (#3360), FLAG epitope (2368), and HA epitope (#2367 and #3724). Antibodies against Raptor (Millipore #09-217), FLAG (Sigma #F1804), LAMP1 (Developmental Studies Hybridoma Bank at the University of Iowa #1D4B), LAMP2 (Santa Cruz Biotechnology #18822) and Actin (Sigma #A5441) were obtained elsewhere. The antibody to c17orf59 was a generous gift from Jianxin Xie at CST.

Inactivated Fetal Bovine Serum (IFS), RPMI, and DMEM were obtained from US Biologicals. Amino acids for re-stimulation experiments were purchased from Sigma and dissolved in water to a concentration of 10x compared to the RPMI amino acid concentrations, as described previously (Sancak et al., 2008).

Cell lysis and immunoprecipitation

Cells were washed once with ice-cold PBS and lysed with CHAPS lysis buffer (0.3% CHAPS [Sigma #C3023], 10 mM beta-glycerol phosphate [Sigma #G9422], 10mM sodium pyrophosphate [Sigma #221368], 40mM HEPES [pH 7.4], and 2.5 mM MgCl₂) with one tablet of EDTA-free protease inhibitor (Roche #11 873 580 001) per 25 ml. Lysates were cleared by centrifugation at 13,000 rpm in a table-top microcentrifuge for 10 minutes. For anti-FLAG immunoprecipitations, cleared lysates were normalized for protein content by Bradford assay (Bio-Rad #500-0006) and incubated for 1.5-3 hours with 30 µl of 50% slurry of FLAG-M2 affinity gel (Sigma #A2220) that had been washed three times in lysis buffer. After incubation, beads were washed three times with lysis buffer containing 150 mM NaCl. Immunoprecipitated proteins were denatured by the addition of 35 µl of sample buffer and boiling for 5 minutes. In experiments using only cell lysates, without immunoprecipitation, 1% Triton X-100 (Sigma T9284) was substituted for CHAPS in the lysis buffer.

In transfection experiments in which epitope-tagged proteins were immunoprecipitated, 2 million HEK-293T cells were seed in 10 cm culture dishes. 24 hours later 500 ng of each pRK5-based plasmids was transfected using XtremeGENE9 (Roche #06 365 809 001) according to the manufacturers protocol: FLAG-Metap2, FLAG-p14/HA-MP1, FLAG-c17orf59, FLAG-RagB/HA-RagC. Empty pRK5 vector was used to normalize total plasmid amount to 2 µg per 10 cm culture dish. Thirty-six hours after transfection, cells were lysed in 1 ml lysis buffer as described above.

For experiments in which c17orf59 was expressed with Rag or Ragulator components, 2 million HEK-293T cells were seeded in 10cm culture dishes. Twenty-four hours later, the following pRK5-based plasmids were transfected using X-tremeGENE9: 100 ng of each FLAG-Metap2, FLAG-p14 with HA-MP1, FLAG-RagB with HA-RagC co-transfected with 1 µg of either HA-c17orf59 or HA-Metap2. Thirty-six hours after transfection, cells were lysed in CHAPS lysis buffer as described above.

For experiments where cells were starved and re-stimulated with amino acids or insulin, 400,000 HEK-293E cells were seeded in 6-well plates coated with fibronectin (Millipore #341635). Forty-eight hours later, cells were washed once with PBS or starvation media and incubated in RPMI lacking all amino acids (US Biological # R9010) supplemented with 5% dialyzed IFS for one hour or in DMEM without serum for 3 hours and stimulated with amino acids or insulin (100 ng/ml; Sigma # I2643) for 10 minutes. Cells were lysed as described above in 130 µl Triton lysis buffer. Alternatively, 500,000 HeLa cells were seeded in 6-well plates and starved, re-stimulated and lysed as described above after culturing overnight.

For dialysis, 100 ml IFS was dialyzed in SnakeSkin Dialysis Tubing with a 3.5 kDa cutoff (Thermo #PI88244) against approximately 3L PBS at 4°C for 48 hours, replacing with fresh PBS after 24 hours.

c17orf59 overexpression in signaling experiments

In experiments where mTORC1 activity was assessed upon overexpression of c17orf59, FLAG-S6K1 co-expression and immunoprecipitation was used as described previously (Bar-Peled et al., 2012). Briefly, 2 million HEK-293T cells were seeded in 10 cm culture dishes. 24 hours later, 2 µg of the cDNA for a control protein, HA-Metap2, 200 ng HA-RagB-T54N (RagB^{GDP}) or between 500 ng and 2 µg of the cDNA for HA-c17orf59 was co-transfected into HEK-293T cells with 2 ng of the cDNA for FLAG-S6K1. Empty pRK5 vector was used to normalize total plasmid amount to 2 µg per 10 cm plate. 36 hours post-transfection, cells were starved of amino acids, stimulated with amino acids and lysed and FLAG-S6K1 was immunoprecipitated as described above.

Mass spectrometry

Immunoprecipitates from nearly confluent 15 cm culture dishes containing HEK-293T cells stably expressing FLAG-Metap2, FLAG-HBXIP, or FLAG-c17orf59 were prepared using CHAPS lysis as described above, except 50 µl of FLAG-M2 affinity gel was used for immunoprecipitations and beads were washed 6 times in lysis buffer containing 150mM NaCl. Bound proteins were eluted from the FLAG-M2 affinity gel by incubation in 50µl 1mg/ml FLAG-peptide (sequence DYKDDDK) for 45 minutes on ice and denatured by addition of loading buffer and boiling for 5 minutes. Samples were resolved on 4-12% NuPage gels (Life

Technologies) and stained with SimplyBlue SafeStain (Life Technologies LC6065). Each lane was cut into 10 pieces and digested in trypsin overnight. Resulting digests were analyzed at the Whitehead Institute Proteomics core using a Thermo Fisher LTQ with Waters NanoAcuity UPLC mass spectrometer. Data were analyzed using Scaffold Free Viewer (Proteome Software).

In vitro binding

Purification of recombinant proteins and in vitro binding assays using GST-tagged Rag GTPases or Ragulator were done as described (Bar Peled et al., 2012). Briefly, 4 million HEK-293T cells were seeded in 15cm culture dishes. Forty-eight hours after seeding, cells were transfected with cDNA for the following genes using PEI (Polysciences #23966; 3 μ l PEI at 1 mg/ml per μ g DNA): for HA-GST-Ragulator: 4 μ g HA-GST-p14, 8 μ g HA-MP1, 8 μ g p18G2A-FLAG (a lipidation defective mutant), 8 μ g HA-HBXIP, and 8 μ g HA-c7orf59; for FLAG-Ragulator: 4 μ g p18G2A-FLAG, 8 μ g HA-MP1, 8 μ g HA-p14, 8 μ g HA-HBXIP, and 8 μ g c7orf59; for HA-GST-Rag GTPases: 8 μ g HA-GST-RagB, 16 μ g HA-RagC; for FLAG-Rag GTPases: 8 μ g FLAG-RagB, 16 μ g HA-RagC; for individual proteins: 10 μ g FLAG-c17orf59; 10 μ g FLAG-Rap2a; 10 μ g HA-GST-Rap2a.

Thirty-six hours after transfection, cells were lysed as described above, using 750 μ l Triton lysis buffer per dish. After clearing the lysates, 50 μ l of 50% slurry of FLAG-M2 affinity resin in lysis buffer or 200 μ l of 50% slurry of immobilized glutathione affinity resin (Thermo #15160) in lysis buffer were added to lysates expressing FLAG- or GST-tagged proteins, respectively. Recombinant proteins were incubated with affinity resin for 2 hours at 4°C with rotation. Each sample was washed once in lysis buffer, five times in wash buffer (0.3% CHAPS, 2.5 mM MgCl₂, 40 mM HEPES, 500 mM NaCl) and three times in binding buffer (0.3% CHAPS, 2.5 mM MgCl₂, 40 mM HEPES). GST-tagged samples were re-suspended in 160 μ l binding buffer and FLAG-tagged samples were eluted in 50 μ l FLAG-peptide in binding buffer. When necessary, eluates were concentrated using centrifugal filters with a 10 kDa cutoff (Millipore #UFC501024).

For the initial binding reactions, 20 μ l of glutathione affinity resin containing immobilized HA-GST-tagged proteins was incubated in binding buffer supplemented with 2 mM DTT and 1 mg/mL BSA (NEB #B9000) with 745 ng (20 pmol) FLAG-c17orf59 or 1.5 μ g (20 pmol) FLAG-Ragulator to a final volume of 50 μ l for 90 minutes on ice. To terminate binding assays, samples were washed three times with 1 ml of ice-cold binding buffer supplemented with 150 mM NaCl followed by the addition of 50 μ l sample buffer.

Binding assays in which increasing amounts of c17orf59 were added to GST-tagged Ragulator or Rag GTPases were done as described above, except that FLAG-c17orf59 was incubated with FLAG-Ragulator for 30 minutes prior to the incubation with other proteins on ice. For experiments where FLAG-c17orf59 was added to GST-Ragulator, 100 ng-10 μ g (2.7 pmol-270 pmol) was incubated

with Ragulator and 2 μg (25 pmol) Flag Rags were added to the reaction for 90 minutes. For experiments where FLAG-c17orf59 was added to GST-Rags, 100 ng-2 μg (2.7 pmol-270 pmol) was incubated with 1 μg (14 pmol) FLAG-Ragulator for 30 minutes prior to addition to GST-Rag GTPases.

Immunofluorescence

1.5 million p53-null MEFs were transfected with 20 ng HA-c17orf59 and 1 μg empty pRK5 using the MEF Nucleofector kit 1 (Lonza #VPD-1004) using a nucleofector (Lonza) and seeded onto fibronectin-coated glass cover slips. Two wells of a 6-well culture dish were seeded per 1.5 million MEFs transfected. The following day, cells were either left untreated or starved and re-stimulated of amino acids or insulin as described above. Slides were fixed and processed as described previously (Zoncu et al., 2011). Briefly the slides were rinsed once with PBS and fixed using 4% paraformaldehyde in PBS for 15 minutes. Slides were washed twice with PBS and permeabilized with 0.05% Triton X-100 in PBS for 15 minutes. Slides were washed three times in PBS and incubated with primary antibody in 5% normal donkey serum (Jackson #017-000-121) for 1 hr at room temperature (1:300 for anti-LAMP1 antibody and 1:150 for anti-HA antibody), washed three times with PBS, and incubated with secondary antibodies produced in donkey (diluted 1:500 in 5% normal donkey serum) for 45 min at room temperature in the dark, and washed three times with PBS. Slides were mounted on glass coverslips using ProLong Diamond Antifade Mountant (Molecular Probes #P36966) and imaged on a spinning disk confocal system (Perkin Elmer).

p18^{-/-} MEFs were transfected, treated and fixed as above. Samples were washed three times in PBS and blocked for 1 hour in 5% normal donkey serum in PBS containing 0.3% Triton. Samples were incubated in primary antibodies diluted in 1% BSA in PBS containing 0.3% Triton overnight in a humidified chamber at 4degC. Primary antibodies used were as follows: anti-LAMP1 (diluted 1:200), anti-HA (diluted 1:100), p18 (diluted 1:100) and LAMTOR4 (diluted 1:800) The next day samples were washed with PBS three times and incubated for 1-2 hours at room temperature with Alexa Fluor-conjugated secondary antibodies (Molecular Probes, diluted 1:500). Samples were then washed two times with PBS and incubated with Hoechst 33342 (Molecular probes H3570, 1:10,000) in PBS for 15 seconds and washed twice in PBS. Cover slips were mounted on glass slides with Vectashield Mounting Media and cured overnight at room temperature and then imaged as described above.

Alternatively, HEK-293T cells were transfected with 1 μg FLAG-c17orf59-IRES-GFP or 1 μg FLAG-GFP with 1 μg empty pRK5 in 10 cm culture plates as described above for signaling experiments. 24 hours after transfection, 300,000 cells were seeded per well on fibronectin-coated cover slips in 6-well plates. The following day cells were processed as described above and stained using anti-

LAMP2 antibody at 1:400, anti-mTOR at 1:200, anti-RagC at 1:100, or anti-LAMTOR4 at 1:800.

Images are max projections of 0.5 μ m z-stacks. For MEF images, 5 slices were used; 10 slices were used for HEK-293T images. Pearson's correlation was calculated for the p18-c17orf59 quantitation using ImageJ Coloc 2 plugin and analyzed using a Students two-tailed t-test.

Generation of CRISPR/Cas9 knockout cells

To generate c17orf59-null cells, guide RNAs were cloned into the pLentiCRISPR vector (Addgene) that was cut with BbsI (NEB #R0539). GuideRNAs were generated by annealing the following pairs of oligonucleotides and ligated into pLentiCRISPR:

Guide 1 fwd: caccGGGGCGGCCCGGGCCCGAGA

Guide 1 rev: aaacTCTCGGGCCCGGGCCCGCCC

Guide 2 fwd: caccgCAAAGTGGGTAAGGTCGCCG

Guide 2 rev: aaacCGGCGACCTTACCCACTTTGc

One million HEK-293E or 500,000 HeLa cells were seeded in 10cm culture dishes. 24 hours later, cells were transfected with 500 ng guideRNA plasmid with X-tremeGENE9. The following day, transfected cells were selected using puromycin. 48 hours after puromycin selection started, cells were re-transfected with guide RNA plasmid and allowed to grow to near confluence. 90% confluent dishes were trypsinized and single-cell sorted with a flow cytometer into the wells of a 96-well plate containing 150 μ l of DMEM supplemented with 30% IFS. Cells were grown until visible colonies were present, and the resultant colonies were trypsinized and expanded. Clones were validated for loss of the c17orf59 via immunoblotting.

Cholesterol depletion

Cells were depleted of cholesterol using a protocol modified from that described previously (Bartz et al., 2009). Briefly, 3 million HeLa cells were seeded in 10cm culture dishes. The following day, cells were washed twice in PBS and media was changed to either full DMEM with 10% IFS or DMEM containing 0.5% lipid depleted serum (LDS, Intracel #RP-056). Twenty-four hours later, cells were incubated with DMEM with 10% IFS, DMEM with 0.5% LDS, or 2% 2-Hydroxypropyl)- β -cyclodextrin in DMEM with 0.5% LDS for 5 hours. Cells were lysed in 1ml Triton lysis buffer as described above.

c17orf59 cDNA cloning

c17orf59 cDNA was PCR amplified from HEK-293T cDNA using PlatinumTaq HIFI (Life Technology) the below gene-specific primers which have Sall and BamHI sites added at the 5' and 3' ends, respectively. The PCR product was purified from a 1% agarose gel and digested with Sall and BamHI restriction endonucleases (NEB #R0138 and #R0136) overnight. The restriction product was gel purified and ligated into previously Sall-BamHI digested pRK5. For further subcloning, a NotI site present in the c17orf59 cDNA was mutated using overlapping PCR with the following primers, digested with Sall and NotI (NEB #R0189), and ligated into Sall-NotI-digested pRK5.

To amplify c17orf59 cDNA from HEK-293T, the following primers were used:
Fwd: ACGCGTCGACGATGGAGTCGTCTCGGGGGCGG
Rev: CGCGGATCCTCACTTGACAGGGCCTCAA

To remove the internal NotI site and add Sall-NotI subcloning sites, the following primers were used:

Fwd1: caagtcgtcgacgATGGAGTCGTCTCGGGGGC
SDM1 rev: CGAGGAGGCTGCAGCGGGCAGC
SDM2 fwd: GCTGCCCGCTGCAGCCTCCTCG
Rev2: catgatgcggcccgTCCTTGACAGGGCCTCC

The 1000 nucleotides upstream of the c17orf59 gene locus were used as its endogenous promoter and amplified by PCR from genomic DNA from HEK-293T cells with the below primers and ligated to c17orf59 and pLEX-TRC202 plasmid cut with XmaI and BsrGI (NEB #R0180 and #R0575) by Gibson assembly (NEB #E5510). The ligation maintains the XmaI site upstream of the promoter, but eliminates the BsrGI site after the gene of interest.

To amplify the c17orf59 promoter the following primers were used:
Fwd: ccggctcgagggggcccgCTTTCCAATGTCGCTGCACCATTGCATTTAG
Rev: catttccatACTGCAGGTGGGGGCCGC

To amplify FLAG-c17orf59 the following primers were used:
Fwd: cctgcagtATGGAAATGGACTACAAGGATGAC
Rev: gtctcgagttaggactTCACTTGACAGGGCCTC

To generate the FLAG-c17orf59-IRES-GFP construct, FLAG-c17orf59 cDNA was generated by PCR using a forward primer adding an NheI site and Kozak sequence to the FLAG-tag and the NotI-Rev2 primer described above, purified, and digested using NheI and NotI restriction endonucleases (NEB #R0131 and #RO189). Digested PCR produce was ligated into pCAGGS-

PSAML141F, Y115F:GlyR-IRES-GFP (Addgene #32480) that had been digested with NheI and NotI to remove the insert.

To amplify FLAG-c17orf59 for cloning into pCAGGS-IRES-GFP the following primers were used:

Fwd: caagtccgtagcgccaccATGGAAATGGACTACAAGGATG

Rev: catgatcgcgcccgcTCACTTGACAGGGCCTCC

Production of the PKA substrate motif logo

The list of PKA substrates and their phosphorylation sites downloaded from Phosphosite.org. Each annotated PKA substrate in the database includes the primary amino acid sequence in the 14 residues surrounding the phosphorylation site (7 residues upstream and downstream of the site). The list of 15 residue sequences was input into the WebLogo algorithm with the default settings (<http://weblogo.berkeley.edu/logo.cgi>).

PKA kinase phosphorylation

Phosphorylation and PKA kinase assays were adapted from previously published protocols (Sancak et al. 2007). Briefly, recombinant PKA (EMD Millipore #539481) and c17orf59 (purified as above) were incubated together with 100mM Tris/HCl (pH 7.5), 20mM MgCl₂, 400uM ATP, and 500nM H-89 (Cell Signaling Technologies #9844), where indicated, for one hour (for kinase assays) or 20 hours (for in vitro phosphorylation prior to binding assays) at 30°C. For kinase assays, the reaction was stopped by adding protein loading buffer and for in vitro binding assays, the phosphorylated (or not) protein was added immediately to immobilized Ragulator and incubated as above with the indicated amounts of c17orf59.

Forskolin treatments

HEK-293E cells were treated with either 20uM Fsk (LC Laboratories #F-9929) and/or 550uM IBMX (Sigma #I5879). For signaling experiments, 1 million c17orf59-null or expressing cells were seeded in 6-well plates 24 hours prior to Fsk treatments. Cells were treated with Fsk or DMSO for 20 minutes and cells were lysed as described above. For experiments investigating c17orf59 phosphorylation, 4 million cells expressing FLAG-tagged c17orf59 were seeded in 10cm plates (for blotting) or 10 million cells in 15cm plates (for mass spectrometry) 2 days prior to treatment. Cells were treated for one hour with Fsk or IBMX and lysed as described above for immunoprecipitations and mass spectrometry.

Expression analysis

WT C57BL/6 mice were sacrificed according to CAC regulations. Tissues were harvested and snap-frozen in liquid nitrogen immediately after sacrifice. Tissues were homogenized in Trizol Reagent (Trizol Reagent, Life Technology #15596-026) using motorized homogenizer (Thermo Fisher Scientific #K7495400000) and RNA was extracted according to manufacturer's protocol. cDNA was transcribed using Super Script III (Thermo Fisher Scientific #18080085). 7900 Applied Biosystems instrument was used for qPCR using Sybr Green master mix (Roche #4472908).

Gene	Forward primer	Reverse Primer
HPRT (control gene)	GTTAAGCAGTACAGCCCCAAA	AGGGCATATCCAACAACAAACTT
UBC (control gene)	CAGCCGTATATCTTCCCAGACT	CTCAGAGGGATGCCAGTAATCTA
C17orf59	AGCTGACAGCGTTGAGTGTG	TGCCCTTAATGCTCATGTCC
Cryptidin 3 (small intestine marker)	CTGTGTCTGTCTCTTTTGGAG	GCAGCCTCTTTTCTACAATAG
Mucin 2 (large intestine marker)	GGTCCAGGGTCTGGATCACA	GCTCAGCTCACTGCCATCTG
CCL5 (T cells marker)	AAGTGCTCCAATCTTGCACTCG	ACTTCTTCTCTGGGTTGGCACA
B220 (B cells marker)	TGATGGGATGGTGTACGTG	CCAGCAGAGGAAGAAAATGC
CDH16/KSP (kidney marker)	GAGACCAGCATCCCAGTCA	GAGACCAGCATCCCAGTCA
Surfactant protein D (lung marker)	GAGAAGGGTGATCCATTTGC	GTTCTCCCTTTGGTCCAGGT
Albumin (liver marker)	AGTCTGCCGCCAACTGTG	GCAGTCAGCCAGTTCACCATAG

ACKNOWLEDGEMENTS

We would like to thank the entire Sabatini lab for helpful suggestions and input as well as critical reading of the manuscript. This work was supported by grants from the NIH (R01 CA103866, R01 CA129105, R37 AI047389, and R21 AG042876-01A1), Department of Defense (W81XWH-07-0448), and the David H. Koch Institute and Ellison Medical Foundation to D.M.S., fellowship support from the NIH to L.D.S. (F31 CA167872), and an award from the David H. Koch Graduate Fellowship Fund to L.B.-P. W.C.C. is supported by an American Cancer Society/Ellison Foundation postdoctoral fellowship (PF-13-356-01-TBE). D.M.S. is an investigator of the Howard Hughes Medical Institute.

REFERENCES:

Bar-Peled L, Schweitzer LD, Zoncu R, Sabatini DM. (2012). Ragulator is a GEF for the rag GTPases that signal amino acid levels to mTORC1. *Cell*. Sep 14;150(6):1196-208.

Bar-Peled L, Chantranupong L, Cherniack AD, Chen WW, Ottina KA, Grabiner BC, Spear ED, Carter SL, Meyerson M, Sabatini DM. (2013). A Tumor suppressor complex with GAP activity for the Rag GTPases that signal amino acid sufficiency to mTORC1. *Science*. 340(6136):1100-6.

Bartz F, Kern L, Erz D, Zhu M, Gilbert D, Meinhof T, Wirkner U, Erfle H, Muckenthaler M, Pepperkok R, Runz H. (2009). Identification of cholesterol-regulating genes by targeted RNAi screening. *Cell Metab*. Jul;10(1):63-75.

Bonfils G, Jaquenoud M, Bontron S, Ostrowicz C, Ungermann C, De Virgilio C. (2012). Leucyl-tRNA synthetase controls TORC1 via the EGO complex. *Mol Cell*. 46(1):105-10.

Brohawn SG, Partridge JR, Whittle JR, Schwartz TU. (2009). The nuclear pore complex has entered the atomic age. *Structure*. 17(9):1156-68.

Brown MS, Goldstein JL. (1997). The SREBP pathway: regulation of cholesterol metabolism by proteolysis of a membrane-bound transcription factor. *Cell*. May 2;89(3):331-40.

Chantranupong L, Wolfson RL, Orozco JM, Saxton RA, Scaria SM, Bar-Peled L, Spooner E, Isasa M, Gygi SP, Sabatini DM. (2014). The Sestrins interact with GATOR2 to negatively regulate the amino-acid-sensing pathway upstream of mTORC1. *Cell Rep*. 9(1):1-8.

Devos D, Dokudovskaya S, Alber F, Williams R, Chait BT, Sali A, Rout MP. (2004). Components of coated vesicles and nuclear pore complexes share a common molecular architecture. *PLoS Biol*. 2(12):e380.

Gürkan C, Stagg SM, Lapointe P, Balch WE. (2006). The COPII cage: unifying principles of vesicle coat assembly. *Nat Rev Mol Cell Biol*. 7(10):727-38.

Han JM, Jeong SJ, Park MC, Kim G, Kwon NH, Kim HK, Ha SH, Ryu SH, Kim S. (2012). Leucyl-tRNA synthetase is an intracellular leucine sensor for the mTORC1-signaling pathway. *Cell*. 149(2):410-24.

Kim YM, Stone M, Hwang TH, Kim YG, Dunlevy JR, Griffin TJ, Kim DH. (2012). SH3BP4 is a negative regulator of amino acid-Rag GTPase-mTORC1 signaling. *Mol Cell*. 46(6):833-46.

Nada S, Hondo A, Kasai A, Koike M, Saito K, Uchiyama Y, Okada M. (2009). The novel lipid raft adaptor p18 controls endosome dynamics by anchoring the MEK-ERK pathway to late endosomes. *EMBO J*. 28(5):477-89.

Okunishi K1, DeGraaf AJ, Zaslona Z, Peters-Golden M. (2014). Inhibition of protein translation as a novel mechanism for prostaglandin E2 regulation of cell functions. *FASEB J*. Jan;28(1):56-66.

Panchaud N, Péli-Gulli MP, De Virgilio C. (2013). Amino acid deprivation inhibits TORC1 through a GTPase-activating protein complex for the Rag family GTPase Gtr1. *Sci Signal*. 6(277):ra42

Parmigiani A, Nourbakhsh A, Ding B, Wang W, Kim YC, Akopiants K, Guan KL, Karin M, Budanov AV. (2014). Sestrins inhibit mTORC1 kinase activation through the GATOR complex. *Cell Rep*. 9(4):1281-91.

Peng M, Yin N, Li MO. (2014). Sestrins function as guanine nucleotide dissociation inhibitors for Rag GTPases to control mTORC1 signaling. *Cell*. 159(1):122-33.

Pu J, Schindler C, Jia R, Jarnik M, Backlund P, Bonifacino JS. (2015). BORG, a multisubunit complex that regulates lysosome positioning. *Dev Cell*. Apr 20;33(2):176-88.

Sancak Y, Peterson TR, Shaul YD, Lindquist RA, Thoreen CC, Bar-Peled L, Sabatini DM. (2008). The Rag GTPases bind raptor and mediate amino acid signaling to mTORC1. *Science*. Jun 13;320(5882):1496-501.

Sancak Y, Bar-Peled L, Zoncu R, Markhard AL, Nada S, Sabatini DM. (2010). Ragulator-Rag complex targets mTORC1 to the lysosomal surface and is necessary for its activation by amino acids. *Cell*. Apr 16;141(2):290-303.

Takahashi Y, Nada S, Mori S, Soma-Nagae T, Oneyama C, Okada M. (2012). The late endosome/lysosome-anchored p18-mTORC1 pathway controls terminal maturation of lysosomes. *Biochem Biophys Res Commun*. Jan 27;417(4):1151-7.

Teis D, Taub N, Kurzbauer R, Hilber D, de Araujo ME, Erlacher M, Offterdinger M, Villunger A, Geley S, Bohn G, Klein C, Hess MW, Huber LA. (2006). p14-MP1-MEK1 signaling regulates endosomal traffic and cellular proliferation during tissue homeostasis. *J Cell Biol*. 2006 Dec 18;175(6):861-8.

Vogel GF, Ebner HL, de Araujo ME, Schmiedinger T, Eiter O, Pircher H, Gutleben K, Witting B, Teis D, Huber LA, Hess MW. (2015). Ultrastructural Morphometry Points to a New Role for LAMTOR2 in Regulating the Endo/Lysosomal System. *Traffic*. 2015 Jun;16(6):617-34.

Xie J, Ponuwei GA, Moore CE, Willars GB, Tee AR, Herbert TP. (2011). cAMP inhibits mammalian target of rapamycin complex-1 and -2 (mTORC1 and 2) by promoting complex dissociation and inhibiting mTOR kinase activity. *Cell Signal*. Dec;23(12):1927-35.

Zoncu R, Bar-Peled L, Efeyan A, Wang S, Sancak Y, Sabatini DM. (2011). mTORC1 senses lysosomal amino acids through an inside-out mechanism that requires the vacuolar H(+)-ATPase. *Science*. 334(6056):678-83.

CHAPTER 5

Discussion And Future Directions

Lawrence D. Schweitzer¹

¹ Whitehead Institute for Biomedical Research and Massachusetts Institute of Technology, Department of Biology, Nine Cambridge Center, Cambridge, MA 02142

SUMMARY AND OUTSTANDING QUESTIONS

mTORC1 is an important regulator of cellular growth and metabolism, responding to the nutritional status of a cell and organism to coordinate processes that are required for either proliferation in cycling cells or for the specific function of post-mitotic cells. It has been well-appreciated that mTORC1 is tightly regulated by nutrient levels, but the proteins that mediate signaling to mTORC1 from amino acid sufficiency have only just been identified in last eight years. As we uncover new proteins and describe their functions, we may be able to accurately describe exactly how amino acids activate mTORC1.

Here we have presented data detailing amino acid sensing upstream of mTORC1. First, we identified HBXIP and its binding partner as new members of the Ragulator complex. The pentameric Ragulator binds the Rag GTPases *in vitro* and is a guanine nucleotide exchange factor (GEF) for RagA and RagB (Bar-Peled et al., 2012). Second, we uncovered non-canonical mTORC1 signaling in RagA-null MEFs, where loss of RagA leads to constitutive activation of mTORC1 regardless of nutrient availability. In addition, loss of RagA in adult mice leads to an accumulation of monocytic cells, likely due to the upregulation of Akt that occurs as a consequence of diminished mTORC1 activity (Efeyan et al., 2014).

Finally, we identified c17orf59, a new Ragulator-interacting protein that can inhibit mTORC1. c17orf59 inhibits the nutrient-sensing arm of mTORC1 activation via a previously undescribed mechanism. c17orf59 competes with the Rag GTPases for binding to Ragulator, such that when c17orf59 is present in excess (compared to the Rag GTPases), the Rag GTPases no longer bind to Ragulator or the lysosome and cannot recruit mTORC1 to the lysosome. This inhibition is completely independent of the nucleotide-bound state of the Rag GTPases, indicating that c17orf59 could override positive signals from amino acids and glucose (Schweitzer et al., 2015).

Despite the advances in the field over the last few years (illustrated in Figure 1), including the data presented here, there are numerous open questions to address. Recently our lab and others have identified a number of new proteins that are important for sensing amino acids, but how these proteins regulate each other and the Rag GTPases is largely unknown.

How does Ragulator activate RagA/B?

When we first identified Ragulator as the scaffold that tethers the Rag GTPases and mTORC1 to the lysosome, the assumption was made that a multi-protein complex likely has more functions than mere protein-protein interaction and thus named the complex “Ragulator,” implying that it was a regulator of the Rag GTPases (Sancak et al, 2010). It was not until further expansion of the Ragulator and inclusion of HBXIP and c7orf59 that this prediction was borne out and the GEF activity towards RagA and RagB was uncovered; however, despite the knowledge of the complete Ragulator and more than three years since its publication we still do not know the molecular basis for Ragulator’s GEF activity.

GEF and GAP complexes exist with similar structural motifs as Ragulator, including multimeric GTPase regulatory proteins. These include longin domain containing proteins, such as the TRAPP complexes, which are GEFs for Rab GTPases (Jones et al., 2000; Langemeyer et al., 2014); the bacterial roadblock-containing protein MglB, which acts as a GAP for its cognate GTPase MglA (Levine et al., 2013; Miertzschke et al., 2011). The structure of the MglA-MglB complex (Miertzschke et al., 2011) and structures of TRAPP complexes have been published (multiple structures summarized in Levine et al., 2013). In these structures, the roadblock- or longin-containing proteins form dimers as expected, and there is evidence of multimers comprising multiple different roadblock/longin dimers (Miertzschke et al., 2011; Levine et al., 2013).

In each case, it appears that the GEF or GAP does not act directly upon the catalytic site of their cognate GTPases; instead, the roadblock- and longin-

Figure 1: Progress in the amino acid pathway upstream of mTORC1 - 2010 to 2015

Top panel: mTORC1 activation by amino acids in 2010. In the absence of amino acids, the Rag GTPases are in an inactive conformation, but maintained at the lysosome by the trimeric Ragulator complex. Upon stimulation with amino acids (labeled non-specifically as “AA”), the nucleotide-bound state of the Rag GTPases changes such that mTORC1 is recruited to the lysosome.

Bottom panel: mTORC1 activation by amino acids in 2015. Adapted from Chapter 1 Figure 2. In the absence of amino acids Sestrins are bound to GATOR2, relieving its inhibition upon GATOR1. Thus, GATOR1 can interact with and facilitate GTP hydrolysis in the RagA or RagB, preventing the Rag GTPases from recruiting mTORC1 to the lysosome. The absence of lysosomal amino acids simultaneously inhibits the GEF activity of Ragulator, likely because both SLC38A9 and the v-ATPase cannot induce activation of Ragulator. Upon stimulation with amino acids, Sestrins bind to cytosolic leucine (labeled as “L”) and dissociate from GATOR2. Dissociation of Sestrins from GATOR2 leads to inhibition of the GAP activity of GATOR1; the inhibitory signal from GATOR1 to the Rag GTPases is relieved. Amino acids within the lysosomal lumen induce the activation of the GEF activity of Ragulator, through binding of arginine (“R”) to SLC38A9 and some aspect of lysosomal amino acids (labeled “?”) to the v-ATPase. Activated Ragulator facilitates nucleotide exchange in RagA and RagB, leading to an activated Rag conformation and recruitment of mTORC1 to the lysosomal membrane. The Ragulator-c17orf59 complex also exists on the lysosome.

containing regulatory proteins act in allosteric manners (Levine et al., 2013). It is likely that Ragulator acts allosterically to induce the release of nucleotide from RagA and RagB. However, this prediction cannot be validated without a crystal structure of the entire Ragulator bound to the Rag GTPases, a structure that has proved elusive. Hopefully, in the next few years, this structure will be solved and perhaps will facilitate our understanding of Rag GTPase activation by Ragulator.

How is Ragulator regulated by amino acid availability?

It is not clear how amino acid availability controls Ragulator function at the molecular level through the amino acid-sensing pathway that activates mTORC1. Two components of the amino acid-sensing pathway, SLC38A9 and the v-ATPase interact with Ragulator and appear to regulate Ragulator function (Wang et al., 2015; Zoncu et al., 2011). We have previously shown that inhibition of the v-ATPase appears to inhibit the GEF activity of Ragulator (Bar-Peled et al., 2012). However, it is not clear if these proteins activate or inhibit GEF activity directly, or if they somehow prevent Ragulator’s interaction with the Rag

GTPases. Also, both SLC38A9 and the v-ATPase interact with the Rag GTPases in addition to Ragulator, so it is possible that they can coordinate the Rag-Ragulator complex to facilitate nucleotide exchange from RagA or RagB.

Both the v-ATPase and SCL38A9 are required for activation of mTORC1 by amino acids, but may act in parallel, not sequentially, in a way that will allow different actions upon Ragulator and the Rag GTPases (Wang et al., 2015). Multiple ways to alter the GEF activity of Ragulator is implied by the finding that SLC38A9 and the v-ATPase act differently upon the complex. New Ragulator interacting proteins may uncover other parallel mechanisms to alter Ragulator function.

It is also possible that there are proteins like c17orf59 that inhibit the Rag-Ragulator interaction in an amino acid-sensitive fashion, which would effectively inhibit the GEF activity of Ragulator. In addition to these hypotheses, Ragulator may be modified by various post-translational modifications in response to amino acid availability changes, a possibility that has not been pursued yet.

What regulates c17orf59?

While overexpression of c17orf59 inhibits mTORC1 activation by amino acid stimulation, the amount of c17orf59 protein required to disrupt the Rag-Ragulator interaction is much higher than is present in the cell lines tested (HEK-293T, HEK-293E, and HeLa). In addition, cell lines with the highest expression of c17orf59 at the mRNA level do not have markedly higher levels of the protein. This indicates that it is unlikely that under normal conditions c17orf59 could successfully act as an inhibitor of mTORC1. While post-translational modifications could increase the potency of inhibition by c17orf59, phosphorylation by PKA, the only identified modification on c17orf59, was not required for inhibition of mTORC1 by PKA agonism. The question remains whether there are cells or tissues that express c17orf59 to a sufficient level to

inhibit mTORC1, possibly following protein modification by PKA, SREBP or an unknown signal transduction pathway to inhibit mTORC1.

These data point to the possibility that c17orf59 is not actually a cellular inhibitor of mTORC1, but rather a Ragulator-interacting protein that uses Ragulator for another function or pathway. It is not known what other pathway or process that the c17orf59-Ragulator participates in, but one possibility is in the trafficking and biogenesis of lysosomes. c17orf59 is a part of the BLOC-1-related complex (BORC; Pu et al., 2015), and this complex could utilize Ragulator in an mTORC1-independent manner.

Regardless of the regulation or role of c17orf59, the disruption of the Rag-Ragulator interaction by c17orf59 also suggests the possibility for the design of a new mTORC1 inhibitor. That c17orf59 can prevent the Rags from binding to Ragulator in vitro, as well as in cells, implies that the binding site between the two complexes is an accessible surface that could be the target of a small molecule or peptide. A molecule that mimics the presence of c17orf59 could provide an mTORC1-specific inhibitor that inhibits mTORC1 completely without affecting mTORC2.

An inhibitor of mTORC1, but not mTORC2, would be a useful research tool to determine the distinct functions of the complex in cells. Currently, mTOR kinase inhibitors target both mTORC1 and mTORC2 by virtue of the shared kinase between the two complexes (Thoreen et al., 2009; Feldman and Shokat, 2010) and rapamycin, which was originally thought to be mTORC1-specific, is a compromised tool to interrogate mTORC1 activity because it only partially inhibits mTORC1 and can inhibit mTORC2 assembly upon prolonged treatment (Thoreen et al., 2009; Feldman et al., 2009; Sarbassov et al., 2006). Peptides derived from c17orf59 could potentially inhibit mTORC1; alternatively a small molecule that binds to the same, accessible surface on the structure of Ragulator that c17orf59 and, likely, the Rags bind to could be an effective mTORC1 inhibitor.

How do different amino acids regulate mTORC1?

We and others have identified proteins that are putative sensors of single amino acids and regulate Rag GTPase activity to signal to mTORC1 (Wang et al., 2015; Wolfson et al., 2015). SLC38A9 binds arginine and is required for activation of mTORC1 in response to arginine (Wang et al., 2015). Sestrins bind leucine and are required for inhibition of mTORC1 in the absence of that amino acid (Wolfson et al., 2015). Both of these proteins have been studied largely in one immortalized cell line, HEK-293T. However, different cell lines diverge in their response to amino acid availability and in their regulation of mTORC1, requiring distinct amino acids to maintain mTORC1 activity. Similarly, different tissues in the mouse show mTORC1 activation in response to treatment with distinct subsets of amino acids (unpublished data).

The different requirements and sufficiencies for amino acids leads to the question of how specificity is generated by different cell types. One possibility is that there are numerous amino acid sensors that control mTORC1 via Ragulator and GATOR complexes, and different cell lines or tissues express different levels of these sensors. In addition to the different sensors themselves, it is not clear how ubiquitous the expression of the Rag paralogs, Ragulator components or GATOR components is. There are also different isoforms of many of these proteins, but since the functions and expression of these has not been examined in depth, many unknown variables might be discovered in the future. Any difference in the function or regulation of these core components of the amino acid-sensing pathway could alter amino acid sensitivities in different cells or tissues.

It is also possible that in some cases amino acids themselves are not always sensed, but rather some indirect readout of their presence is recognized, such as activity of or flux through amino acid transporters on the lysosome. In this case some amino acids (such as arginine and leucine) could be sensed by sestrins, SLC38A9 and other amino acid-binding proteins that directly interact

with Rag-modifying proteins, but other important amino acids could be sensed through more indirect means to alter Ragulator or v-ATPase function, for example.

CONCLUSION

Recently there have been leaps in our understanding of how amino acid availability to cells regulates mTORC1 activity (outlined in Figure 1). The Rag GTPases themselves were only identified seven years ago and we have continued expanding the universe of proteins that respond to amino acids to control mTORC1 localization, which is required for activation. However, we do not know the mechanism of action for many of these proteins at the molecular level. Hopefully in the coming years the crystal structures of many of these proteins will be solved and facilitate the study of the molecular activity of these proteins. While this alone will not describe how this signaling pathway works, structures could provide valuable information that leads to hypotheses about how amino acids are sensed and the this signal is propagated to the Rag GTPases.

In conjunction with deeper understanding of the mechanisms of amino acid sensing, the physiological role of the components of the pathway needs to be better described. Most of the work characterizing Rag- and Ragulator interacting proteins has been carried out cultured cell lines. Generating mouse models of null alleles or important mutations will allow us to better understand exactly how amino acids are sensed in an organism, taking into account physiological levels of amino acids in different organs as well as the relevant co-stimulation with growth factor and hormones.

It is remarkable that in less than a decade our understanding of the amino acid sensing pathway to mTORC1 has expanded exponentially. While we now know many of the players in the pathway and what their functions are, there are many questions left to answer before we fully understand how mTORC1 is regulated in response to the presence or absence of amino acids.

REFERENCES

Bar-Peled L, Schweitzer LD, Zoncu R, Sabatini DM. Ragulator is a GEF for the rag GTPases that signal amino acid levels to mTORC1. *Cell*. 2012 Sep 14;150(6):1196-208.

Efeyan A, Schweitzer LD, Bilate AM, Chang S, Kirak O, Lamming DW, Sabatini DM. RagA, but not RagB, is essential for embryonic development and adult mice. *Dev Cell*. 2014 May 12;29(3):321-9.

Feldman ME, Apse B, Uotila A, Loewith R, Knight ZA, Ruggero D, Shokat KM. Active-site inhibitors of mTOR target rapamycin-resistant outputs of mTORC1 and mTORC2. *PLoS Biol*. 2009 Feb 10;7(2):e38.

Feldman ME, Shokat KM. New inhibitors of the PI3K-Akt-mTOR pathway: insights into mTOR signaling from a new generation of Tor Kinase Domain Inhibitors (TORKinibs). *Curr Top Microbiol Immunol*. 2010;347:241-62.

Jones S, Newman C, Liu F, Segev N. The TRAPP complex is a nucleotide exchanger for Ypt1 and Ypt31/32. *Mol Biol Cell*. 2000 Dec;11(12):4403-11.

Langemeyer L, Nunes Bastos R, Cai Y, Itzen A, Reinisch KM, Barr FA. Diversity and plasticity in Rab GTPase nucleotide release mechanism has consequences for Rab activation and inactivation. *Elife*. 2014 Feb 11;3:e01623.

Levine TP, Daniels RD, Wong LH, Gatta AT, Gerondopoulos A, Barr FA. Discovery of new Longin and Roadblock domains that form platforms for small GTPases in Ragulator and TRAPP-II. *Small GTPases*. 2013 Apr-Jun;4(2):62-9.

Miertzschke M, Koerner C, Vetter IR, Keilberg D, Hot E, Leonardy S, Søgaard-Andersen L, Wittinghofer A. Structural analysis of the Ras-like G protein MglA and its cognate GAP MglB and implications for bacterial polarity. *EMBO J*. 2011 Aug 16;30(20):4185-97.

Pu J, Schindler C, Jia R, Jarnik M, Backlund P, Bonifacino JS. BORC, a multisubunit complex that regulates lysosome positioning. *Dev Cell*. 2015 Apr 20;33(2):176-88.

Sancak Y, Bar-Peled L, Zoncu R, Markhard AL, Nada S, Sabatini DM. Ragulator-Rag complex targets mTORC1 to the lysosomal surface and is necessary for its activation by amino acids. *Cell*. 2010 Apr 16;141(2):290-303.

Sarbassov DD, Ali SM, Sengupta S, Sheen JH, Hsu PP, Bagley AF, Markhard AL, Sabatini DM. Prolonged rapamycin treatment inhibits mTORC2 assembly and Akt/PKB. *Mol Cell*. 2006 Apr 21;22(2):159-68.

Schweitzer LD, Comb WC, Bar-Peled L, Sabatini DM. Disruption of the Rag-Ragulator Complex by c17orf59 Inhibits mTORC1. *Cell Rep*. 2015 Sep 1;12(9):1445-55.

Thoreen CC, Kang SA, Chang JW, Liu Q, Zhang J, Gao Y, Reichling LJ, Sim T, Sabatini DM, Gray NS. An ATP-competitive mammalian target of rapamycin inhibitor reveals rapamycin-resistant functions of mTORC1. *J Biol Chem*. 2009 Mar 20;284(12):8023-32.

Wang S, Tsun ZY, Wolfson RL, Shen K, Wyant GA, Plovanich ME, Yuan ED, Jones TD, Chantranupong L, Comb W, Wang T, Bar-Peled L, Zoncu R, Straub C, Kim C, Park J, Sabatini BL, Sabatini DM. Lysosomal amino acid transporter SLC38A9 signals arginine sufficiency to mTORC1. *Science*. 2015 Jan 9;347(6218):188-94.

Wolfson RL, Chantranupong L, Saxton RA, Shen K, Scaria SM, Cantor JR, Sabatini DM. Sestrin2 is a leucine sensor for the mTORC1 pathway. *Science*. 2015 Oct 8. pii: aab2674.

Zoncu R, Bar-Peled L, Efeyan A, Wang S, Sancak Y, Sabatini DM. mTORC1 senses lysosomal amino acids through an inside-out mechanism that requires the vacuolar H(+)-ATPase. *Science*. 2011 Nov 4;334(6056):678-83.